INSTITUTO TECNOLOGICO Y DE ESTUDIOS SUPERIORES DE MONTERREY

CAMPUS MONTERREY

SCHOOL OF ENGINEERING AND SCIENCES

FULL POTENTIOSTAT SYSTEM WITH WIRELESS COMMUNICATION IN A PROGRAMMABLE-SYSTEM-ON-A-CHIP AND A PC.

A THESIS PRESENTED BY

ADRIÁN IVÁN MUÑOZ MARTÍNEZ

SUBMITTED TO THE SCHOOL OF ENGINEERING AND SCIENCES IN PARTIAL FULFILLMENT OF THE REQUIREMENTS FOR THE DEGREE OF

MASTER OF SCIENCES IN ELECTRONICS ENGINEERING

MONTERREY NUEVO LEÓN, DECEMBER 1, 2017

Instituto Tecnológico y de Estudios Superiores de Monterrey

Campus Monterrey

School of Engineering and Sciences

Full Potentiostat System with wireless communication in a Programmable-System-On-a-Chip and a PC

A thesis presented by

Adrián Iván Muñoz Martínez

Submitted to the
School of Engineering and Sciences
in partial fulfillment of the requirements for the degree of

Master of Sciences

In

Electronics Engineering

Monterrey Nuevo León, December 1, 2017

Instituto Tecnológico y de Estudios Superiores de Monterrey

Campus Monterrey

School of Engineering and Sciences

The committee members, hereby, certify that have read the thesis presented by Adrián Iván Muñoz Martínez and that it is fully adequate in scope and quality as a partial requirement for the degree of Master of Science in Electronics Engineering.

Dr. Graciano Dieck Assad
Tecnológico de Monterrey
School of Engineering and Sciences
Principal Advisor

Dr. Alfonso Ávila Ortega
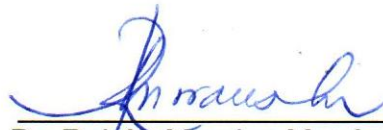Tecnológico de Monterrey
Committee Member

Dr. José Manuel Rodríguez Delgado
Tecnológico de Monterrey
Committee Member

Dr. Jordi Colomer Farrarons
University of Barcelona
Committee Member

Dr. Omar Israel González Peña
Tecnológico de Monterrey
Committee Member

Dr. Rubén Morales Menéndez
Dean of Graduate Studies
School of Engineering and Sciences

Monterrey Nuevo León, December 1, 2017

Declaration of Authorship

I, Adrián Iván Muñoz Martínez, declare that this thesis titled, "Full Potentiostat System with wireless communication in a Programmable-System-On-a-Chip and a PC" and the work presented in it are my own. I confirm that:

- This work was done wholly or mainly while in candidature for a research degree at this University.
- Where any part of this thesis has previously been submitted for a degree or any other qualification at this University or any other institution, this has been clearly stated.
- Where I have consulted the published work of others, this is always clearly attributed.
- Where I have quoted from the work of others, the source is always given. With the exception of such quotations, this thesis is entirely my own work.
- I have acknowledged all main sources of help.
- Where the thesis is based on work done by myself jointly with others, I have made clear exactly what was done by others and what I have contributed myself.

_____

Adrián Iván Muñoz Martínez
Monterrey Nuevo León, December 1, 2017

Dedication

To Maria Guadalupe Martínez Monjaraz for her incomparable love and support through all the time since I was studying. Her mentoring was fundamental to keep me in the right way. Hence, this success is the result of all her teachings.

To Guadalupe Muñoz Garza for his concern about my education and my wellness. He has believed in me as no one has done. All the help he provided is priceless to me, and this degree is the best inheritance that he can leave me.

To Cynthia Aidee Torres Alarcón for her love and patience in the difficult times. She always cared about me, and she always gave me a hand when I had troubles. Thus, this achievement is for our future.

Furthermore, I want to dedicate this success to my whole family because they were there to help me when I needed it most. Their love and companion were crucial every day. In this work, I have given my best effort, and I hope they feel proud of me.

Acknowledgements

Full Potentiostat System with wireless communication in a Programmable-System-On-a-Chip and a PC

By

Adrián Iván Muñoz Martínez

Abstract

This thesis is about the development of a Potentiostat System. The objective is to have a device capable of being embedded in rotary disk platforms and watches. Hence, some of the features are the small size and the low power consumption. The dissertation addresses those concerns thought a Programmable-System-on-a-Chip demonstrating that this solution is a good approach. Thus, this document explains from the circuit design until the validation of the entire system.

A series of steps establish the path to reach the objectives. The circuit review describes relevant configurations to control the voltage and read the Redox current. The prototype design explains the circuits implementation in hardware and the development of electrochemical trials in software. A characterization allows us to make the proper compensations to have accurate results. The completion of several electrochemical experiments validates the embedded system capacity, and it establishes the working range of the applications. Therefore, it is easy to accomplish the objectives with all this in mind.

As results, the Potentiostat System is capable of handling negative and positive Redox currents in the range of 86.44 to 3000 nA and the voltage control is of ± 2 volts. The samples per second of this device goes from 50 to 2000. All these features make the prototype suitable for health, environmental, and research applications. Biosensors to detect glucose, melatonin, hydrogen peroxide, nitrite, and the xanthine oxidase enzyme are examples of specific applications for this electronic system. Therefore, the Programmable-System-on-a-Chip strategy is suitable to develop portable and low energy devices.

List of Figures

List of Tables

Contents

Chapter 1. Introduction

Exists several applications in medical diagnosis, environmental engineering, and industrial control that required the detection of analytes in a solution, and information about its concentration [1]. Many methods have been created to address those issue as magnetic, optical, and electrochemical techniques. However, electrochemical methods have the following advantages:

- Reasonable speed.
- Good sensitivity.
- A wide range of applications.
- Low cost of instrumentation and maintenance.

Today, the electrochemical biosensors are an opportunity area for research and development [2]. One line of investigation is wearable monitoring devices [3]. Those sensors focus on fitness and health issues to track relevant human body variables. The challenges of an electrochemical biosensor instrument are the small size of the components, great autonomy, and wireless data transmission capabilities. Those opportunities for development can be seen as well in the centrifugal microfluidic platform commonly called Lab-on-a-Disc [4]. Someone can use this platform as a clinical diagnostic tool with the ability to detect glucose [5], and cancer cells [6].

Moreover, doctors often use electrochemical biosensors as Point of Care Technologies (POCT) inside or outside of the human body [7]. POCT has features as short analyze periods, portability, and its measurements most of the time are taken out of a clinical laboratory. This last characteristic is helpful to those who are far away from hospitals, or when it is too risky to move a patient. Also, this kind of technology can be implantable in humans for continuous monitoring, bringing advantages to the medical care [8].

Electrochemical biosensors require a potentiostat system for the electrical manipulation of the electrodes to make the proper detections [9]. This electronic instrument has been studied since 1940 [10]. The goal of this device is to accurately control and condition the potential of the sensor, despite impedance changes that could happen in the Electrochemical Cell (EC). The key to maintaining a stable voltage is a feedback loop with advanced electronic components that allows precise measurements to get reliable information.

In recent years, the developments in microelectrodes fabrication and microfluidics technology have brought to the potentiostats systems more challenges to their designs [11]. Likewise, the advances in the electronic systems allow developing potentiostats for specific and precise applications, taking advantage of better practices in operating and driving electrochemical biosensors [9]. These technological advances will lead us to sophisticated systems capable of:

- DNA identification.
- Protein classification.
- Neural recording.
- Glucose level determination.

- pH detection.
- Drugs concentration quantization.

Thus, it is not hard to imagine that all this technological progress will end in remote health devices allowing to doctors faces illness such diabetes and cancer with new tools and perspectives [2]. However, to reach such a goal, a well-described and characterized potentiostat system is needed, but many commercial potentiostats lack information about its circuit [10]. It turns this device into a "black box" bringing all kind the problems to those who are developing new measurement techniques.

All the potentiostat systems make the analyte detection through Redox reactions [7], [10], [12]. Those reaction takes place at the sensor surface driving the proper potentials. The key to detecting an analyte is the current measurement circuit sensibility. Without that component, it is impossible to know the Redox current. Also, the biosensors materials play a relevant role in the detection of analytes. However, this research focuses on the development of the electronic circuits and the software to drive Redox reactions.

The next sections deal with issues according to the following descriptions:

- State of the art presents a literature review of the last technology about wireless potentiostat instruments and some without wireless capabilities.
- The Problem Description explains the investigation opportunities where the project can provide a solution.
- The Objectives describes the goals of this research and the contribution to the scientific community.
- The Premises shows the investigation and the ideas that sustain the problem solution and the hypothesis.
- The Solution Overview presents the concepts to develop during the investigation and how the potentiostat system will be.
- The Hypothesis shows the ideas submitted to study. Thus, the investigation tries to approve it or reject it.
- The Methodology presents a set of steps to solve the problem and how to approve the hypothesis.
- The Scope and Limitations explain the parts that the investigation will not cover and the potentiostat system boundaries.

1.1 State of the Art

Potentiostats are taking advantage of microelectronics to provide with unique features. For example, Jafari et al. made a wireless electrochemical instrument with DNA analysis capabilities [13]. A highlight is the number of channels for current-to-digital recording, being 54. Also, the device has 54 pH sensors. The integrated circuit achieved is 3 mm x 3 mm in 0.13 µm standard CMOS technology. This kind of integration is called System-on-a-chip (SoC), and it has been used lately to build potentiostat systems [14], [15]. The linear range of the device comes from 350 nA and goes to 8.6 pA.

Two years after Jafari et al. [13], Dorta-Quiñones et al. used 65 nm CMOS technology getting an Integrated Circuit (IC) of 1.5 mm x 1.0 mm for dopamine detection in small animals [15]. Additionally, to the size enhancements, a hybrid Analog to Digital

Converter (ADC) was made. The idea behind of this electronic component is to delete the background current (measured without dopamine) of the resulting Reduction-Oxidation (Redox) reaction. The design has a power consumption of 30 μW for the whole device. Moreover, the area of the embedded device is of 4.7 cm x 1.9 cm making it suitable for embedded applications.

Dorta-Quiñones et al. recognize as an enhancement the use of a Delta-Sigma ($\Delta\sum$) converter [15]. However, Bozorgzadeh et al. had already used this strategy for the generation of neurochemical pattern *in vivo* [16]. The use of such converter brings significant advantages as good speed and resolution. Moreover, a 3rd-order $\Delta\sum$-Converter was chosen to be a middle point among system complexity, clock frequency, and power consumption. The improvement is in the input noise, where Dorta-Quiñones et al. got 92 pA, Bozorgzadeh et al. achieved 55 pA. Although, this enhancement will be greater if the design focus on noise reduction rather than power consumption.

Besides to the SoC technology, Programmable-System-on-a-Chip (PSoC) has been used to build wireless potentiostats [17]. Kim et al. utilized a PSoC 5LP from Cypress Semiconductor which is a flexible platform where all the hardware can be reconfigured. This feature sets the genuine possibility to build circuits beyond the potentiostat capacity. Moreover, there are several components ready to be implemented as ADC's, Digital to Analog Converters (DACs), Operational Amplifiers (OPAMPs), Pulse-Width Modulators (PWM), and so on. The research demonstrates the ability of the PSoC to be part of a full potentiostat system.

Nowadays, Dryden et al. had reached one of the lowest current detection limit (600 fA) in the literature [10]. That device can take 30,000 samples per second using one of the fastest ADC reported. The careful selection of the electronic components was a key to enhancing the potentiostat system performance. It has an analog multiplexor of 10 Ω for each channel in on mode, a $\Delta\sum$-Converter of 24 bits, a femtoampere input bias current for the Transimpedance Amplifier (TIA), and low offset rial-to-rial OPAMPs. Thus, the limits of detection drop drastically. However, the size of the Printed Circuit Board (PCB) and the lack of wireless data transmission are unwanted features for certain applications.

In the market, there are several potentiostat instruments. However, PalmSens has one of the smallest called EmStat [18]. This instrument has an area of 5.5 cm x 4.1 cm, turning it into an interesting option for embedded applications such a Lab-on-a-Disc and POCT. However, for wearable monitoring systems, the size could be an issue. Moreover, the device can execute nine electrochemical techniques with a range of detection from 100 mA to 1 pA. The main drawback of this device is the power consumption of 2.5 W and the price difference compared to homemade potentiostats.

Additionally to PalmSens, another company in the market sells a portable potentiostat [19]. However, the concept of portability depends on the application. For Lab-on-a-Disc, POCT, and wearable monitoring systems, this instrument is not good enough due to its big area (16.5 cm x 10 cm). On the bright side, the device has more electrochemical techniques than the EmStat with capabilities beyond of a potentiostat. Thus, someone can perform methods such Galvanostatic, Corrosion, Rotating Disk, Open Circuit Potential (OCP), and Spectroelectrochemistry without to have to use another instrument.

Recently, Sun et al. embedded a potentiostat system in a smartphone [2]. However, he went even further having as well Potentiometric, and Electrochemical Impedance Spectroscopy (EIS) circuits in a cellphone. This instrument has a limit of detection in the amperometric mode of 1 nA. The experiments confirm the capacity for monitor and diagnose diabetes through the glucose sensing. Moreover, the creation of applications in Android or iOS gives to the potentiostat the facility of being used for anyone who has access to a smartphone.

Also, some potentiostats have taken advantage of smartphones without being inside [20]. The idea is to have a remote device in contact with the electrochemical sensor. The communication for this case is by Bluetooth, and an Android application programmed in Java is employed for the user interface. The potentiostat relies on the open-source CheapStat [12]. However, the performance of this instrument falls short of other instruments because it uses relatively old technology.

Table 1 and Table 2 show several potentiostat characteristics. For smaller instruments, the power consumption decreases, as well the performance. Those instruments are commonly used with one or two electrochemical techniques. The efficiency in one or more features improves when the device space increase and the applications are wider. However, sacrifices in portability and power consumption are strictly necessary for those enhancements. Thus, the electronic design for a potentiostat system is always a trade-off between the instrument size and the performance.

Table 1 and Table 2 demonstrate that it is possible to build a potentiostat for applications as Lab-on-a-Disc, wearable monitoring systems, and POCT. This change takes place due to the advances in manufacturing microelectronics devices. However, the size restrictions of such applications decrease the performance of the device. If the applications for this research will not have space restrictions, we could have more components like a powerful a workstation. Though, the actual manufacturing techniques allow us to make a modest device given the size constraints.

1.2 Problem Description

When someone bought a potentiostat, the main disadvantage is the lack of information about the circuit by any supplier [10]. New electrochemical detection methodologies require this information for the manipulation of certain variables as the voltage waveforms. Thus, researchers have to adapt the methodologies under development to the available potentiostats in the market. Discoveries in the electrochemical field require flexible electronic platforms where the researcher can manipulate all the parameters. Therefore, new electrochemical instruments have to be developed to be highly customized.

The literature describes some homemade potentiostat systems [10]. They have an advantage its well-described circuit, but most of them are protected by copyrights. However, three of them are open source, and the researchers can use them for their investigations. The problem with those potentiostats shows up when they do not fit in some embedded applications, due to its size, current range, or accuracy [10], [12], [21]. Also, the available potentiostats lack wireless data transmission which is a very desirable feature for Lab-on-a-Disc, wearable monitoring systems, and POCT applications.

Table 1. Electrochemical Instruments Comparison.

Electrochemical Instrument	Jafari et al. [13]	Dorta-Quinones et al. [15]	Bozorgzadeh et al. [16]	Dryden et al. [10]
Highest Current Detection Limit	350 nA	430 nA	950 nA	22 mA
Lowest Current Detection Limit	8.6 pA	***	***	600 fA
Electronic Chip Area	3 mm x 3 mm	1.5 mm x 1.0 mm	3.16 mm x 3.16 mm	***
PCB Area	***	4.7 cm x 1.9 cm	***	8 cm x 8 cm
Maximum Samples Per Second	2 ksps	10 ksps	10 ksps	30 ksps
ADC Effective Number of Bits	9 bits	10.95 bits	***	21.3 bits at 1.45 ksps
Wireless Connectivity	Ultra-Wideband Transmitter	Ultra-Wideband Transmitter	FSK Transmission with Manchester Encoding	No
Number of Techniques Implemented	1	1	2	More than 3
Channels	54	1	1	1
SoC Present	Yes	Yes	Yes	No
Capabilities additional to a potentiostat	No	No	No	Yes
Maximum Power Consumption	1543.3 µW for each channel	30 µW	Approximately 0.4 mW	Less than 1 W

A basic electrochemical instrument for a potentiostat management will need three essential parts: a potentiostat system, a recording and display system, and a function generator [22]. However, the literature does not provide any information whatsoever about the last two parts. Mainly, the literature deals with the circuit issues making aside the algorithms for a complete electrochemical system. It brings all kind of problems to someone who is not familiar with electronics and software development.

Wireless potentiostats have relevant applications in POCT, Lab-on-a-Disc, and wearable monitoring systems [3], [4], [7]. Moreover, the transmission capabilities bring advantages in the field. One example is the elimination of the noisy slip-ring in Lab-on-a-

Disc applications [23]. Also, Bluetooth communication has been used, with advanced smartphones and electrochemical application [2], [20], [24]. However, detail explanations about the integration of the Bluetooth protocol are no common.

Table 2. Electrochemical Instruments Comparison (Continuation).

Electrochemical Instrument	EmStat 3+ Embedded / OEM [18]	WaveNow AFTP1 [19]	Sun et al. [2]	Giordano et al. [20]
Highest Current Detection Limit	100 mA	100 mA	200 uA	50 uA
Lowest Current Detection Limit	1 pA	80 nA	1 nA	100 nA
Electronic Chip Area	***	***	***	***
PCB Area	5.5 cm x 4.1 cm	16.5 cm x 10 cm	3.9 cm x 1.62 cm	9.7 x 5.7 cm
Maximum Samples Per Second	Less than 1 Ksps	1 Ksps	200 ksps	***
ADC Effective Number of Bits	***	***	***	***
Wireless Connectivity	Bluetooth or Wifi	No	No	Bluetooth
Number of Techniques Implemented	9	33	3	4
Channels	up to 16	1	2	1
SoC Present	***	***	No	No
Capabilities additional to a potentiostat	Yes	Yes	Yes	No
Maximum Power Consumption	2.5 W	10 W	111 mW	***

Most of the equivalent methods to the electrochemical techniques are high cost, they are not user-friendly, they lack rapid quantification, they require a careful treatment of samples, and a very skilled person needs to manage the instrument [25]–[31]. Thus, a potentiostat system can be used in implantable medical biosensors [32], clinical diagnosis [5], analyte detection [1], and pharmaceutical analysis [33] overcoming the explained issues. Moreover, all these benefits will lead us to develop instruments capable of monitoring a patient from home, saving time, effort, and money [2].

1.3 Objectives

The objective of this research is to provide a well-characterized potentiostat using new embedded technology with the capacity of being easily scalable. This information will allow the researchers to know the instrument and make the appropriate modifications to suit their specific needs. Moreover, the description of the potentiostat system components, besides of the potentiostat, will present the basis of a functional instrument capable of performing electrochemical experiments.

The research outcome is a potentiostat instrument prototype with the capacity of being modifiable at hardware and software levels. The current detection limits have to be on the scale of nanoampere. Also, the device will have methods as Double Step Chronoamperometry (DSC), Linear Sweep Voltammetry (LSV), and Cyclic Voltammetry (CV), because of their capacity to get relevant electrochemical data [34]. Likewise, the prototype will have a program with a function generator and a recording and display system. Thus, the researchers and engineers will have an idea to start making a complete potentiostat instrument.

The capacity of the instrument to be embedded in watches and rotating disk are highly desirable. Hence, the potentiostat system must have wireless communication capabilities. That feature will turn it suitable for applications where the potentiostat cannot be physically connected to the user interface. Also, size and cost must be kept as low as possible. Moreover, the system needs to prove its functionality by making the identification of some analyte. Furthermore, this research has to determinate the working range of the prototype. The specific objectives of this investigation are:

- Provide a low cost and low size hardware design for a potentiostat system.
- Explain of the potentiostat system components.
- Describe the electronic circuits for a potentiostat system.
- Develop a device with a sensitivity in the nA scale for the Redox current measurements.
- Develop algorithms for the function generator considering the waveform of the electrochemical techniques mentioned.
- Include a data logger for the electrochemical experiments.
- Design a user-friendly interface.
- Develop a wireless protocol for the data transmission.
- Reduce noise using software and hardware techniques.
- Detect some analyte to prove the hardware, software, and wireless functionality of the device.
- Compare test results against a commercial potentiostat.
- Determination of the working range of the potentiostat developed.
- Demonstrate the feasibility and features of the instrument.
- Review and visualize applications for the prototype.

The main contribution of the thesis is the analysis of several potentiostat circuits and the current measurements strategies to read the Redox reaction. Also, it explains the effects of the ADC and DAC features in the potentiostat system. Moreover, another contribution is the use of new technology like Programmable-System-on-a-Chip (PSoC)

and the Programmable-Radio-on-Chip (PRoC) to explore the feasibility of these ICs to make potentiostat systems for embedded applications. Thus, those issues will provide the innovation to this research.

1.4 Premises

Today, new IC are available in the market providing advanced features and tools to the designers [35]. The integration of analog and digital hardware in one chip is part of the technological advances [36]. This kind of integration is known as a SoC, and it can manipulate analog and digital signals in the same IC. Moreover, researchers have been taking SoC approach recently to address their investigation [14], [37]–[39]. The main advantages of the SoC technology are moderate accuracy, portability, small size, and low cost.

The PRoC and the PSoC have all the advantages of a SoC, and they have reconfigurable features [40]. A PSoC is a general platform where electronic devices like ADC, OPAMPs, configurable digital filters, DAC, timers, counters, and PWM are in one single chip [41]. A PRoC is like a PSoC, but it focuses on wireless transmissions. Moreover, the reconfigurable features of both SoC let us test several configurations. Thus, someone can change the design until the application matches the research objectives.

Moreover, the PSoC technology has already been using to build a wireless electrochemical instrument [17]. In this case, Kim developed a real-time neurochemical prototype for brain activity observation. The device showed aptitudes for dopamine measurements through an amperometry method. However, the potentiostat system can use another approach to improving its performance. Also, the design needs more trials to probe the PSoC capabilities as a potentiostat instrument.

LabVIEW (Laboratory Virtual Instrument Engineering Workbench) is a programming language developed by National Instruments [42]. This language relies on graphical programming. Engineers commonly use this software for measurements, instrumentation control, test, automation, data acquisition, and data analysis applications. Moreover, LabVIEW has been suggested and employed in applications to take advantage of the PSoC technology [37], [38]. Also, this language has been used to program some potentiostats systems [43]–[45]. Hence, it is going to be used to develop the prototype.

Nowadays, the firmware generates the waveforms in the new embedded potentiostat applications [2], [10], [20]. One effective way to develop any program is using design patterns. The State Machine design pattern is highly acceptable by programmers because its implementation is very flexible and easy to follow [46]. Also, the modularity of the pattern makes feasible the additions of states to implement more electrochemical methods in a given device. Thus, the State Machine is an excellent choice to have a friendly firmware because it is very explicit.

In embedded potentiostat applications as in many others, the user interface performance is a relevant aspect. The Producer/Consumer design pattern shows good features for data acquisition, and in this case, the data is the Redox current [47]. This pattern is very helpful because the designer can have a process to collect the data and

another one to display it. Therefore, the task division allows us to have an efficient program and a user interface responsive to events.

1.5 Solution Overview

Figure 1 shows a possible solution to have a highly customized potentiostat system for applications like Lab-on-a-Disc, wearable monitoring systems, and POCT. The idea is to have an embedded system small enough to meet the application requirements. In this case, the PSoC and the PRoC have shown their worth [17], [40], [41]. The interface system will use LabVIEW in a computer to deal with the user because of its good features [37], [38], [43], [45]. The communications between computer and PSoC is wireless. The scalability of the system takes place using pattern designs at the software level. Thus, the design can address the problems explained in sections behind.
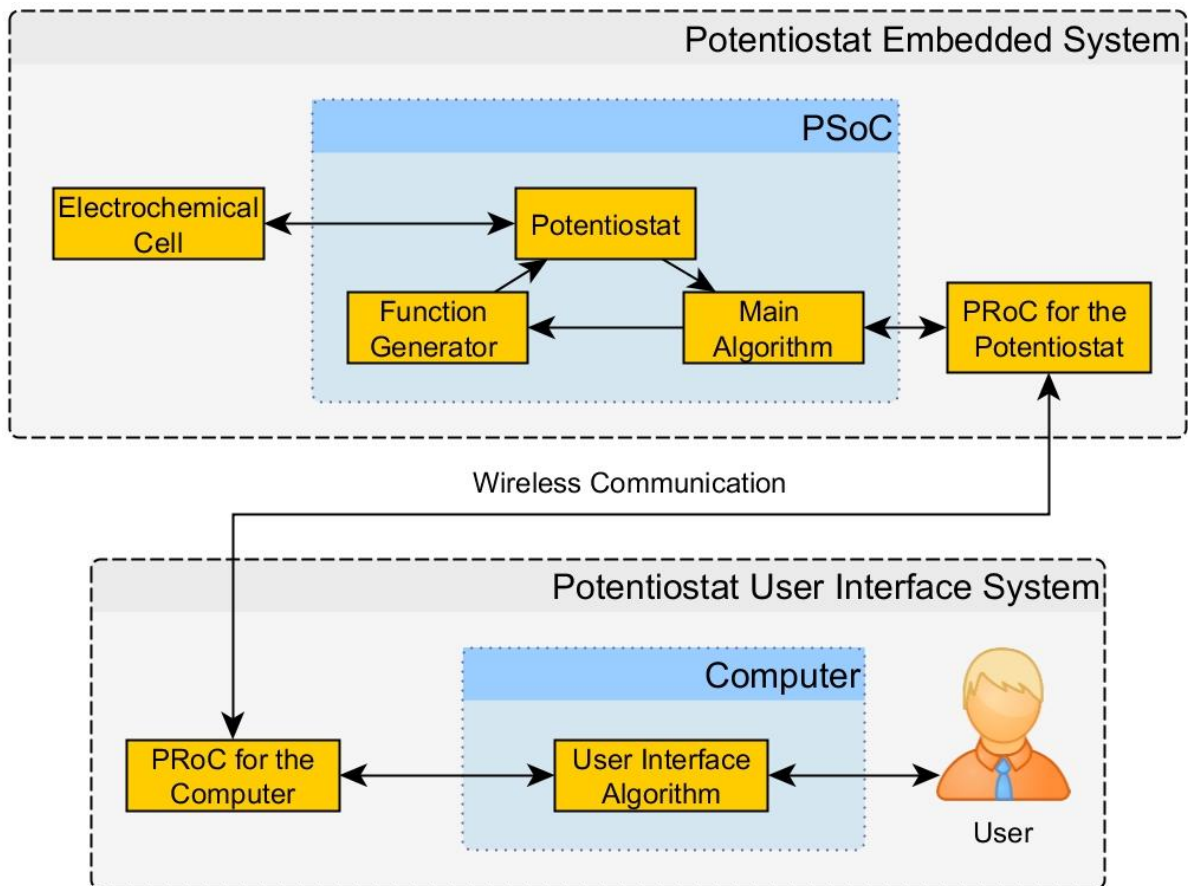
Figure 1. Solution Overview.

The PSoC can handle analog and digital signals in the same chip [40], [41]. Thus, it can hold a digital function generator and the analog circuit of the potentiostat system. Moreover, the PSoC microcontroller can have a firmware based on a pattern design like a State Machine. Hence, several issues can be addressed in a single chip allowing to keep the prototype size low. Therefore, it is a good idea to use this electronic device in the potentiostat system prototype.

9

The computer needs a clear interface system for the user. There are many programs to do that. However, LabVIEW has remarkable features in data acquisition, and analysis besides the controls and indicator for the user interface creation [37], [38], [43], [45]. Moreover, someone can use pattern designs in LabVIEW as well to improve the performance and the scalability of the prototype. The Producer/Consumer design pattern shows good features for data acquisition [47]. Thus, the computer software can use this pattern and the State Machine to have an efficient program for the potentiostat system.

1.6 Hypothesis

This research consists of developing a specialized potentiostat system. Also, it focuses on embedded applications such a Lab-on-a-Disc, POCT, and wearable sensors. Thus, the instrument needs to make wireless transmission to communicate with the recording and display system using new technology. Hence, the following questions are going to be the object of study:

1. Can the PSoC work as a potentiostat embedded system with a digital function generator for the waveforms of the electrochemical techniques?
2. Can a State Machine design pattern for the PSoC main algorithm perform Double Step Chronoamperometry, Linear Sweep Voltammetry and, Cyclic Voltammetry experiments?
3. Can the prototype reach a current sensing capability in the nanoampere range where relevant applications take place?
4. Can the PSoC and the PRoC technology address the size requirements for embedded applications such a Lab-on-a-Disc, POCT, and wearable monitoring systems?
5. Can the cost of the resulting prototype system be competitive with similar instruments in the market?
6. Can a State Machine and a Producer/Consumer design pattern address the basic functionality of a user interface for a potentiostat management in LabVIEW?
7. Can PRoC technology transmit all the information of the experiments from the potentiostat embedded system to a computer in a wireless manner?

The previous questions pretend to prove the following hypothesis:

1. The PSoC can generate several waveforms in a single chip to keep the potentiostat system size low.

2. A State Machine design pattern is a good approach to develop efficient firmware for potentiostat systems.

3. The PSoC can reach limits of detection in the nanoampere range where relevant applications for potentiostat systems can be developed.

4. The PSoC and the PRoC can hold a potentiostat system small enough to be embedded in applications such Lab-on-a-Disc, POCT, and wearable monitoring systems.

5. The potentiostat electronic system can be affordable for people who need special equipment in the house or wear monitoring devices.

6. A State Machine and a Producer/Consumer design pattern is a good approach to develop a user interface for potentiostat systems.

7. The PRoC technology can deal with the all the data traffic from the PSoC to the computer.

1.7 Methodology

The following steps are going to take place in this research to reach the objectives and approve or reject the hypothesis:

1. Description of the potentiostat system in a general way with all its components to have a complete view of the electronic system.
2. Description of the electrochemical techniques that a potentiostat system can perform to know the prototype capacity to carry out electrochemical experiments.
3. Description of several potentiostat circuits with their equations and their advantages to choosing the best circuit for the prototype.
4. Description of the Randles Cell to make simulations for the potentiostat circuits.
5. Simulations of the potentiostat circuits to know the performance of each circuit.
6. Description of the OPAMP features for a potentiostat circuit.
7. Description of several Current-to-Voltage Converters with its equations and its advantages to choosing the best for the prototype.
8. Simulation of the Current-to-Voltage Converters to know the performance of each converter.
9. Description of the OPAMP features for the Current-to-Voltage Converters.
10. Description of the ADC effects in a potentiostat system to make a selection for the prototype.
11. Description of the DAC effects in a potentiostat system to make a selection for the prototype.
12. Develop a Basic Potentiostat System to implement it in the prototype based on the simulations and the ADC and DAC effects.
13. Description of a suitable embedded architecture to develop the prototype.
14. Description of the PSoC and PRoC to know the ICs capacity.
15. Description of the Master/Slave design pattern to know its advantages in the prototype.
16. Slave design to develop the embedded device.
17. Master design to develop the user interface.
18. Description of the waveforms for the LSV, CV, and DSC experiments to implement them in the prototype.
19. Implementation of the analog and digital circuits in the PSoC to have a potentiostat embedded system.
20. Development and implementation of the PSoC firmware to generate the waveforms and deal with the Master commands.
21. Development and implementation of the wireless communication protocol to interchange information inside of the system.
22. Development and implementation of the interface system to communicate with the user.

23. Development and implementation of the user interface algorithm to control the slave.
24. Description of the prototype scalability to implement more electrochemical techniques.
25. Measurement of the reference voltage to make any adjustment necessary. Also, this measurement allows the programmable gain amplifier characterization.
26. Determination of the potentiostat capacity to supply current to a Redox reaction and the potential range.
27. Recording of three LSV waveforms with different parameters in an oscilloscope. Thus, hypothesis one is accepted if the waveforms are consistent with the parameters for this technique.
28. Recording of three CV waveforms with different parameters in an oscilloscope. Thus, hypothesis one is accepted if the waveforms are consistent with the parameters for this technique.
29. Recording of three DSC waveforms with different parameters in an oscilloscope. Thus, hypothesis one is accepted if the waveforms are consistent with the parameters for this technique.
30. Current measurement circuit characterization to know the real resistor values inside of the PSoC and measure the output offset voltage.
31. ADC characterization to compensate its offset voltage and its gain.
32. Measurement of the power consumption of the slave system.
33. Description of all the compensations in the user interface algorithm.
34. Description of the electrochemical cell design, the analyte, the electrolyte, and the electrodes for the Redox experiments.
35. Description of the materials, solutions, and procedures for the Redox experiments.
36. Experimental design to evaluate the potentiostat performance. Also, this design has some experiments where the wireless data traffic is as high as possible to probe hypothesis seven.
37. Presentation of the electrochemical result comparing the prototype with a commercial potentiostat system like some researchers has been done [2], [10], [20]. This comparison allows us to probe hypothesis two and six.
38. Analysis of the electrochemical results taken as reference the current values from the commercial instrument. This comparison will describe in a quantitative way how far is the prototype measurements from that instrument.
39. Explanation of the electrochemical results to establish the limitations of the prototype system.
40. Description of the possible size of the embedded system to review applications for the prototype system to probe hypothesis four.
41. Description of the cost of the embedded system to review applications for the prototype system to probe hypothesis five.
42. Description of the possible applications for the prototype system.
43. Review of the objectives.
44. Review of the hypothesis.
45. Description of the enhancements to the prototype and future work.

1.8 Scopes and Limitations

The scope of this research is just for making a prototype, and an end device will not take place. Thus, the researchers will have to adapt the instrument to their investigation because of the different necessities of each one. However, a complete report of the potentiostat system performance will be done. Also, Cyclic Voltammetry, Linear Sweep Voltammetry, and Double Step Chronoamperometry are going to be the only electrochemical techniques programmed in the prototype.

Moreover, the potentiostat hardware can execute certain trials in the prototype because it can only condition the electrodes voltage. Thus, this device cannot perform any other measurements out of the capacity of the potentiostat. Also, the instrument does not make ohmic compensation because there is no such a goal in the objectives. The PSoC 5LP family constrains the electronics components because the investigation is also about the capacity of this IC of being an electrochemical instrument. Just the wireless module will be as an external because it is vital for the applications.

Besides to the prototype development, a PCB area estimation will be done for a comparison in hypothesis four. However, the elaboration of the PCB is out of the scope of this research. Moreover, the user interface has just the purpose of handling the potentiostat system by showing the collected data and saving it into a file. Thus, this program cannot perform any treatment or analysis of the electrochemical information, and it has to take place in another software.

1.9 Thesis Organization.

Chapter one introduces the reader to the investigation describing the problematic situation, state of the art, the objectives, and the contribution to the scientific community. Also, it presents a possible solution for the issues founded. Moreover, chapter one states the research limitation and how to test the hypotheses.

Chapter two introduces the analog circuits of the potentiostat system. It covers several potentiostat circuits, the Redox current measurements, and the Analog-to-Digital and Digital-to-Analog conversion. Moreover, the chapter has some simulation to show the difference between the circuits presented.

Chapter three explains everything about the potentiostat system creation. It describes the embedded architecture of the electronic platform selected. Also, it provides a general view of the whole system. Then, it explains the specific issues about the implementation using schematics and flows charts. Finally, it illustrates the capacity of the system to be customizable.

Chapter four describes the hardware characterization and the advantage of this. It analysis the control of the potentiostat voltage and provides an equation to make adjustments to the Redox current. Moreover, it explains about the energy consumption and the changes in the software to make the compensation.

Chapter five presents all the electrochemical trials to validate the functionality of the potentiostat system. It gives more details about the materials and the solutions. Also, the chapter contains the design of the chemical experiments and the procedures.

Furthermore, a result analysis in this chapter illustrates the working range of the prototype and its capabilities.

Chapter six provides an interpretation of the results, and it declares how the hypotheses were accepted or rejected as well. Also, it describes the objectives accomplished in this dissertation and the possible applications of the prototype. Furthermore, it gives ideas to make enhancements, and it suggests a possible continuation of this work.

Chapter 2. A Basic Potentiostat System.

This chapter deals with all the hardware behind of the construction of the potentiostat system. It provides a description of the electronic components and the advantages or disadvantages of certain circuits to control the voltage and read the current. Also, it describes the effects of the converters Analog-to-Digital and Digital-to-Analog (ADC and DAC) in the system. Moreover, the reader needs a background in electrochemistry to get a better comprehension of the EC models. Thus, it is important to know about circuit theory, electronic design with OPAMPs, digital signal processing, ADCs, DACs, and Redox reactions at electrodes.

This chapter gives more information about the following points presented in the methodology:

1. Description of the potentiostat system in a general way with all its components to have a complete view of the electronic system.
2. Description of the electrochemical techniques that a potentiostat system can perform to know the prototype capacity to carry out electrochemical experiments.
3. Description of several potentiostat circuits with their equations and their advantages to choosing the best circuit for the prototype.
4. Description of the Randles Cell to make simulations for the potentiostat circuits.
5. Simulations of the potentiostat circuits to know the performance of each circuit.
6. Description of the OPAMP features for a potentiostat circuit.
7. Description of several Current-to-Voltage Converters with its equations and its advantages to choosing the best for the prototype.
8. Simulation of the Current-to-Voltage Converters to know the performance of each converter.
9. Description of the OPAMP features for the Current-to-Voltage Converters.
10. Description of the ADC effects in a potentiostat system to make a selection for the prototype.
11. Description of the DAC effects in a potentiostat system to make a selection for the prototype.
12. Develop a Basic Potentiostat System to implement it in the prototype based on the simulations and the ADC and DAC effects.

2.1 Potentiostat Overview

Sometimes, definitions as simple, basic, and full potentiostat system may be different if someone reads several books and investigations about this instrument [10], [22], [48], [49]. Thus, the following definitions are valid for this research, and they are congruent with Figure 2:

- **Potentiostat.** This circuit provides the current for the Redox reaction, and it keeps a potential difference between WE and RE according to a control signal at the input of the potentiostat [49].
- **Basic Potentiostat System.** Most of the time, the intention of a potentiostat system is to control the voltage to measure the Redox current [48]. Also, nowadays the devices record the data and generate the waveforms digitally

[22]. Hence, a basic potentiostat system needs to have a circuit to measure the current and digital data management for the communication of the computer with the analog variables.

- **Full Potentiostat System.** This system completes the Basic Potentiostat System with a function generator, and a recording and display system. Thus, the outcome is an electronic device capable of getting relevant electrochemical information making some trials.

A potentiostat is an electrochemical instrument responsible for controlling the potential in an EC [48]. Mainly, scientist and engineers use this instrument to work with the three-electrode cell [22]. Sometimes, a person can confuse this instrument with a galvanostat or with a hybrid between them. However, they differ a lot in the circuits. A potentiostat fixes the voltage to get current values while a galvanostat changes the current to measure the voltage. Also, the potentiostat functionality is just for controlling the voltage, and it does not have a circuit to measure the current [49]. Thus, this device conditions the WE vs. RE potential according to a control signal.

The potentiostat can perform the following electrochemical techniques with stirred or unstirred solutions [50]:

- Chronoamperometry.
- Chronocoulometry.
- Sampled Current Voltammetry.
- Differential Pulse Voltammetry.
- Square Wave Voltammetry.
- Anodic Stripping Voltammetry.
- Double Step Chronoamperometry.
- Double Potential Step Chronocoulometry.
- Linear Sweep Voltammetry.
- Cyclic Voltammetry.

If someone needs to use another technique, that person has to find the proper hardware to carry out.

A potentiostat instrument needs at least a basic potentiostat system, a function generator, and a recording and display system to perform controlled Redox reactions [22]. Figure 2 shows that the potentiostat is one part of major systems. This circuit and the nearby electronics determinate the limit of the detection and quantification. The potentiostat digitalization capabilities and the recorder system determinate the number of Samples Per Second (SPS). Thus, the designer needs a careful potentiostat design to take advantage of the last technology.

A potentiostat by itself just control the potential in an EC [49], and more electronic components are necessary to get more information about the electrochemical phenomenon. Figure 2 shows the nearby potentiostat electronic components. The DAC provides the control signal for the potentiostat. The current measurement circuit reads the electrons flow from the Redox reaction. The ADC turns the analog current values in digital. Thus, the Basic Potentiostat System defines the performance of the entire instrument as we shall see in the rest of the chapter.

The Full Potentiostat System completes the Basic one with more components to have a useful instrument in Figure 2 [22]. The function generator can give the waveform values in an analog or digital way. However, a computer generates the digital signals most of the time. Also, the recorder system has to handle digital values because it is the

easiest way to save data. The display system can be any device capable of showing information. Though, one of the fastest is a screen. Hence, all these components and the Basic Potentiostat System let us have a complete device to perform some experiments.
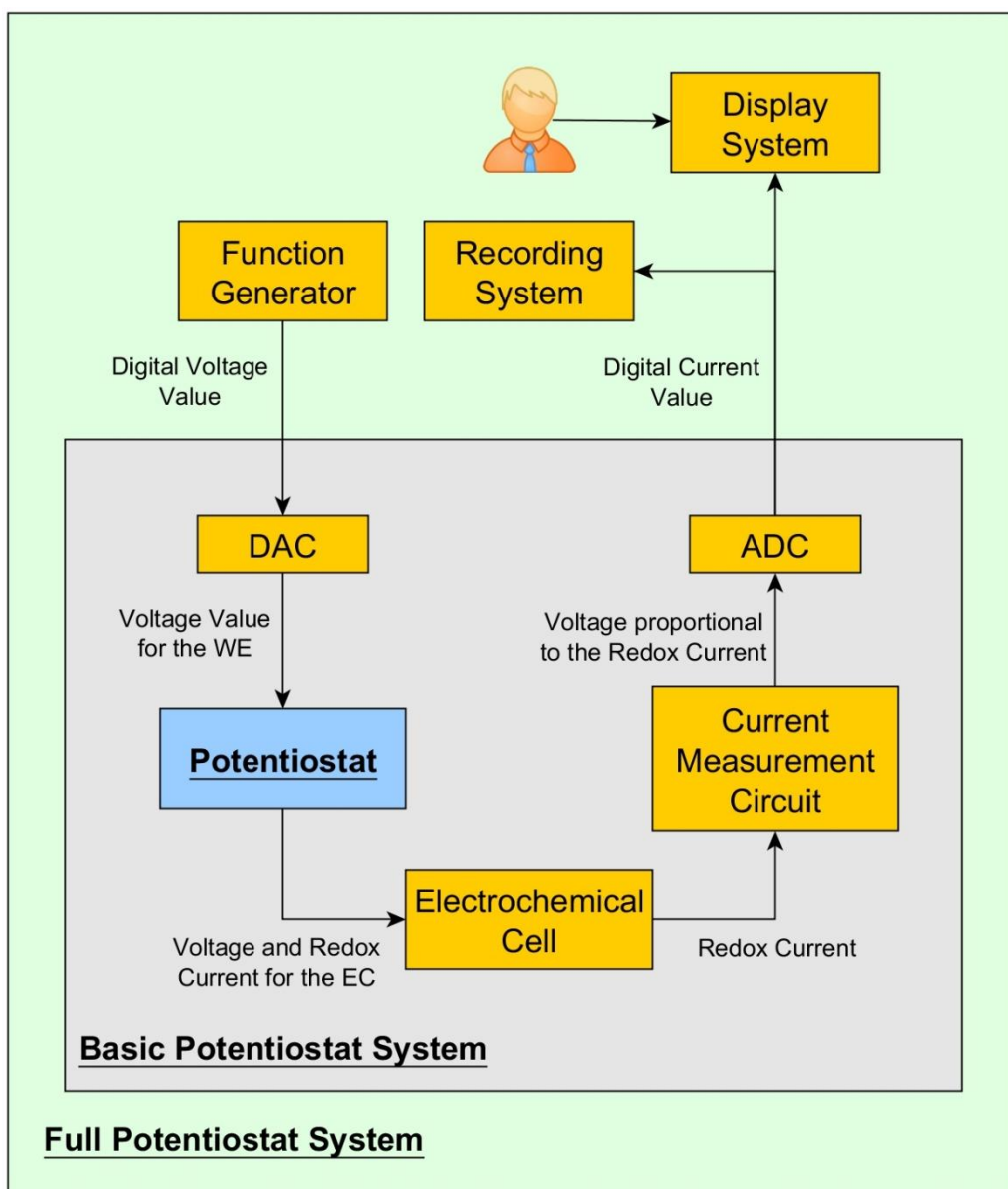
Figure 2. Potentiostat and the relationship with the electronic components.

The following sections of this chapter explain the Basic Potentiostat System. These sections require special attention because it defines the instrument capacity. Therefore, this chapter gives more information about potentiostats and current measurement circuits. Also, the last section describes the Analog-to-Digital and Digital-to-Analog converters with its effects in the device. The next chapter covers the Full Potentiostat System.

2.2 Potentiostat Circuits

The main issue with a potentiostat is to control the WE voltage (Vwe) accurately [10]. Thus, this device needs a Three-Electrode cell to achieve it as Figure 7 shows. The advantage of this cell is that the RE is not vulnerable to polarization errors, and the WE can be close to the RE to reduce measurement errors. In this cell, the CE is responsible for supply the current to the Redox reaction, the RE controls the WE voltage, and the electrochemical phenomenon takes place on the WE surface. Hence, this section presents three different circuits to choose the best for the applications mentioned.

2.2.1 Simple Potentiostat Circuit

Figure 3 presents one of the simplest circuits to make a potentiostat [10]. The Voff terminal can be ground or an offset voltage. The OPAMP U1 supplies the current to the Redox reaction, and its features impose the maximum current for it. Also, it is necessary to watch the voltage output of the OPAMP because it can reach saturation if the cell resistance or the current is too high (Ohms law). Hence, the OPAMP output has to be inside of an operational range to keep the desired voltage in the EC according to the control signal.
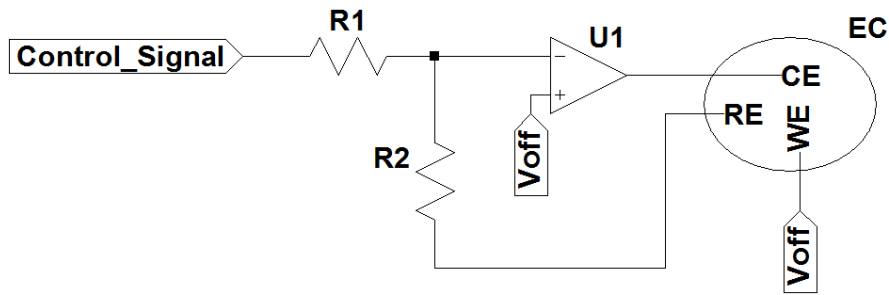
Figure 3. Simple Potentiostat Circuit [10].

The Kirchhoff and Ohms law let us calculate the voltage at the RE according to the following assumptions. Figure 4 is a representation of the R1 and R2 resistors from Figure 3 with an 'R' value for each one. U1 connects virtually the resistors to Voff. Vcs makes reference to the control signal voltage and Vre to the RE voltage. Because Vcs is an input signal, the current i1 goes to the node n1. Thus, i2 goes out of node n1 due to the OPAMP is considered as an ideal and no current flows to it.
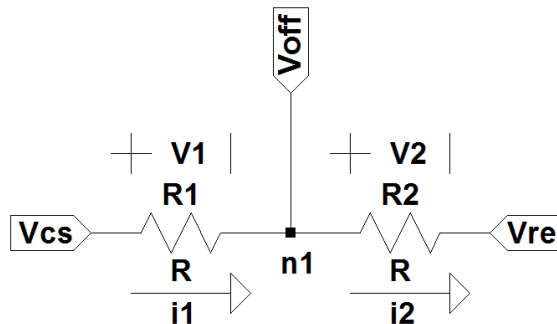
Figure 4. Schematic representation for the RE voltage calculation.

18

The polarization sign of V1 and V2 from Figure 4 are according to the current direction. A positive sign applies where the current gets into the resistor. Hence, a negative sign applies where the current gets out of the resistor. Equations 2.1 and 2.2 show the Kirchhoff law with different variables. The equation 2.3 shows the relation between Vcs, V1, V2, and Vre. Thus, the Vre vs. Voff is the negative potential of the Vcs vs. Voff. However, the WE vs. RE voltage is the same as the control signal vs. Voff because the WE is connected to the Voff terminal in Figure 3.

$$i1 = i2 \qquad\qquad\qquad 2.1$$

$$\frac{V1}{R} = \frac{V2}{R} \qquad\qquad\qquad 2.2$$

$$Vcs - Voff = V1 = V2 = -(Vre - Voff) = Vwe - Vre \qquad\qquad 2.3$$

The Kirchhoff analysis shows that the potentiostat manipulates the RE voltage to set WE voltage. Also, this analysis demonstrates one of the problems of the Simple Potentiostat Circuit (SPC). In Figure 3, the current through R2 reduces the power available for the Redox reaction because it comes from the OPAMP U1 [10]. Furthermore, R1 and R2 are low values most of the time to reduce thermal noise. However, it increases the electrons flow through the R2. Hence, the designer can use an Advanced Potentiostat Circuit (APC) to solve this issue.

2.2.2 Advanced Potentiostat Circuit

The APC adds an OPAMP to the SPC to have the schematic of Figure 5 [10]. This change brings different considerations to the circuit. Now, OPAMP U2 supplies the RE voltage and the current to R2 instead of U1 as in the SPC. The previous Kirchhoff analysis is still valid. However, the Vre terminal now arrives at the inverting input of U2 and its output instead of being connected to the RE. U2 assures no current flow from U1 to R2. Thus, the OPAMP U1 power is just for the Redox reaction in the APC. The relationship between the Vcs and the WE vs. RE voltage is still the same of the SPC (Equation 2.4).

$$Vcs - Voff = Vwe - Vre \qquad\qquad\qquad 2.4$$
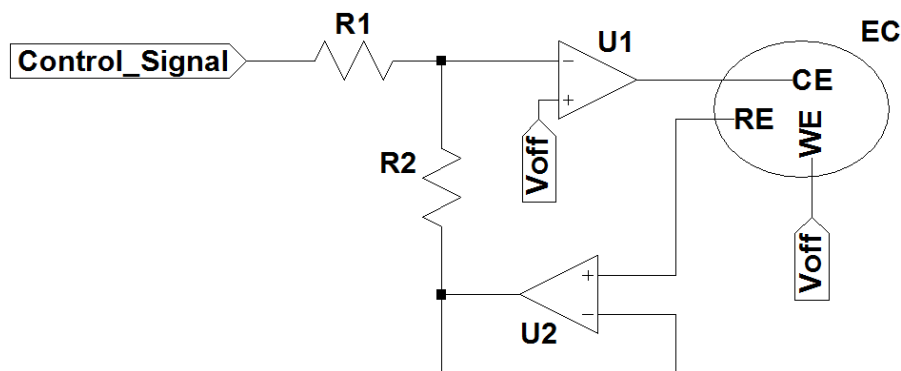
Figure 5. Advanced Potentiostat Circuit [10].

2.2.3 Follower Potentiostat Circuit

Figure 6 presents a Follower Potentiostat Circuit (FPC) for the voltage control in an EC [51]. The WE has the Voff potential to make a relationship between the Vcs vs. Voff and the WE vs. RE according to Equation 2.5. Also, this circuit does not have any resistor and just one OPAMP making the easiest to build. The high impedance of the OPAMP U1 at its inputs reduces polarization errors making better than the SPC in this aspect. One of the drawbacks of the FPC is the stability and the dynamic response [52]. Moreover, it needs summing point in the non-inverting terminal of U1 to have more input signals.

$$Vcs - Voff = Vre - Voff = -(Vwe - Vre) \qquad 2.5$$

The OPAMP U1 provides the Vcs virtually to the RE in the FPC (Figure 6). However, there is always a small potential difference at the inputs of every OPAMP called Input Offset Voltage (Vos) [53]. The easiest way to fix this problem is compensating the Vos through software. Thus, the designer needs to program the function generator to make the proper arithmetic correction. Another way to compensate the Vos is creating a summing point in the FPC with the Vos value. However, it increases the circuit complexity. Furthermore, it is not necessary to make a compensation if the Vos is negligible.
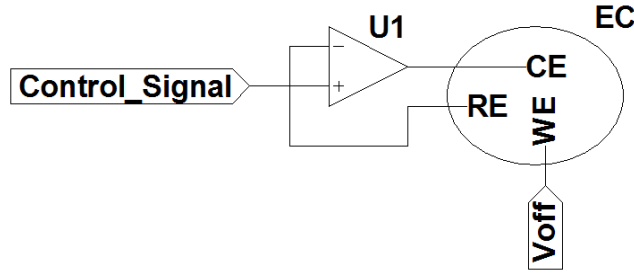
Figure 6. Follower Potentiostat Circuit [51].

2.2.4 Electric representation of an Electrochemical Cell

Researchers and engineers commonly use the three-electrode cell of Figure 7 for their experiments especially when the solution resistance is high [50], [54]. This arrangement shows accuracy improvements at the voltage and current measurements from those taken with the two-electrode cell (Figure 7). This advantage is due to the addition of a CE where most of the current flows. Thus, the RE keeps a very stable voltage in the solution because the current through this electrode is worthless.

A network of electronic components as impedances, resistors, and capacitors can model the behavior of an EC [49]. Figure 8 represents the three-electrode cell with impedances and resistors. Zc and Zwk make reference to the interfacial impedances at the respective electrodes [22]. Ru represents the uncompensated resistor while Rc the compensated resistor. Also, the distance between electrodes and the solution conductivity determinate the value of each resistor. Moreover, the presence of Ru in the solution is highly undesirable. Hence, someone can improve the cell design to keep Ru as low as possible.

The regular Randles cell of Figure 9 gives a more detail circuit between the RE and the WE [55]. This representation is very useful to understand the phenomenon from an electrical point of view [49]. There is no representation of between CE and RE because at the CE is inert most of the times [50]. The regular Randles cell represents an irreversible electrode process where no diffusion limit exists, and a single-step Redox reaction happens. It means that the Faradic process can be simplified to a resistor (R2). This model is not best for electrochemical analysis. However, it is very useful for simulation and tests.
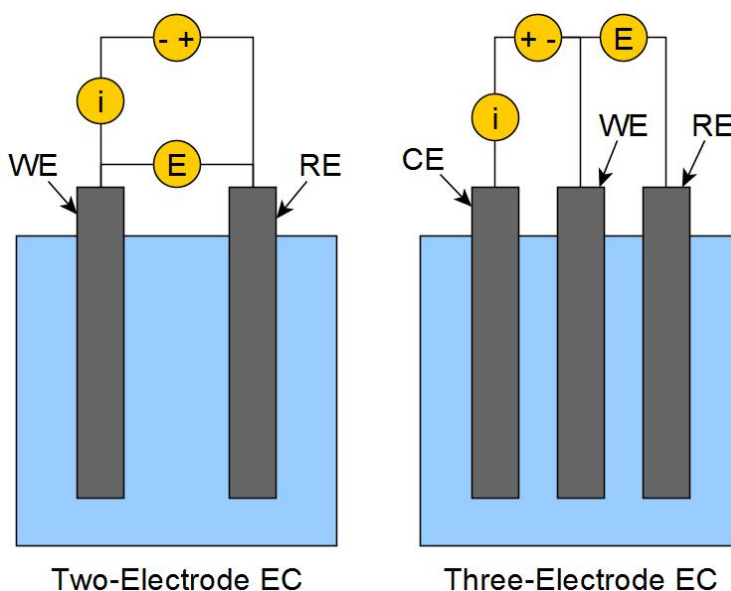
Figure 7. Schematic representation of two EC designs [50].

The regular Randles circuit is one of the simplest representation of the Redox phenomenon through resistors, and capacitors [22], [55]. The components of this model have a direct relationship with the physical variables. In Figure 9, R1 describes the resistance between WE and RE, R2 describes the charge-transfer resistance, and C1 describes the double layer capacitance. Thus, the Randles circuit is suitable to make some simulations and comparisons between potentiostats as we shall see in the next subsection.
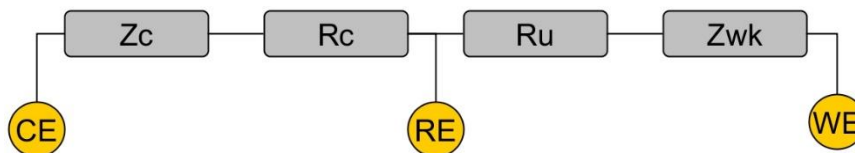
Figure 8. Three-Electrode cell as an impedance network [22].

Gamry Instruments provides the values for the Randles circuit in Figure 10 (dummy cell) [56]. That company recommends these values to check the performance of the instrument. There is no need for a complex representation between RE and CE due to an interest reaction does not take place between them normally [50], and the potentiostat compensates that resistor [22]. The relevant values here are R1 and R2 because they represent the current to supply by the potentiostat. C1 has no effect in a steady-state

simulation. Hence, R2 and R1 are well suited to watch the accuracy of the different circuits without force the OPAMP output.
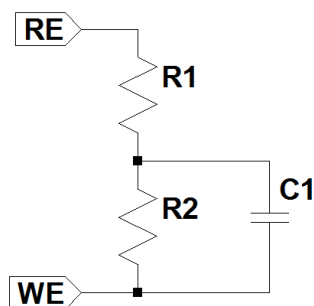
Figure 9. Randles circuit between RE and WE.
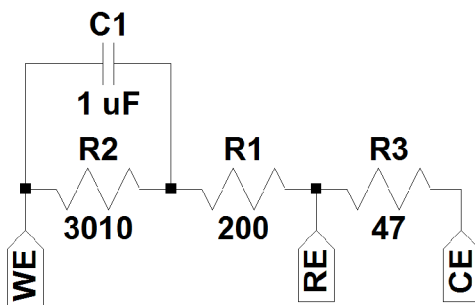
Figure 10. Randles circuit from Gamry Instruments for the Three-Electrode Cell [56].

2.2.5 Potentiostats Circuit Simulations

The simulations of the potentiostat circuits from Figure 11, Figure 12, and Figure 13 show the accuracy of each circuit to control the WE vs. RE potential and the capacity to provide current to the Redox reaction. However, the simulation conditions have to be carefully watched to the results be comparable. Thus, the same software needs to perform the tests with the proper values for the passive elements in each circuit. The only changes allowed came from the different circuit arrangements. Hence, these conditions assure congruent conclusions for the potentiostats.

The potentiostats circuits share several voltage values and an analog component. Dryden et al. suggest the use of the OPAMP LMP7702 in this instrument due to its good features [10]. A bipolar supply powers all potentiostats with ±5 volts and Gamry Instruments provides the Randles circuit values [56]. The Voff is set to ground, and the Vcs value is of one volt for all the circuits. TINA software version 9.3.150.4 SF-TI distributed by Texas Instruments carries out all the simulations. Hence, the different currents and voltages values from the simulations obey to the features of each potentiostat.

The results for the SPC and the APC are minus one volt at the RE and one volt at WE vs. RE in Figure 11 and Figure 12. However, the current supply of the CE for each circuit is not equal. The OPAMP U1 provides -378.22 µA to R3 in the SPC while U1 delivers -311.54 µA to R3 in the APC. The current disagreement corresponds to Vcs/R2, and it is around of 66.667 µA in this case. Thus, the APC can provide more current to the Redox reaction than the SPC because the OPAMP U2 supply the current to R2.

Nowadays, modern instruments rely on the APC and it is going to be used for the prototype construction in this research [22].
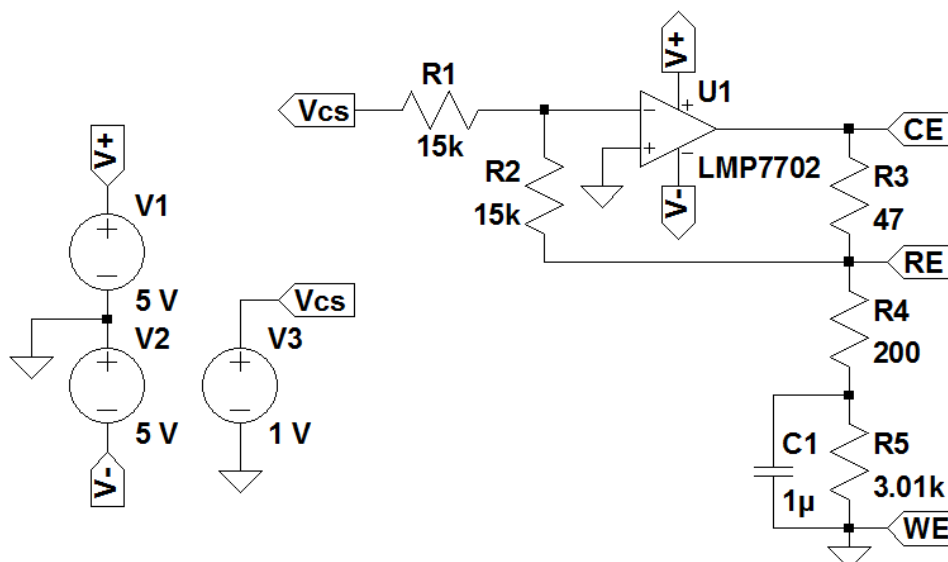
Figure 11. Schematic diagram for the simulation of the Simple Potentiostat Circuit.
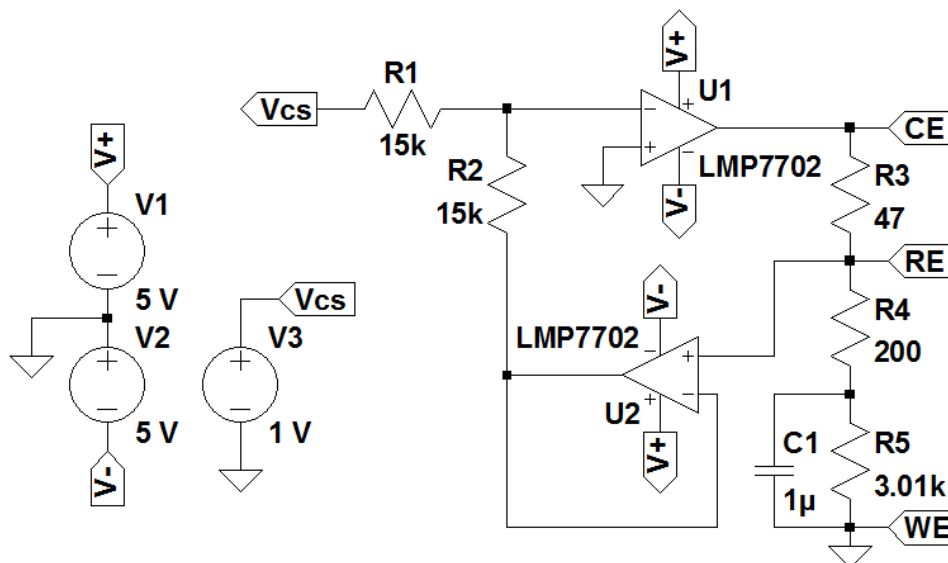
Figure 12. Schematic diagram for the simulation of the Advanced Potentiostat Circuit.

The results of the APC and the FPC are very similar in the current values from Table 3. However, there is a slight difference in the voltage accuracy. The Vos is of 40 μV in the simulation of the FPC from Figure 13. Though, the Vre is practically the Vcs (one volt). This Vos is just valid using this OPAMP; another device can have a different outcome. The advantage of the APC is its voltage accuracy, and the relationship between the Vcs and the WE vs. RE is straightforward. However, someone can choose the FPC due to its simplicity when the Vos is neglectable.

Table 3 summarizes the potentiostats simulations results for voltage and current variables. The APC and the SPC are the most accurate controlling the EC potential. However, the CE current is not totally for the Redox reaction in the SPC because it has

to supply some energy to the circuit. The FPC with the LMP7702 shows remarkable features and a behavior practically like the APC. However, there is a small error in the voltage at the WE vs. RE, and it always is going to depend on how big is the Vos. Thus, the designer has to consider these differences to choose a potentiostat for a certain application.
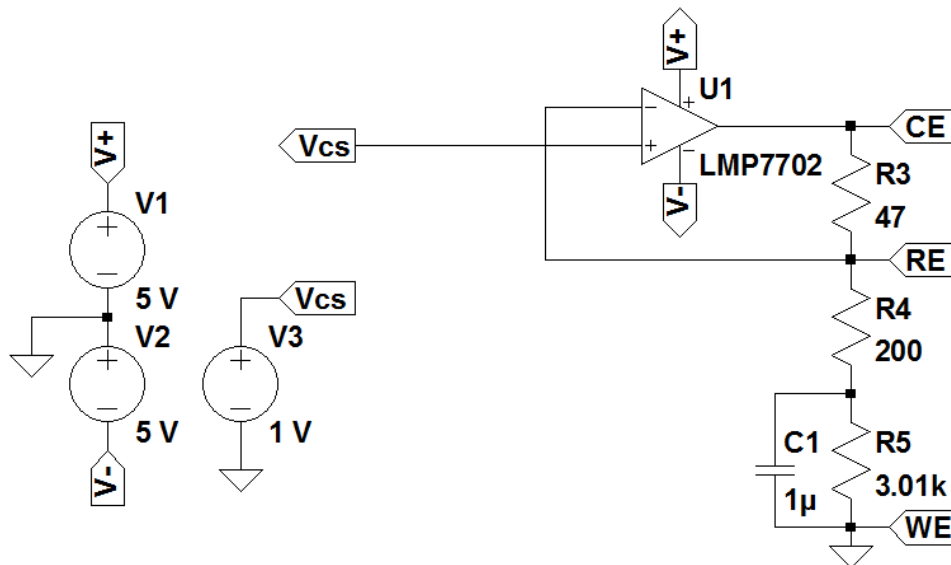
Figure 13. Schematic diagram for the simulation of the Follower Potentiostat Circuit.

Table 3. Simulation results of the Potentiostats.

	SPC.	APC.	FPC.
Real WE vs. RE voltage.	1 V	1 V	-1 V
Measure WE vs. RE voltage.	1 V	1 V	-999.96 mV
WE vs. RE voltage error.	0.0 %	0.0 %	0.004%
CE Current.	-378.22 µA	-311.54 µA	311.51 µA
Redox Reaction Current.	-311.55 µA	-311.54 µA	311.51 µA
CE Current for the Reaction.	82.373 %	100 %	100 %

2.2.6 Potentiostat Circuit Features

Certain OPAMP features are suitable for an optimum circuit performance in a potentiostat. Devices with low input bias currents are very helpful to keep minimum polarization errors [10]. The closed loop gain error of the amplifier has to be low to establish a precise control of the potential. Thus, the OPAMP needs huge open loop gains to achieve it. Moreover, the noise density and the input offset voltage of the OPAMP must be low as well. Table 4 shows some of the OPAMPs features for the potentiostat built by Dryden et al. in their research.

The OPAMP bandwidth should be according to the potentiostat purpose [10]. The amplifier needs bandwidths of several megahertz if the potentiostat performs fast scanning experiments as those presented in EIS trials. However, few hundred of kilohertz may be right if the rate of the scanning is not fast. Also, the power consumption and the size of the electronic components need to be as low as possible when an embedded

application is under development. With all this in mind, the designer can accomplish a good circuit design.

Table 4. Some OPAMP features for the potentiostat built by Dryden [10].

	LMP7702 [57]	**LMP7721** [58]
Input Offset Voltage.	±200 µV Maximum	±180 µV Maximum
Input Bias Current.	±1 pA Maximum at 25°C	±20 fA Maximum at 25°C
Input Voltage Noise.	9 nV/√Hz at 1 kHz	6.5 nV/√Hz at 1 kHz
CMRR.	130 dB	100 dB
Open-Loop Gain.	130 dB	120 dB
Gain Bandwidth.	2.5 MHz	17 MHz
Supply Current.	1.5 mA	1.3 mA
Supply Voltage Range.	2.7 V to 12 V	1.8 V to 5.5 V
Rail-to-Rail I/O.	Yes	Yes
OPAMPs Number	2	1

2.3 Current-to-Voltage Converters

Most of the times it is not enough the potential control in an EC. Thus, the instrument has to measure the Redox current to know more about the phenomenon [10]. Modern potentiostat relies on digital data making use of ADC. However, not all the ADCs can handle currents directly, and instead, they use analog voltage values to digitize. Normally, this instrument turns the current in a voltage using a current-to-voltage converter (I-V converter) to get digital values of the Redox reaction [1], [12], [22], [59]. This section exposes five circuits with the capacity of convert current in a potential.

2.3.1 Shunt Resistor

Figure 14 presents the simplest way to measure the Redox current using a shunt resistor between CE and the OPAMP U1 out [60]. The current through the shunt resistor makes a voltage drop according to Ohms law. This potential is proportional to the Redox current just for the FPC and the APC according to the Equation 2.6 [10]. The designer should avoid the SPC (Figure 3) because the current flow through R2 is not part of the reaction and it comes from the CE as well. Also, someone can use this technique over any range of currents. Hence, the suitable potentiostats for the shunt resistor strategy are the FPC and the APC.

$$V_{R1} = R1 * I_{Redox}$$ 2.6

The shunt resistor has several disadvantages. The voltage drop at R1 (Figure 14) is not referenced to the ground [10]. Thus, the ADC must have differential inputs, or R3 will need an instrument amplifier at its terminals. However, add more components to the measurement is not desirable. Also, R1 reduce the capacity of the OPAMP U1 to provide voltage because it forms a tension divider with the EC. Furthermore, the shunt resistor can be noisy sometimes, and it will need a capacitor to reduce it. However, this affects the circuit bandwidth.
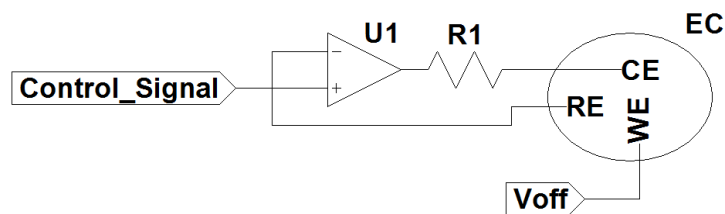
Figure 14. Follower Potentiostat Circuit with a Shunt Resistor (R1).

2.3.2 Transimpedance Amplifier

The Transimpedance Amplifier (TIA) of Figure 15 is an I-V converter, and it solves two main problems from the shunt resistor strategy [10], [61]. The OPAMP U3 eliminates the voltage divider. Thus, the energy for the current measurement comes now from this amplifier letting to U1 supply all its voltage to the Redox reaction. Also, U3 has just one output terminal, and it is referenced to ground according to the Equation 2.7. Thus, the OPAMP U3 makes this circuit more suitable than the shunt resistor for current-to-voltage conversions.

$$V_{U3\_out} = -R3 * I_{Re\,dox} + Voff \qquad\qquad 2.7$$

The TIA and the shut resistor share the gain factor of the respective resistors (R1 and R3). However, they are different in the potential sign because the U3_out terminal is in a negative feedback through R3 (Figure 15). The issue of having one resistor as a gain factor shows up when someone needs unrealistic values for the amplification of ultra-low currents [61]. Thus, high-sensitivity circuits allow keeping the resistors values inside of the commercials. Another drawback of the TIA is its susceptibility to the noise, and it has stabilization issues [51], [62].
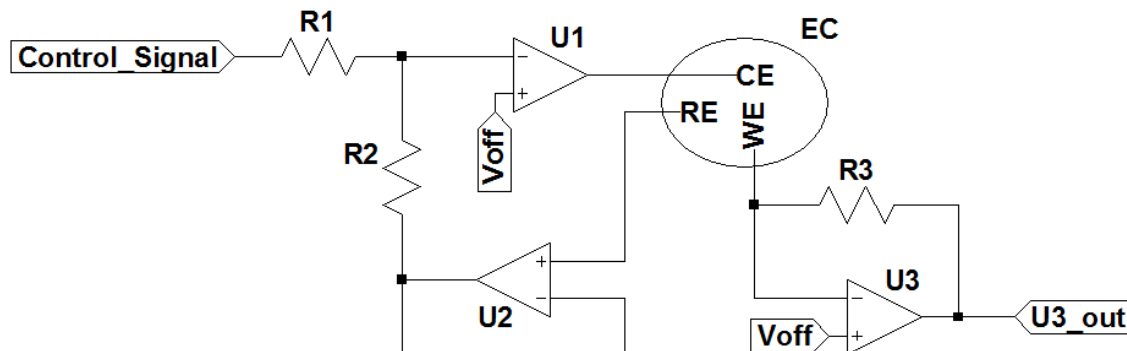
Figure 15. Advanced Potentiostat Circuit with a Transimpedance Amplifier [22].

2.3.3 I-V converter with Two OPAMPs

Figure 16 presents Two OPAMPs for high-sensitivity current measurements [51]. OPAMP U2 provides a factor of amplification R3/R2 (extra sensitivity) while U3 keeps a polarization voltage near to zero for the WE if R3/R2 is equal to R5/R4. This circuit, according to Souto, is more stable than the TIA. However, it is evident the active element (U3) in the feedback. Thus, the designer should do a careful analysis of the circuit to avoid any stability problems during the steady-state operation. The Equation 2.8 shows the voltage output of the circuit.

$$V_{U2\_out} = I_{Re\,dox}R1 * R3 / R2 \qquad\qquad 2.8$$
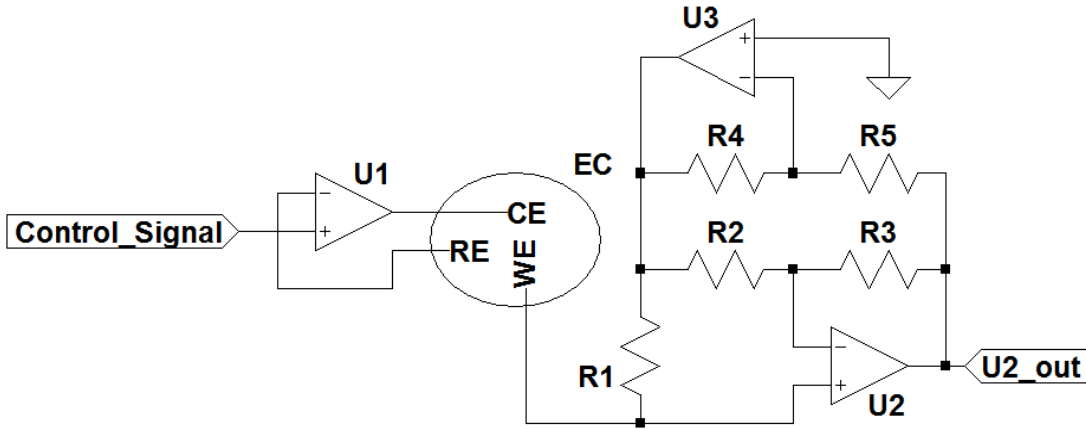
Figure 16. Follower Potentiostat with Two OPAMPs for I-V conversion.

2.3.4 High-Sensitivity I-V converter

Another circuit for ultra-low current detection is the High-Sensitivity I-V converter [61]. This circuit adds two resistors to the classic TIA converter presented in Figure 15 forming the T-network in Figure 17 (R5, R4, R3 with U3,). In the Equation 2.10, the gain 'k' provides the extra sensitivity for the current measurements in the Equation 2.9. However, the price to pay for this sensitivity is the accuracy loss. In this circuit, the designer needs to watch the input bias current, and it has to be much lower than current to detect to avoid any measurements mistakes.

$$V_{U3\_out} = -k * R3 * I_{Redox} + Voff \qquad\qquad 2.9$$

$$k = 1 + R4 / R5 + R4 / R3 \qquad\qquad 2.10$$
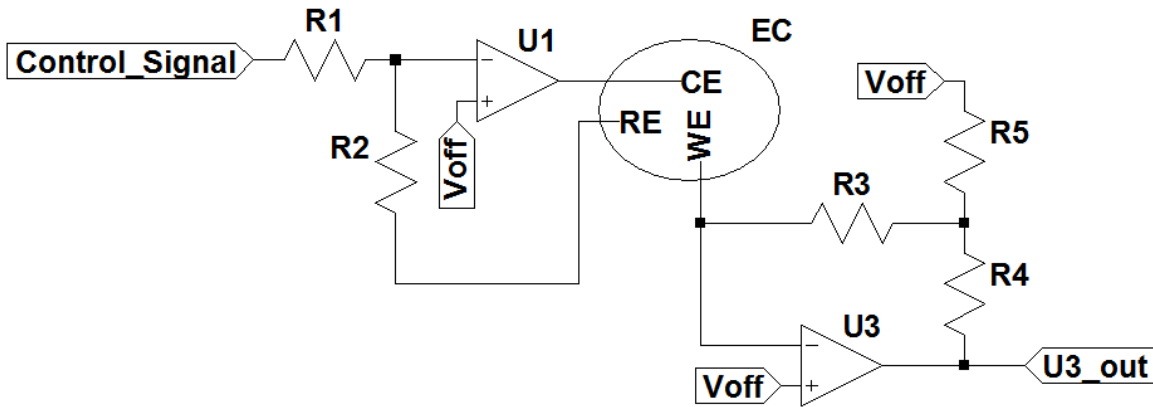
Figure 17. Simple Potentiostat with a High-Sensitivity I-V converter.

2.3.5 Capacitive Feedback

The High-Sensitivity I-V converters sacrifice accuracy by sensitivity [61]. Thus, if someone wants ultra-low current detection and accuracy, the designer needs the Integrator Amplifier of Figure 18 [63]. The Integrator Amplifier strategy is suitable when the currents to detect are below of 100 pA. The circuit, eliminate the problem of the

thermal noise in the resistors because it uses a capacitor in the negative feedback. This strategy relies on measuring the voltage change over the time to calculate the current according to the Equation 2.11.

$$I_{Re\,dox} = C_1 \frac{d(V_{U3\_out} - Voff)}{dt} \qquad\qquad 2.11$$

A computer needs the Equation 2.11 discretized to work with digital values. The good side of this process is that the capacitor makes an average of the incoming electrons every sample period reducing noise. However, this strategy imposes more complexity than any other circuit because the device needs two voltage values to get one measurement. Another drawback shows up when a constant current flow to the capacitor making the OPAMP gets saturation. Thus, the circuit needs a discharge method for the capacitor to solve this problem increasing the complexity even more.
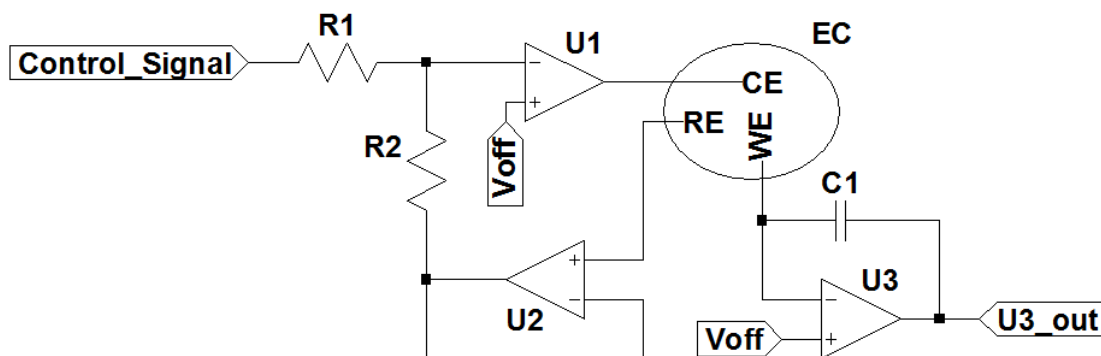
Figure 18. Advanced Potentiostat Circuit with an Integrator Amplifier.

2.3.6 Current Measurement Simulations

The simulations of the current measurement circuits from Figure 19, Figure 20, and Figure 21 show the accuracy of each circuit. With this, the difference between circuits is going to be quantitative. However, the Shunt Resistor strategy and the Capacitive Feedback were not simulated, one for having several disfavors, and the other one for being too complex. The rest of the I-V converters have the proper values in the simulation to the results be comparable. The only changes allowed come from the different circuit arrangements. Hence, these conditions assure congruent conclusions for the current measurement circuits.

These simulations share several voltage values and an analog component. Dryden suggests the use of the OPAMP LMP7721 from Texas Instrument to make the I-V conversion due to its good features [10]. A bipolar supply powers all circuits with ±5 volts and a current source represent the Redox reaction with a fixed value of 10 nA. The gain for every circuit is of 100 M. TINA software version 9.3.150.4 SF-TI distributed by Texas Instruments performs all the simulations as before. Hence, the different errors correspond to the circuit accuracy.

The high-sensitivity converters show the biggest errors according to Table 5. The High-Sensitivity I-V converter has an error of 3.249 % while the I-V converter with Two OPAMPs has 4.0 %. The TIA converter has just an error of 0.044%, and it can be reduced

even more through a proper characterization. Thus, the TIA circuit is the most accurate of the I-V converter. Also, this circuit can reach a limit of detection of 600 fA with a proper ADC [10]. Hence, TIA converter is the most suitable to make the prototype instrument.
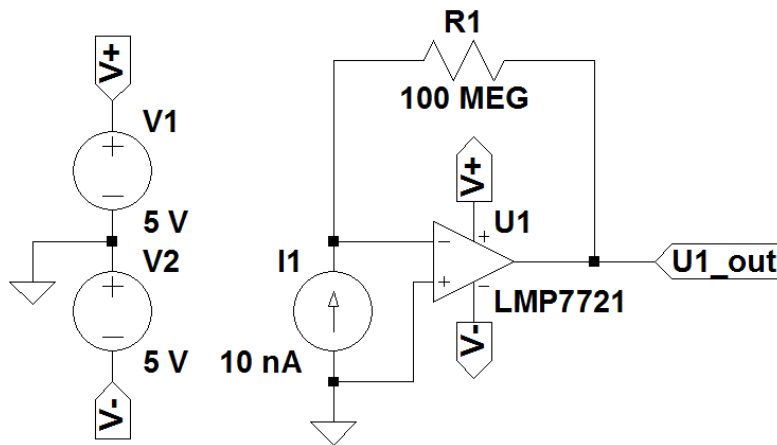
Figure 19. Schematic diagram for the simulation of the TIA converter.
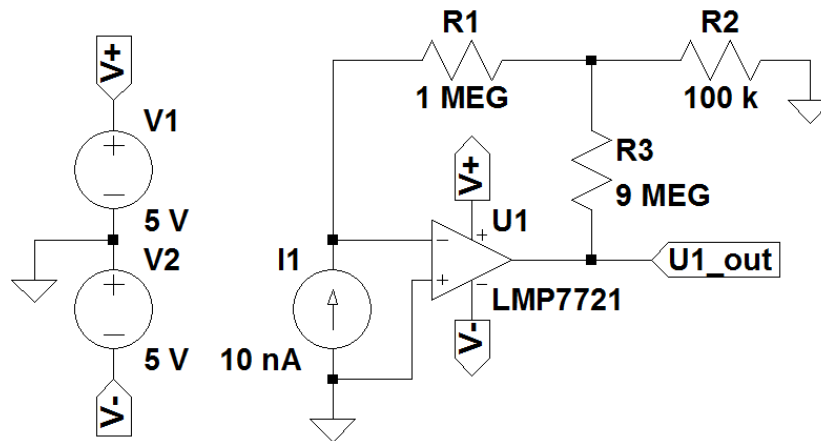
Figure 20. Schematic diagram for the simulation of the High-Sensitivity I-V converter.

The High-Sensitivity I-V converter is a little bit more accurate than the I-V converter with Two OPAMPs. Also, it is the simplest of the High-Sensitivity circuits. Hence, when the resistor value for the TIA circuit is not for sale, the designer should use the High-Sensitivity I-V converter for the applications of this research. However, the Integrator Amplifier and the High-Sensitivity circuits detect ultra-low currents in the same range. Thus, someone can choose and Integrator Amplifier due to its accuracy.

Table 5. Simulation results of some I-V converters.

	Measure Value.	Real Value.	Error.
TIA converter.	-999.56 mV	-1 V	0.044%
High-Sensitivity I-V converter.	-967.51 mV	-1 V	3.249%
I-V converter with Two OPAMPs.	1040.00 mV	1 V	4.0 %

Table 6 summarizes the I-V converters features. The designer can use the shunt resistor for currents above of 1µA when the voltage supply and floating measurements

are not a problem [60]. The TIA is suitable for low current detection caring the resistor values and the input bias current. The High-Sensitivity I-V converter or the I-V converter with Two OPAMPs are helpful when the values of the resistors for the TIA become unavailable, or when the designer wants to avoid the Integrator Amplifier complexity. Finally, the Capacitive Feedback is worthy for ultra-low current sensing where the accuracy is a concern.
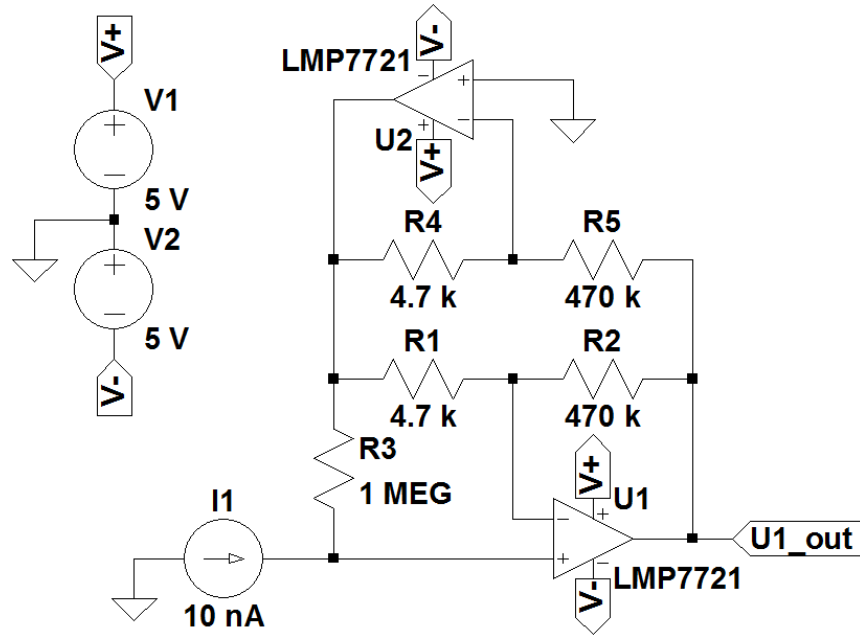
Figure 21. Schematic diagram for the simulation of the I-V converter with Two OPAMPs.

Table 6. Principal features of the I-V converters.

	Shunt Resistor.	TIA.	I-V converter with Two OPAMPs.	High-Sensitivity I-V converter.	Capacitive Feedback.
Floating Measurement.	Yes	No	No	No	No
Low current detection.	Yes	Yes	Yes	Yes	No
Ultra-low current detection.	No	No	Yes	Yes	Yes
Gain of one resistor.	Yes	Yes	No	No	No
High complexity.	No	No	Yes	No	Yes
Good Accuracy.	Yes	Yes	No	No	Yes

2.3.7 OPAMP Features and Signal Quality for I-V converters

The most relevant characteristic of the OPAMP is the input bias current when someone designs a low and ultra-low current detection system [10]. The bias current is the current that goes into the OPAMP at its inputs [53]. Ideally, this electron flow should

be zero, but the reality is different. In a Redox reaction, part of the current gets into the OPAMP as part of the conversion of every I-V converter. However, the key to keeping trustworthy information about the phenomenon is that the current to detect be much greater than the bias current.

Let us consider the OPAMP LM741 of Figure 22 from Texas Instruments with a maximum input bias current of 500 nA [64]. If someone tries to make a TIA for 100 nA detection, a significant part of the current will flow to the OPAMP inwards. Hence, the measurement through the TIA resistor will be wrong. TINA software performs the simulation of the schematic as before. This test shows that the OPAMP inverting input sinks more than the capacity of the current source. Thus, the OPAMP itself has to supply some current through its feedback leading to an error above of 100%. The exact values of the simulation are in Table 7.
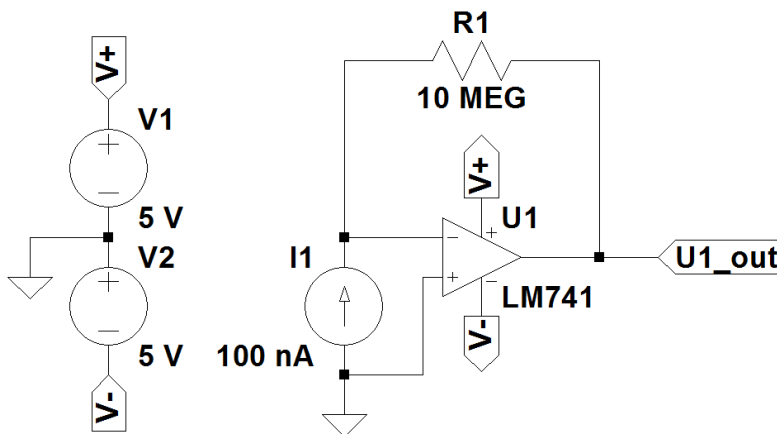
Figure 22. Schematic diagram for the simulation of the TIA converter with the LM741 from Texas Instrument.

This research does not provide information about analog filters because there are plenty in the literature [65]. However, the potentiostat designer needs to keep a good quality of the current signal. The SNR (Signal-to-Noise Ratio) describes how big the signal against the noise is. Hence, the measurements are accurate when the SNR is high. Analog filters cut down the noise improving the SNR. However, the main filter drawback is the bandwidth reduction. Thus, the potentiostat designer needs a good comprehension of filtering to choose the best for the application.

Table 7. Some simulation results of Figure 22.

	Value.	Reference.
TIA output voltage Real.	-1 V	Ground
TIA output voltage Measured.	19.67 mV	Ground
TIA Error voltage.	101.967%	Real Value
OPAMP Inverting Input Current.	101.87 nA	Direction to the Inverting Input
R1 Current.	1.87 nA	Direction to the Inverting Input

Someone can create simple filter adding a capacitor in parallel to the TIA resistor of Figure 19 taking place to the schematic of Figure 23. This addition increases the SNR in a wide range of frequencies according to Figure 24. TINA software performs the

simulation as before with bipolar supply of ±5 volts and the LMP7721. Thus, the simulation illustrates the SNR improvement with a simple analog filter. However, with a more sophisticated filter, the ratio can be even better.
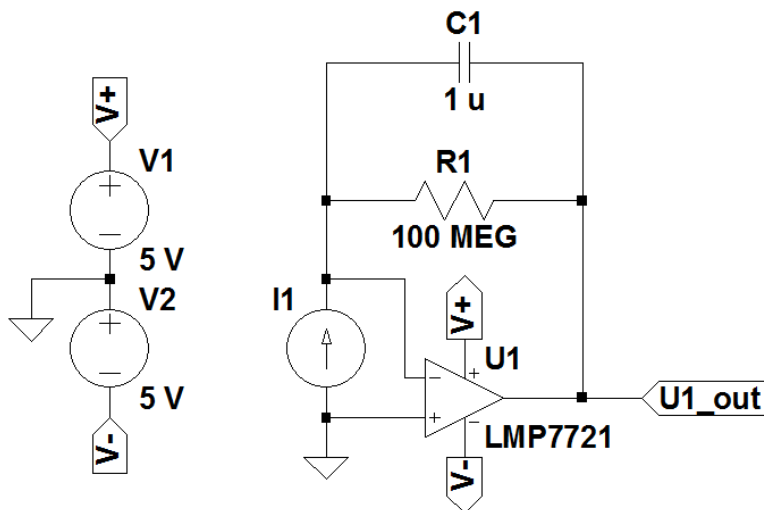
Figure 23. Schematic diagram of the TIA with a filter for the simulation of the SNR.
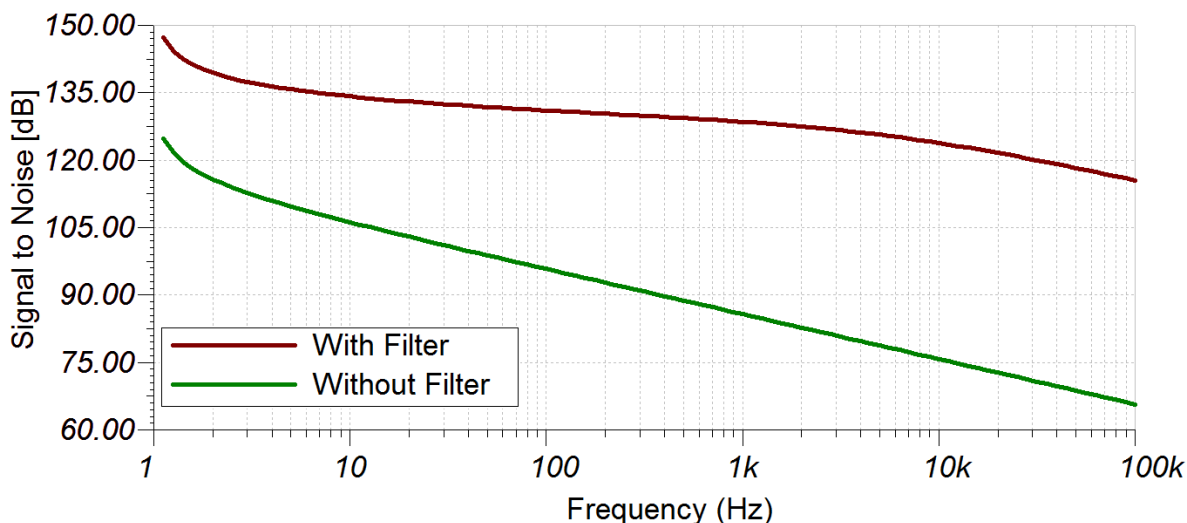
Figure 24. SNR of the TIA converter with filter and without it.

2.4 Digital Signals in a Basic Potentiostat System

Today digital signals are widely used everywhere, and the potentiostats are part of that progress [22]. A Redox reaction delivers analog currents but modern potentiostat use microcontrollers at some point to make a Full Potentiostat System [10]. Thus, the microcontroller needs ADCs and DACs to communicate with the analog world. Both converters determinate factors as sample rate, quantitation limit, and data size in a Basic Potentiostat System.

2.4.1 Analog-to-Digital Converter and Current Measurements

The ADC is the responsible for transforming the analog values of the current to a digital in a Basic Potentiostat System. The main features of this component are the conversion speed and resolution [10]. When the resolution of ADC is high, a huge number of quantization levels are available allowing measurements with more sensitivity (Table 8). However, the RMS noise value at the ADC input limits its resolution. Thus, a good practice is to record some noise in the ADC and get rid of it through digital or software filters to get the lowest limits of detection in a potentiostat system.

The ADC conversion speed and the SPS describe the amount of time between samples [10]. Depending on the application and its purpose, the conversion speed can be fast or slow. An electronic system cannot recover the original signal if aliasing takes place [66]. Thus, the ADC can record as maximum half of the sampling frequency avoiding aliasing in this way according to the Nyquist criterion. The ADC can use an alias filter to stop frequencies above this criterion. Moreover, an electronic system can get a better quality of the signal if the SPS are greater than two times the signal bandwidth. This process is called oversampling [67].

The noise-free bits and the effective resolution in ADC describe how accurate is the converter [68]. Most of the ADCs generate some noise during the conversion process. This noise degrades the converter outcome. The effective resolution expresses the number of bits not affected by the RMS noise value of the ADC. The noise-free bits express the number of bits without any ADC noise. Thus, it is a good practice to look up for this data when someone is designing a potentiostat system.

One of the highest resolution available in the market is the 24-bit ADC of the type Delta-Sigma ($\Delta\sum$) [10]. This kind of converters use a $\Delta\sum$ modulator to reduce noise at low frequencies, and a digital filter called sinc filter [69], [70]. The $\Delta\sum$ converter has a good tradeoff between performance and silicon area. Also, most of these converters provide different samples rates. However, faster conversions are noisier than the slowest. Hence, the designer can choose the proper speed conversion with this ADC to have precise information or record fast signals.

It is usual that 24-bits $\Delta\sum$ ADC can achieve more than 20 noise-free bits. It means over a million of quantization levels without the ADC noise [70]. Let us consider a converter with an input range of ±1.024 volts and 20 noise-free bits with the TIA of Figure 19. It implies that the Least Significant Bit (LSB) has a value of 19.5 fA. Also, the maximum quantization error is ±0.5*LSB [71], and for this case, that value is ±9.8 fA. Therefore, all the data in a range of ±195.3 fA is irrelevant for a measurement with an accuracy above of 95%. These calculi do not take into account the noise at the ADC input. However, an electronic system can measure ultra-low currents when the quantization levels are high.

Table 8 shows the effects of changing the ADC number of bits for the TIA converter of Figure 19. The calculus is for a converter with an input range of ±1.024 volts, and they just take into account the ADC quantization error. The LSB is in amperes because the TIA allows establishing the relationship. Therefore, the noise-free bits of the ADC impose the limit of detection and not the number of bits of the ADC. According to the table, the addition of one bit to the ADC noise-free bits reduces its detection limit by half of the

converter detection limit without this bit. Thus, the designer should choose an ADC with the highest number of noise-free bits to reduce the limit of detection.

Table 8. Limit of detection varying the ADC number of bits for the TIA of Figure 19.

ADC	LSB Value	Quantization Error	Inaccurate Data Range (below 95%)
20-bits	19.53 fA	±9.77 fA	±195.31 fA
16-bits	312.50 fA	±156.25 fA	±3.13 pA
12-bits	5.00 pA	±2.5 pA	±50.01 pA
8-bits	80.31 pA	±40.16 pA	±803.14 pA

2.4.2 Digital-to-Analog Converter and the Potentiostat

In a Basic Potentiostat System, the DAC provides the control signal voltage to the potentiostat [10]. Before of the digital revolution, analog circuits created the waveforms for this device. However, it was very complex when the user needed to perform several techniques because the designer had to add an especial circuit for each waveform. Nowadays, an algorithm generates the signals for each electrochemical method, and a DAC takes the waveforms to the analog world saving space in a PCB.

The DAC, as the ADC, bring some constraints to the potentiostat system operation. The DAC resolution determinates the smallest potential change at the WE, and the half of that value determinates the maximum quantization error. Let us consider a range from zero to five volts and a DAC with eight bits of resolution. In this case, the maximum quantization error will be around ±10 mV. Hence, the Redox reaction voltage cannot be accurate control because of the poor resolution of the converter.

The DAC converting rate describes how fast the potentiostat changes values at the WE [10]. The designer chooses this value depending on the speed of the electrochemical application. Also, half of the converting rate determinate the maximum frequency that a DAC can deliver at its output to make a signal properly. A reconstruction filter is commonly used to have a better quality of the control signal. This filter is a low-pass filter with a cut-off frequency according to the Nyquist criterion. Likewise, the designer needs to make a careful design of this filter to reduce as much as possible the shift phase errors.

The best way to improve the signal quality in a DAC is having a sampling frequency much higher than the maximum frequency at the DAC output [10]. It results in a reconstruction filter design more feasible because the bandwidth between the sampling frequency and the maximum output frequency is wider with oversampling. However, electrochemical step techniques require fast settlement times. Thus, a potentiostat system can bypass a reconstruction filter when the user needs to perform these electrochemical methods.

2.5 Design of a Basic Potentiostat System

The design of a Basic Potentiostat System for this research relies on the Advanced Potentiostat Circuit and the Transimpedance Amplifier. Both circuits demonstrated their

worth in the respective simulations. The APC has an accuracy of 100% controlling voltage, and the current goes to the Redox reaction. The TIA is the simplest and the most accurate strategy to convert according to previous simulations. The other I-V converters were not considered due to complexity or disadvantages. Thus, Figure 25 shows the circuit to develop in the next chapter.
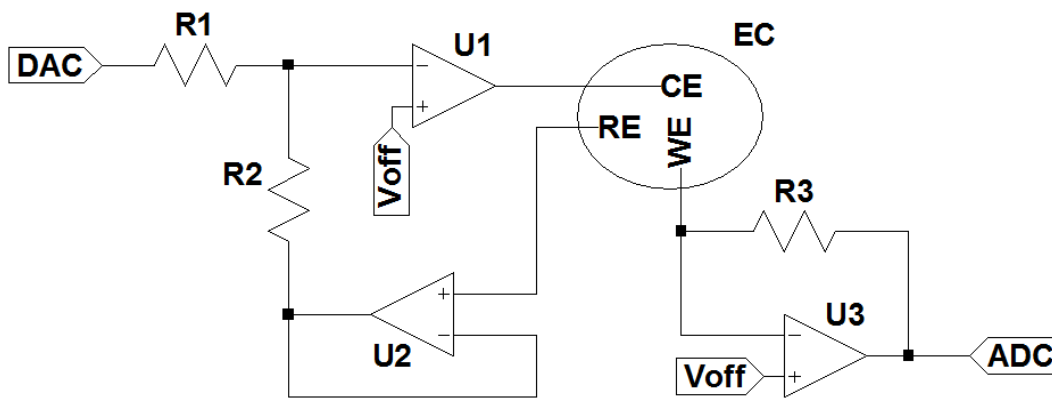
Figure 25. Schematic for the Basic Potentiostat System.

There are many features to considerate in the selection of OPAMPs, ADCs, and DACs as was explained in subsections behind. However, one of the objectives if this research is to know the capacity of the PSoC to work as a potentiostat embedded system. The PSoC has its OPAMPs, DACs, and ADCs, the only external circuit to use is the Bluetooth module. Hence, the schematic of Figure 25 will work with the features of these modules to build the prototype.

The effects to consider in the ADC and the DAC are resolution and conversion speed. Poor resolution cause problems as an increment in the detection limit and voltages errors in the EC due to the ADC and DAC respectively. Thus, highest resolutions eliminate those issues. Based on the application, someone can choose the conversion speed. Applications to detect transients need fast conversions while analysis in the steady-state does not require it. Thus, it is important to keep in mind conversion rate effects when the designer develops a potentiostat system.

Chapter 3. Prototype Design

This chapter describes the potentiostat´s prototype design and explains some modifications to incorporate additional electrochemical techniques. The main aspects are the description of the embedded systems and design patterns for programming. Also, the prototype explanation is through flow charts and schematics. Thus, the reader does not need to know about a specific programming language. However, the appendices related to this chapter will need a domain in C language and LabVIEW. Hence, it is enough to know about embedded systems and design patterns for this chapter.

This chapter gives more information about the following points presented in the methodology:

13. Description of a suitable embedded architecture to develop the prototype.
14. Description of the PSoC and PRoC to know the ICs capacity.
15. Description of the Master/Slave design pattern to know its advantages in the prototype.
16. Slave design to develop the embedded device.
17. Master design to develop the user interface.
18. Description of the waveforms for the LSV, CV, and DSC experiments to implement them in the prototype.
19. Implementation of the analog and digital circuits in the PSoC to have a potentiostat embedded system.
20. Development and implementation of the PSoC firmware to generate the waveforms and deal with the Master commands.
21. Development and implementation of the wireless communication protocol to interchange information inside of the system.
22. Development and implementation of the interface system to communicate with the user.
23. Development and implementation of the user interface algorithm to control the slave.
24. Description of the prototype scalability to implement more electrochemical techniques.

Furthermore, some subsection relies on previous chapters. Thus, the reader needs to be aware of that information.

3.1 Embedded Mixed-Signal Architecture

An embedded mixed-signal architecture deals with applications where the acquisition, processing, and manipulation of the variables are necessary [72]. Most of the times in a potentiostat system, the Redox current is the variable to sense, the voltage at the electrodes is the variable to control, and the microcontroller algorithm generates the appropriate waveforms for an electrochemical trial. Thus, a potentiostat application matches with an architecture like this. The main functions to perform by this kind of embedded system are [72]:

- Sensing the analog signals.

- Transmission and reception of data inside and outside of the embedded system.
- Firmware execution.
- Actuation signals generation.

The PSoC from Cypress Semiconductor is one of the icon devices in an embedded mixed-signal architecture [73]. The selection of this device relies on the incorporation of several features in a single chip. Hence, analog, digital, and processing systems are inside of a PSoC with the capacity to address several applications. The main feature of the PSoC is its reconfigurability. That allows to scientist and engineers to have new solutions to the most challenging problems [17], [40], [41].

According to Figure 26, the main subsystems in an embedded mixed-signal architecture to achieve a reliable application are the following [74]:

- **CPU**. The CPU process all the data executing an established program and it also controls the analog and digital peripherals behavior [73]. The CPU architecture defines features as cost, power consumption, and simplifies the complexity of compilers and simulators.
- **Memory System.** The memory system has two types of memories: volatile and nonvolatile. The volatile memory (RAM) stores all the operations results and variables for computing [73]. The nonvolatile (flash, EPROM) stores the firmware. The PSoC footprint space defines the capacity of both memories. Thus, the applications have to deal with low memory space when the chip area is low as well.
- **Analog Peripherals**. The analog peripherals provide the ability of the embedded system to read or manipulate fiscal variables out of the IC [73]. The connection between the CPU (digital component) and the analog world is through DACs and ADCs. Theses converters impose certain restrictions to keep in mind. Also, this set of peripherals condition the signal to work in a proper range, and they are reconfigurable in a PSoC.
- **Digital Peripherals**. This set of peripherals have specialized modules for determined tasks, and they are common in embedded applications. Also, they can free the CPU from trivial tasks [73]. An example is the use of a PWM instead of making a program to create a square waveform. Also, reconfigurable digital blocks can be part of the applications to provide more flexibility to the design.
- **Interconnect Buses.** In an embedded architecture, there are system and local buses [73]. The buses provide the necessary connections between modules inside of the chip. However, system buses focus on the connection of several subsystems while local buses make CPU connections with specialized digital circuits. System buses provide more connectivity than local buses, but they are slower and less reliable.
- **Input and Output ports**. Input and Output (I/O) ports provide a path for the connection with the modules outside of the chip [73]. Exist three types of ports: analog I/O ports, digital I/O ports, and global I/O ports. Most of the time input buffers are necessary to decouple the signal from the source and output drivers to provide enough power.

- **Interrupt Controllers**. The interruptions are an efficient way to develop embedded firmware. When an interrupt signal is on, the CPU starts to execute and Interrupt Service Routine (ISR) to handle the event [73]. Several modules might trigger an ISR as timers to make real-time applications, general-purpose I/O, and external peripherals. The interrupt controller decides which ISR executes first through a ponderation when several requests arrive.
- **Power supply, clocking units, and other hardware support**. Additional to the last main subsystems there are more modules less complex but with the same relevance [73]. Some examples are oscillators, sleep, watchdog timer, and reference voltage modules.

A Full Potentiostat System, as Figure 2 showed, requires the management of analog and digital signals. A PSoC provides an architecture for the treatment of mixed-signals in one chip [73]. These features bring advantages as fast development times, space reduction, and simplification of the application. Thus, with all the attributes of the PSoC, it is not hard to think that someone can make a potentiostat system on this device.
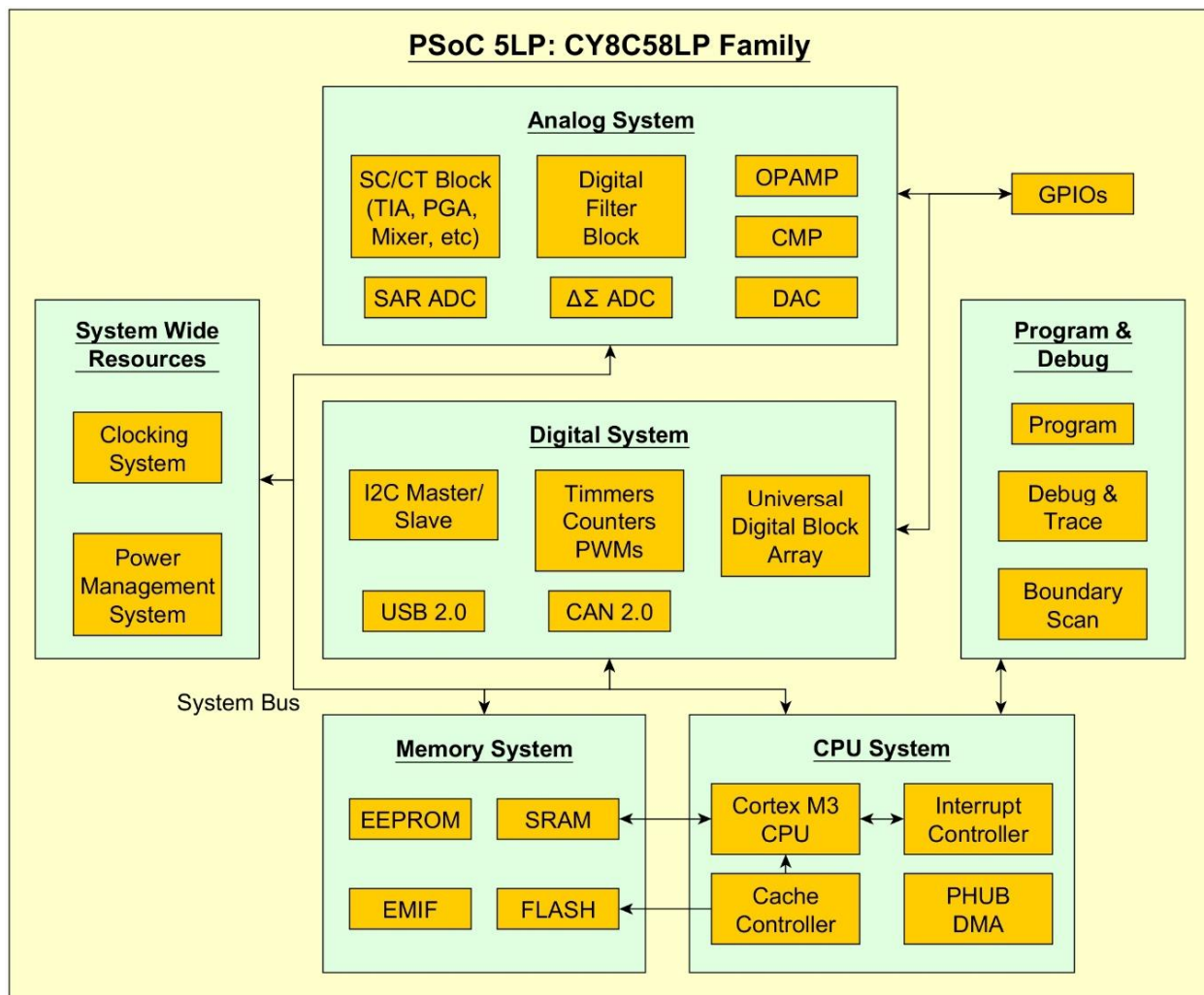
Figure 26. Diagram of the components of the PSoC 5LP: CY8C58LP Family [74].

3.1.1 PSoC 5LP: CY8C58LP Family

The PSoC chosen for the potentiostat application is the CY8C5888LTI-LP097, and it belongs to the CY8C58LP family. This PSoC has analog and digital modules with custom functions, ultra-low power consumption, a 32-bit ARM Cortex-M3 microcontroller, and flexible routing for analog and digital signals [74]. Moreover, the PSoC might have until one hundred analog and digital peripherals in a single chip, reducing PCB space, and cost. Hence, this chip meets the desired characteristics of the embedded system.

The PSoC has many features due to it is made to handle a lot of applications. However, the key characteristics of the prototype are [74]:

- Voltage range from 1.71 to 5.5 V.
- 32-bit ARM Cortex-M3 CPU up to 80 MHz.
- Up to 64 Kbytes for the SRAM.
- Universal Asynchronous Receiver-Transmitter (UART).
- 3 to 74 MHz internal oscillator.
- 8 to 20-bit $\Delta\Sigma$ ADC.
- One Dithered Voltage Digital to Analog Converter up to 12 bits.
- Programmable gain amplifier (PGA).
- 46 to 72 I/O pins.

- Temperature range: -40 to 85 ºC.
- Up to 256 Kbytes program flash, with cache and security features.
- Universal Digital Blocks for 24-bit timers.
- Internal PLL clock generation up to 80 MHz.
- Four OPAMPs.
- One TIA.
- Serial Wire Debug (SWD) 2-wire.

The PSoC Creator is an Integrated Design Environment (IDE) where the development of hardware and firmware takes place [74]. The hardware programming is by dragging and dropping components as the schematics creation of analog circuits. The code development is through C language, and the IDE has a GCC compiler with support for the Keil/ARM MDK. Thus, advanced tools are available for the designer in a single friendly IDE.

3.1.2 PRoC BLE: CYBL10X6X Family

The only missing feature in the PSoC for the potentiostat prototype is the wireless data transmission. Thus, a Bluetooth Low Energy (BLE) module inside of a PRoC is necessary to accomplish the potentiostat system objectives. The selection of this device relies on the fact that the same company manufactures the PRoC and the PSoC. Thus, once knowing one of the Cypress devices, the others do not change a lot making easier the development of the embedded application.

The PRoC has many features because it is made to handle a lot of applications. However, the most important for the prototype are [75]:

- Voltage range from 1.9 to 5.5 V.
- 32-bit ARM Cortex-M0 CPU up to 48 MHz.
- Up to 16 Kbytes SRAM.
- Two blocks for UART.

- Temperature range: -40 to 105 ºC.
- Up to 128 Kbytes flash memory.
- Serial Wire Debug (SWD) 2-wire.
- 2.4 GHz BLE radio and baseband with an integrated balun.

- 3 to 48 MHz internal oscillator.
- 36 general purpose I/O pins.
- Bluetooth 4.1 single-mode device

- TX output power: -18 dBm to 3 dBm.
- RX sensitivity: -89 dBm.

The potentiostat prototype needs two chips to establish a wireless communication as Figure 1 shows. The CYBL10162-56LQXI is the one which is in contact with the computer through wires while the CYBL10563-56LQXI is in contact with the embedded system. More details about the arrangement of the embedded system are in the following section. Furthermore, the differences between both devices are negligible because they belong to the same family. With both IC, the establishment of the wireless communication matches the research objectives.

3.2 Prototype Overview

The potentiostat instrument prototype has two main aspects: the embedded and the interface system. The Potentiostat Embedded System (PES) is responsible for the manipulation of the EC sending and receiving data wirelessly. The Potentiostat User Interface System (PUIS) deals with the user and controls the PES behavior. Both parts constitute a Master/Slave design pattern where the PES is the slave, and the PUIS is the master.

The Master/Slave design pattern brings many advantages to the prototype [76]. The work division allows the completion of the research objectives by using a small embedded system as a slave. Also, the modularity of this pattern is a good feature when the master needs to be changed by another device. An example will be the replacement of a computer by a smartphone. Thus, both devices can use the same slave system without any modification of this one at different times. Hence, the Master/Slave design pattern is very useful to customize the system.

To implement the potentiostat instrument prototype, the master sends commands to the slave, and the slave returns the task response as Figure 27 shows [77]. In this prototype, there is a command for each electrochemical method, and the response is a lot of digital values from the trial. Taking advantage of concurrency, the PUIS focuses on manage the recording and display system. The PES focuses on generating the appropriate waveforms and it sends the Redox current and the voltage values from the trial to the PUIS. Hence, multiprocessing allows achieving a full potentiostat system.
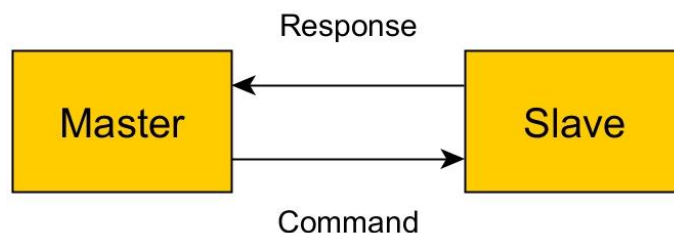
Figure 27. Master/Salve design pattern [77].

3.2.1 Potentiostat Embedded System

The PES is a set of electronic components small enough to be embedded in a potentiostat system application. This system has three main aspects: Bluetooth, PSoC, and the EC as Figure 28 shows. The Bluetooth establish a wireless communication and works as UART bridge to send and receive data. The PSoC has analog and digital modules to implement a potentiostat. Also, the PSoC has a microcontroller, and it executes the firmware. The EC is where the Redox reaction takes place. However, the relevant aspect of this subsection is the PSoC.
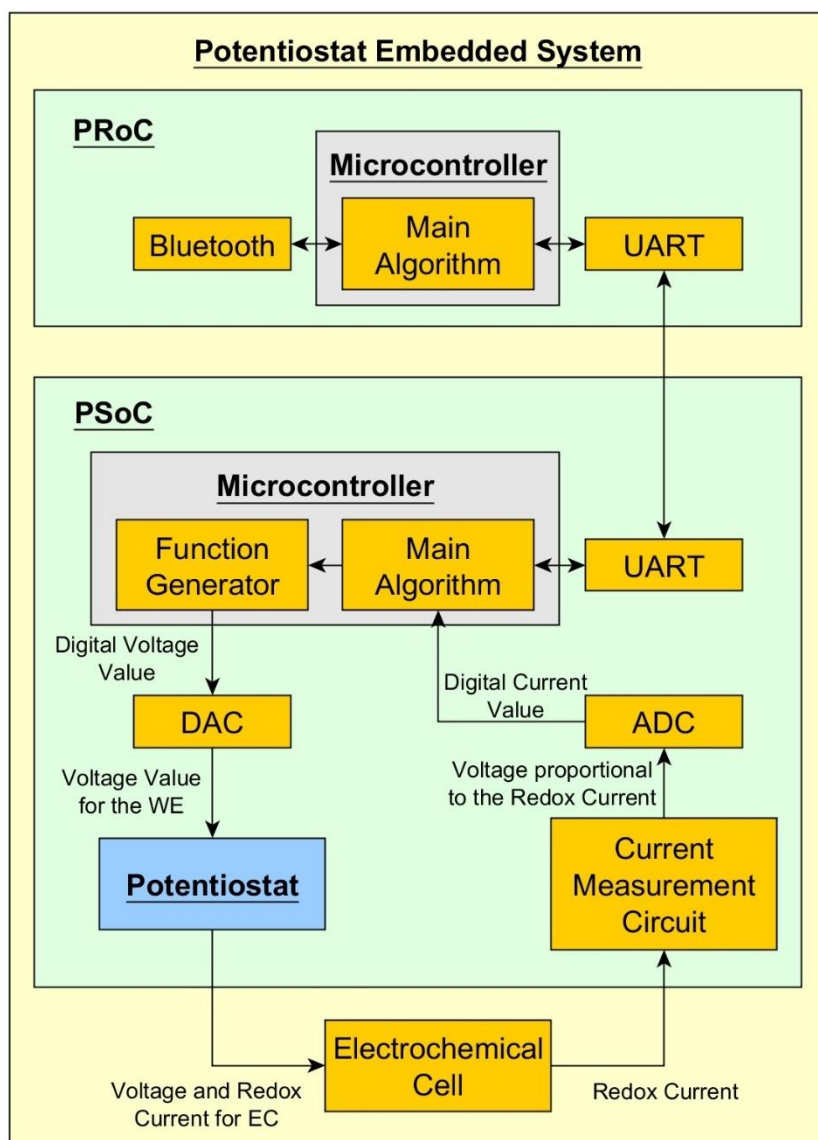
Figure 28. Potentiostat Embedded System Schematic.

The most complex part of the electronic design of the PES is the PSoC because it contains several peripherals in the same chip. The PSoC analog hardware allows to the designer the development of a basic potentiostat system with all the electronic components of Figure 28. Moreover, the microcontroller has the code for the generation of the waveforms according to the electrochemical technique selected and the

parameters to stop a running experiment. Hence, the PSoC has unique advantages having almost everything in one chip for the potentiostat system application.

The main algorithm of the PSoC has a State Machine design pattern programmed in C language. This design pattern is highly acceptable by programmers because its implementation is very flexible and easy to follow [46]. Also, the modularity of the pattern makes feasible the additions of states to implement more electrochemical methods in the same PSoC. Thus, the State Machine is an excellent choice to have a friendly firmware because it is very explicit.

Besides the PSoC, Figure 28 shows another chip called PRoC. Because the PSoC does not have wireless communication capabilities inside of it, an additional electronic component is necessary. The PRoC is like a PSoC, but it focuses on Bluetooth communication instead of hardware modules. The addition of this device increases the prototype size. However, this element is extremely important for a successful PES functionality. Also, the PRoC is one of the best options considering that it comes from the same manufacturer of the PSoC.

3.2.2 Potentiostat User Interface System

The PUIS schematic of Figure 29 uses Bluetooth communication to send commands to the slave. The commands come from a computer with a particular program and the PUIS is always waiting for any events at the interface to start the electrochemical experiment. Also, it has a recording system to save the data in the computer in a TDMS format.
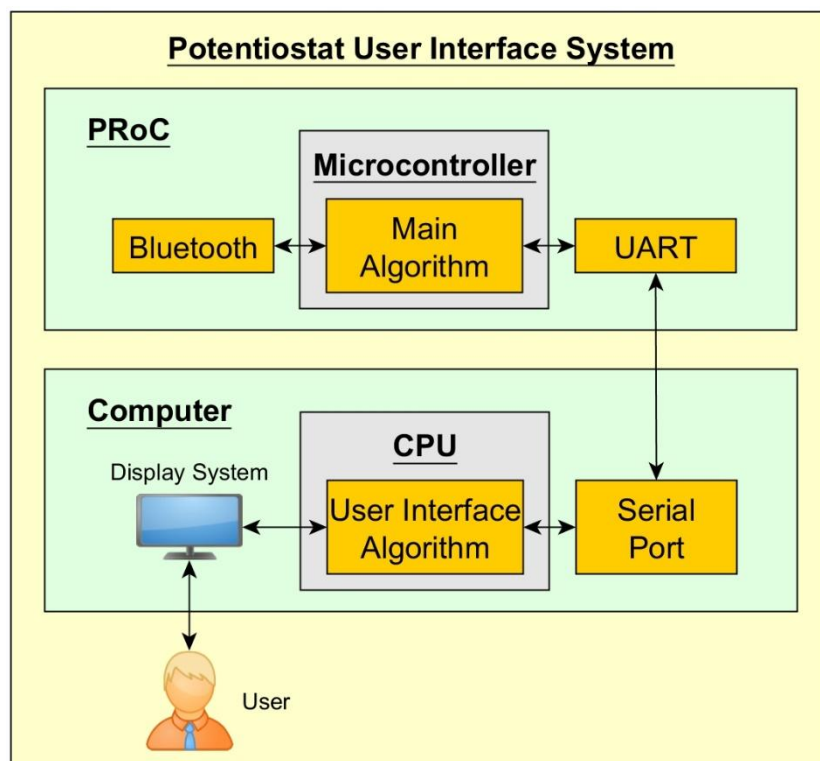
Figure 29. Potentiostat User Interface System Schematic.

Figure 29 shows that the Bluetooth device is out of the computer, and it controls all the communication of the master. Moreover, the Bluetooth version is the BLE 4.2 with a data rate up to 25 Mbps for this prototype [78].

The Bluetooth communication works basically as a UART bridge allowing the design of a simple communication protocol for sending commands. Thus, it is easy the manipulation of bytes to send tasks to the slave and receive the voltage and the current values. However, the Serial Port Profile (SPP) is just for the classic Bluetooth, and the designer needs a custom profile for the PRoCs. Hence, the PSoC sees the communication as serial once accomplish the SPP for the BLE.

A recording and display system is a challenge for any designer. However, the use of advanced design patterns is very helpful. Thus, LabVIEW allows the creation of user interface systems with advanced programming techniques. The algorithm performed by the computer uses a Producer/Consumer and a State Machine design pattern. A later subsection provides more information about these techniques. The advantage of a well-known programming method relies on the information available for making the appropriate modifications by programmers. Thus, LabVIEW is an excellent tool for developing and testing this prototype.

3.3 Waveforms of the Electrochemical Techniques

Before to start programming, it is essential to know the waveforms of the respective electrochemical trails to implement. This section provides an idea of the algorithms to implement in the waveform generator. Also, it describes the parameters of each waveform to give a better idea of the user interface controls. It is noteworthy that all the waveforms represent the WE vs. RE voltage and the potentiostat control signal fix this potential. The Equation 2.4 describes the relationship between these variables.

All these electrochemical techniques unleash Redox reactions at the electrode surface [34], [79]. Each technique provides different information to know more about the phenomena in the EC. With these data, someone can infer the amount of the analyte and its kinetics. Thus, the capacity of the system to provide valuable data to the user relies on the accurate generation of the waveforms.

The LSV is a ramp, and it has an initial and final value with a certain slope as Figure 30 shows [79]. The initial voltage is the first value of the ramp while the final voltage represents the last value of this ramp. The slope of the LSV is known as the scan rate, and it describes the voltage change over time of the signal. With all these parameters, someone can write a program to generate the waveform.

The CV is a triangular wave with a maximum, minimum, and initial value where the cycles and the slope can vary as Figure 31 shows [34]. The maximum voltage is the highest value of the signal while the minimum is the lowest. The initial value is the first value of the signal, and the initial scan direction is the slope of this signal. The scan rate describes the voltage change over time of the triangular wave. The cycles number is the number of periods of this signal. Hence, with all these parameters is easy to build the waveform.

The DSC is a square wave of one cycle as Figure 32 ilustrates. It has two voltage values with a fixed time width for each one [34], [80]. The pulse width is the time where the voltage stays without change. The first step is the voltage value after the time zero and corresponds to the experiment beginning. The last step is the voltage value after the first step. The quiet time is the time before to start the experiment [81]. The value of the quiet time according to Zanello and Brett is the last step voltage. Therefore, someone can make a DSC waveform with these variables.
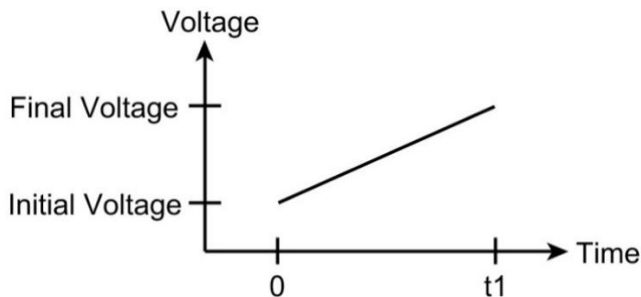
Figure 30. Linear Sweep Voltammetry waveform [34].
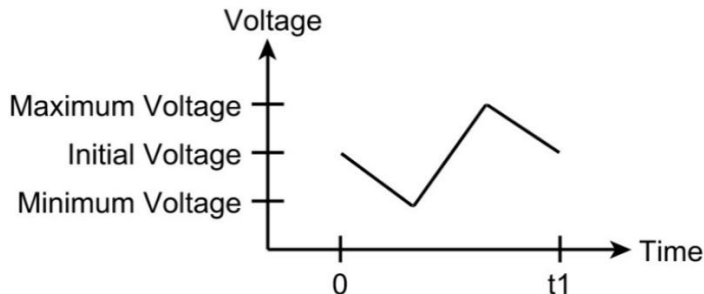
Figure 31. Cyclic Voltammetry waveform [34].
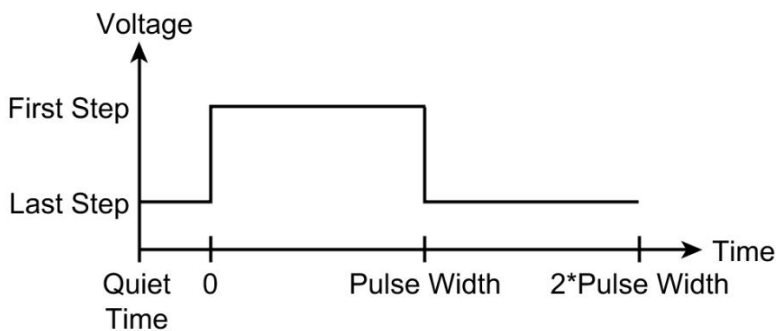
Figure 32. Double Step Chronoamperometry waveform [34].

3.4 Potentiostat Embedded System Design

The PES design has three main aspects for its accomplishment. The analog circuit was the first step in the development as chapter 2 describes. The firmware relies on the waveforms of the electrochemical techniques explained before. The wireless communication has its protocol to have an adequate dialogue between master and slave. Moreover, the PSoC Creator can handle these three aspects: circuit, firmware, and

wireless communication under the same IDE. Thus, the prototype development is not as complicated as having products from different manufacturers.

The PES uses two kits from Cypress Semiconductor: CY8CKIT-059 and CY8CKIT-042-BLE because one of the research goals is to have a prototype and not an end device. The CY8CKIT-059 kit has the chip CY8C5888LTI-LP097 with all the CY8C58LP family features. The CY8CKIT-042-BLE kit has four devices, but the prototype just needs the PRoC and the USB Dongle. Figure 33 shows the PES prototype with the PRoC (left side) and the PSoC (right side).
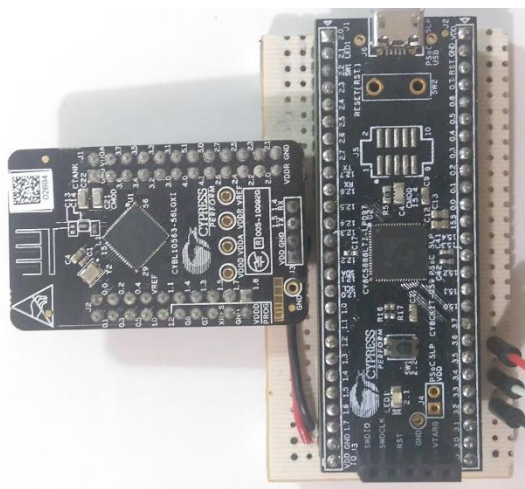
Figure 33. Potentiostat Embedded System Prototype.

3.4.1 Analog and Digital Circuits in the PSoC

Figure 34 shows the digital circuit of the PSoC which provides a firmware execution in real-time and the communication to the PRoC. Figure 35 presents the PSoC analog hardware to make a Basic Potentiostat System. The advanced potentiostat circuit with a TIA from Figure 25 has remarkable features [10], [22]. Hence, The PSoC uses this circuit to make the electrochemical trials. Moreover, the design of the analog circuitry is the most relevant to have a good performance in the system.

The digital circuit from Figure 34 works with separate modules to complete determined tasks. The Timer_ADC triggers an ISR to start a conversion in the ADC. The Timer_DAC triggers an ISR to generate the appropriate waveform according to the electrochemical technique selected. The UART module communicates with the Bluetooth module to send data and receive commands wirelessly. The implementation of this circuit is simpler than the analog because there is no interaction between modules.

The analog hardware from Figure 35 relies on the advanced potentiostat circuit with the TIA, and it has some extra features. Opamp_0 and Opamp_2 control the potential at the WE through the RE. The Opamp_1 supplies the energy for the waveform while the DAC throws the waveform values at the proper rate. The PGA provides a reference voltage of 2.048 V because the RE can be just manipulated in a range of 0 to 4.08 V. Hence, this floating potential gives a chance to work with ±2 V approximately in the EC. The TIA and the ADC transform the current into digital values. Thus, the analog modules of the PSoC can hold a basic potentiostat system.

The PES DAC brings some restriction to the embedded application. The maximum quantization error is 0.5 mV because every step is of 1 mV. The minimum time for the DAC to change a value at its output is of 4 µs. Hence, the maximum scan rate for the prototype is 250 V/s in a range of 0 to 4.08 V. The DAC needs the digital waveform value in 12 bits to make the conversion. Also, the DAC requires a buffer at the output to keep the right potential and supply the energy to the potentiostat control signal. Thus, with these features, the PSoC DAC meets the research objectives.
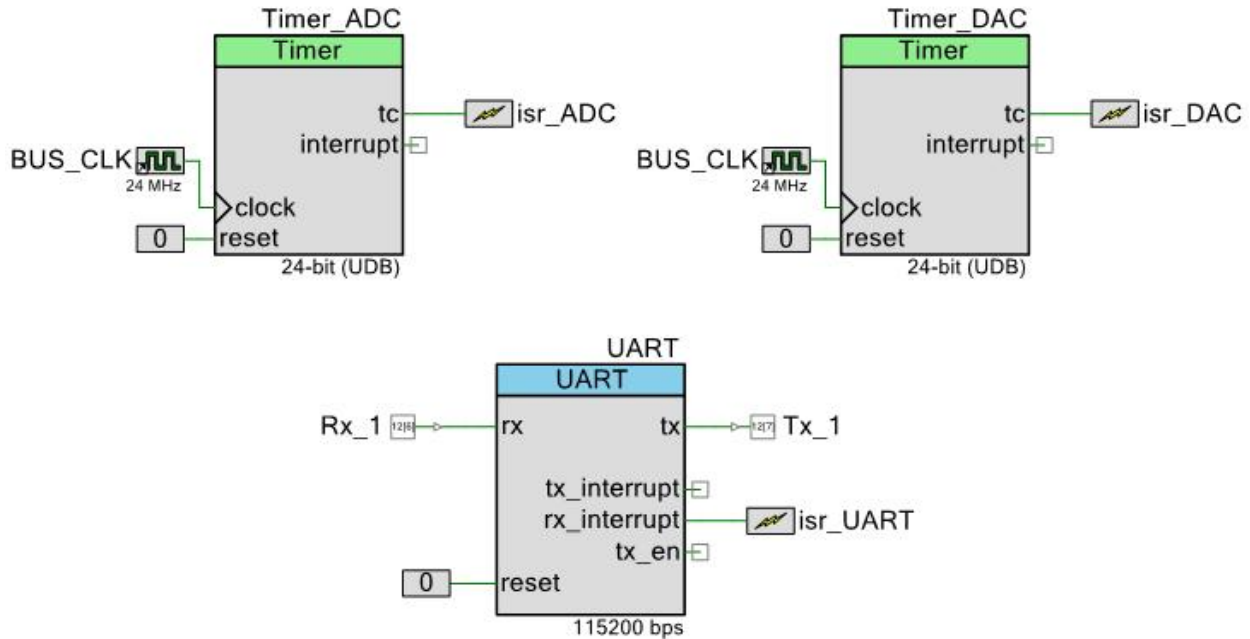
Figure 34. Digital peripherals of the PSoC

The TIA module and the $\Delta\Sigma$ ADC define the sensitivity of the current measurement. The TIA has eight resistors to have eight different quantization levels. However, Cypress Semiconductor does not provide any information about the input bias current of the TIA module. Hence, the potentiostat application sensitivity is unknown. The maximum current value to measure with the TIA is ±51.2 µA. Those limits come from the Equation 3.1 relying on Equation 2.7, and the values for the operation come from the minimum resistor of the TIA module (20 kΩ) and the ADC voltage range at its input (±1.024 V). Furthermore, the missing data needs to be calculated through a characterization.

$$\frac{\pm 1.024 \text{ V}}{20000 \text{ }\Omega} = \pm 51.2 \text{ µA} \qquad\qquad 3.1$$

The $\Delta\Sigma$ ADC has several features that define the behavior of this module in the prototype. The conversion mode is a single sample. Thus, one trigger makes one conversion. The resolution bits of the ADC are of 18, and it takes 414 µS approximately to get one conversion. The clock frequency is around 3071 kHz, but the output rate is slower because it uses oversampling to get a better signal quality. The input range is ±1.024 V, and the ADC has a buffer at its input to avoid any measurement error by impedance mismatching. Hence, the $\Delta\Sigma$ ADC is well suited for the prototype necessities.
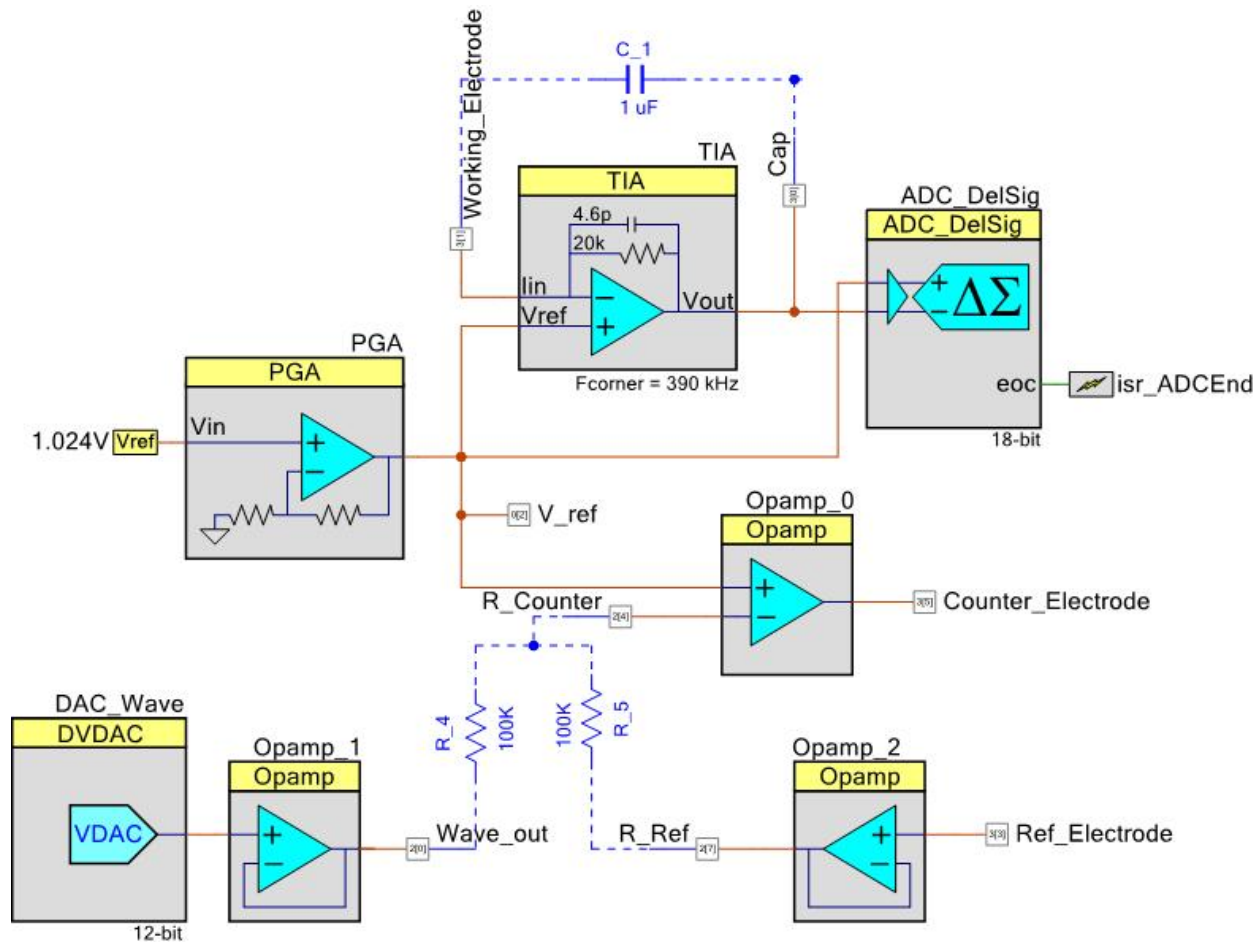
Figure 35. Analog circuit of the PSoC.

3.4.2 The PSoC Firmware

The PSoC firmware has all the logic of the slave according to Figure 36. The program has an initialization procedure and then waits for the master commands while the CPU is off. The reception of a command or the execution of a trial causes the CPU wakes. Through some commands, the user can configure the ISRs to perform an electrochemical assay. When the ISRs are already set up, the experiment takes place. The end of the trial happens when the PSoC sends all the samples to the master or when the user stops its execution. Moreover, this algorithm is not as complicated as the one for the PUIS.

The initialization procedure enables several features for the functionality of the whole algorithm. First of all, the global interrupts and the UART module are on to wake the CPU by any interrupt. After this, the UART receiver buffer is clear. Finally, the variable for counting the measurements taken initiates with zero value. Hence, the initialization procedure ensures the proper conditions for the PES to start its execution as a slave.

After the initialization, the CPU is off. This action freezes the program execution to wait for a command from the master. When a command arrives at the UART module, an interruption is on. However, there is no ISR to assist the interruption. Thus, the CPU

continues with the program flow. Moreover, the CPU wakes as well by the execution of an experiment as it also uses interruptions. One of the advantages of freezing the CPU in the application is the reduction of energy consumption. Hence, disable the PSoC processing system is a good strategy for extending battery life.
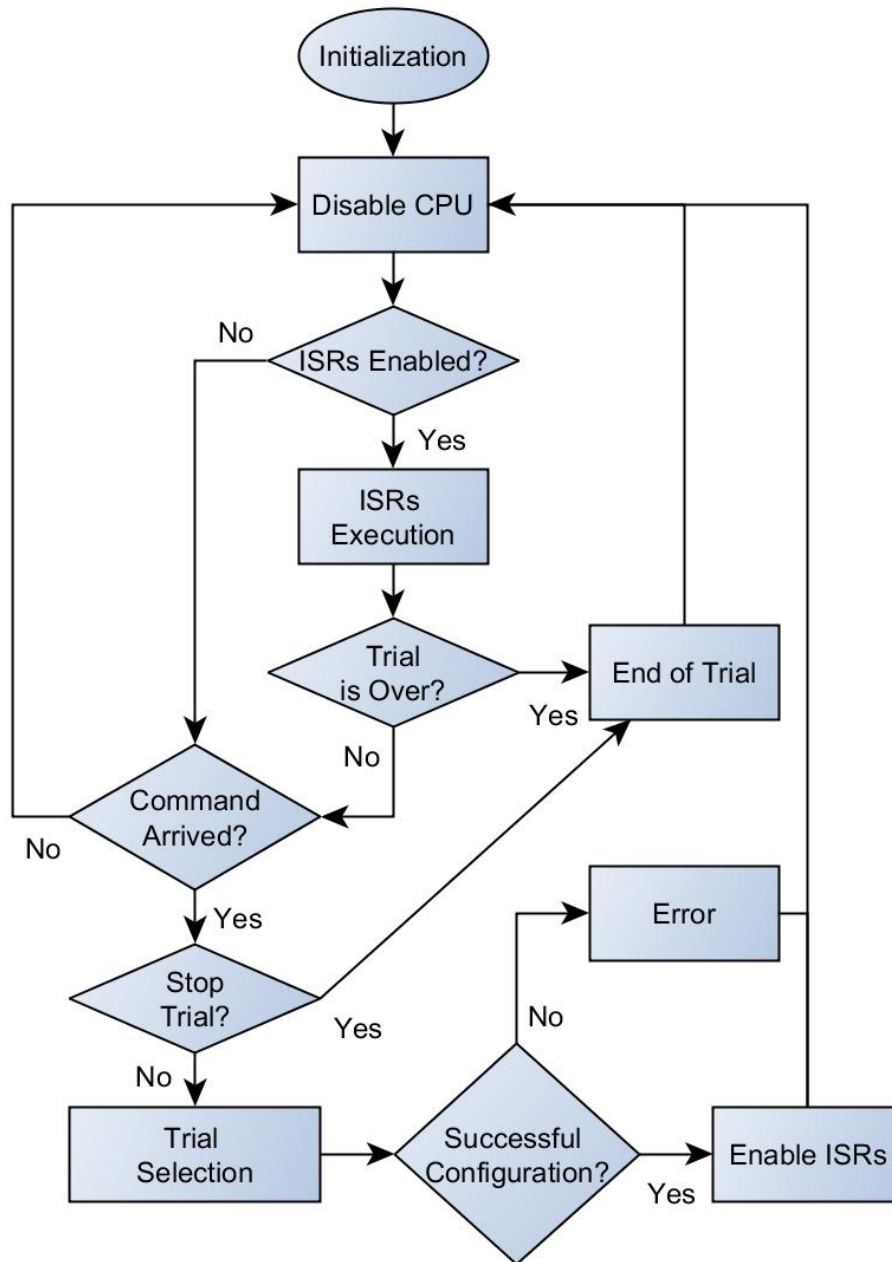
Figure 36. Flowchart of the PSoC Firmware.

The selection of the electrochemical trial depends on the command value. A byte with number one means the execution of the LSV, number two is for CV, and number three is for DSC. When an unknown number arrives, the application ignores it, and the slave returns an error to the master. The program uses a switch statement to make this

behavior possible. Hence, the commands are variables of one byte with numeric values to perform an electrochemical assay.

When the user chooses an experiment, a subroutine according to the electrochemical trial selected starts a configuration procedure. The procedure covers the following points:

- Reception of all the settings to arrange them in the proper variables.
- Calculation of some parameters as the number of samples, and DAC rate for the waveform creation.
- Waveform and timers initialization.
- Interruption configuration.

Four main ISRs exist in the algorithm to send the voltage and current values to the master. However, there are just two sources for triggering these ISRs: isr_ADC and isr_DAC (Figure 34). The isr_DAC is responsible for trigger the proper ISR according to the electrochemical experiment selected by the user. Hence, there are three ISRs to deal with the different waveforms, and one more ISR handles the current measurements. It is noteworthy that the ISRs for the ADC and DAC are executed simultaneously at different times. These ISRs controls the voltage at the WE, measure the current, and send the respective values to PUIS.

The end of trial takes place for two reasons: the experiment is over, or the user finishes it. The assay reaches its end when the PSoC sends all the samples to the master for displaying and storing. Also, the user can send a command with number 255 to terminate the trial when something goes wrong. After the experiment is over, the program shut down the CPU and waits for a command again. Thus, the assay end allows the beginning of a new one. Appendix B provides more information about the firmware code.

3.4.3 Wireless Communications Protocol

The wireless communication uses BLE to transmit all the data from the slave to the master and vice versa. There are two main issues in the communication to establish an understanding in the prototype: the profile and the protocol. The profile is the features to keep a wireless connection between two devices while the protocol makes reference to the arrangement of the data for transmission and reception. Thus, the master and the slave must have the same profile to make a Bluetooth connection.

Cypress Semiconductor provides a custom profile called UART-BLE bridge in one of its blogs [82]. When the Bluetooth appeared at the first time, a serial port profile was given to manage serial ports. However, there is no such profile for BLE because this kind of Bluetooth is not for high data rate. Instead, it is for low power consumption. Though, this company developed a UART-BLE bridge to deal with serial ports. This profile once implemented works basically as UART.

The Bluetooth needs a broadcaster and an observer to make a connection between master and slave. Thus, the PUIS (broadcaster) is the responsible for announcing its presence while the PES (observer) listens to it. Also, the changes to the respective PRoC programs for the PUIS and the PES are minimum selecting the proper

chip number and erasing the logging message. Hence, the firmware given by Cypress Semiconductor for broadcaster and observer are almost ready to use.

Once the bridge is working, all the communication takes place in a serial manner. Figure 37 describes the PSoC firmware from the communication point of view. The color purple is for variables of one byte, yellow for two bytes, and green for five bytes. The Waveform Parameters state has two colors because it has to deal with several data types. The dotted line is for bytes coming from the master, and they go to the slave while the scripted line is vice versa. This algorithm is more detailed than Figure 36 due to it shows how the communication happens.
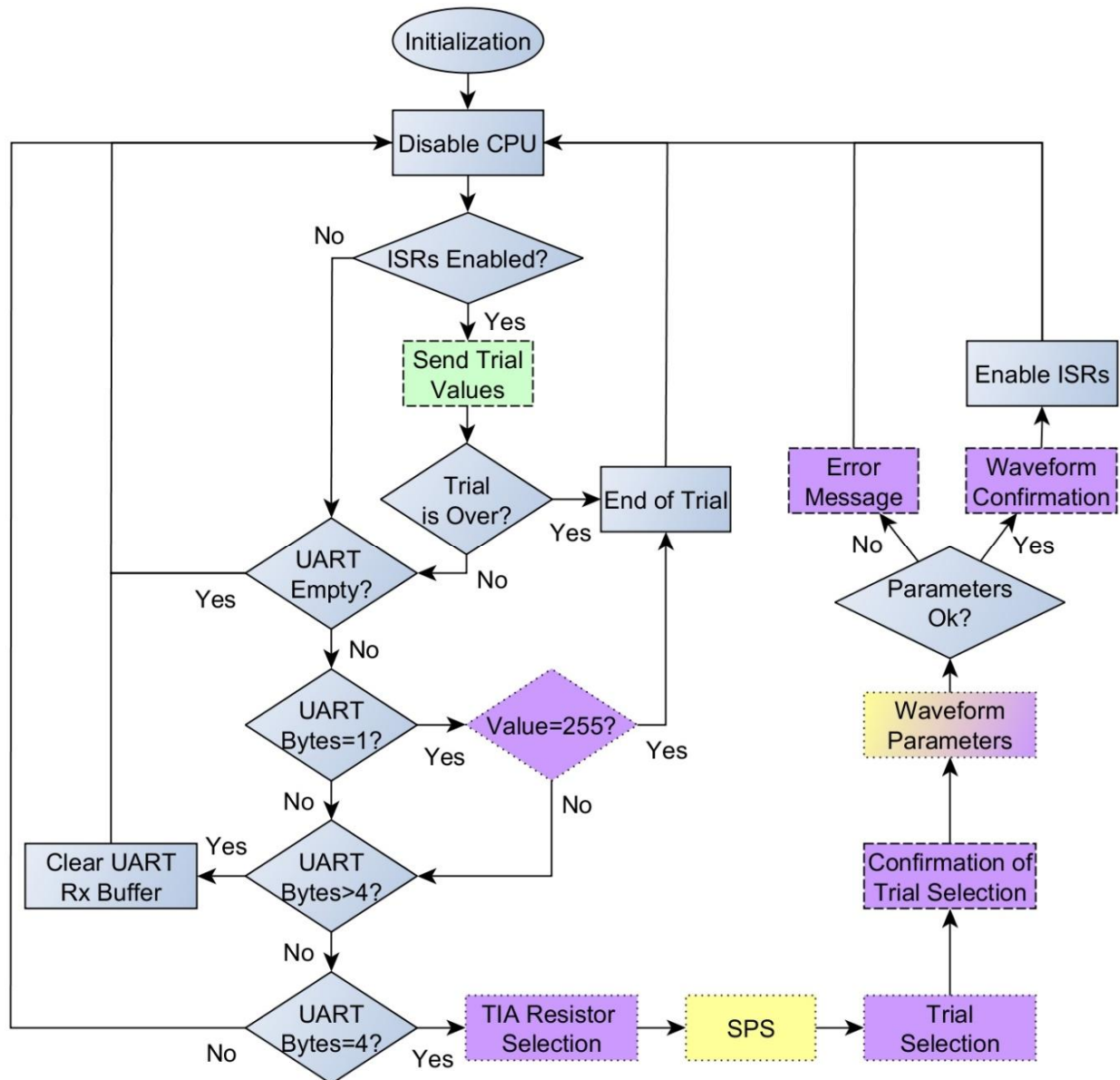
Figure 37. Flow chart of the PSoC Firmware from the Communication Point of View.

In Figure 37, the master starts the communication sending three variables selecting the proper TIA resistor, the number of SPS, and the kind of trial. Then, the PES

replays with a confirmation if the settings are good. After that, the master gives the waveform parameters to the slave. Then, the PES checks these settings, and it sends an error message if the parameters are incongruent. Once the trial configuration is ready, the ISRs start their execution sending the current and the voltage values of the experiment to the PUIS. Hence, the protocol is the interchanged bytes congruence between the PUIS and the PES.

When the waveform settings arrive from the PUIS, the number of variables vary because the waveform necessities for each experiment are different. From Table 9 most of the parameters are of two bytes. However, Cycles Number and Initial Scan Direction are of one byte while Pulse Width and Quiet Time are of four bytes. Depending on the selected trial, this kind of information is expected by the PES. Hence, the ISRs use this information to create the proper waveform to for an experiment.

Table 9. Waveforms Parameters for the different techniques.

LSV	CV	DSC
• Initial Voltage • Final Voltage • Scan Rate	• Initial Voltage • Maximum Voltage • Minimum Voltage • Cycles Number • Initial Scan Direction • Scan Rate	• Last Step • First Step • Pulse Width • Quiet Time

3.5 Potentiostat User Interface System Design

The PUIS has two main matters: the interface system and the algorithm behind of this interface. At the interface, all the interaction with the user takes place. The main features of the interface are about the understanding of the controls and indicators by the user. The algorithm for PUIS is just sequences of step and choices to deal with the user. Also, the manner of how is coding the algorithm defined the comprehension by programmers and the scalability of the system. Hence, the PUIS has to be friendly with the user and the programmer.

3.5.1 Controls and Indicators for a Potentiostat Application

The user interface was developed in LabVIEW 2013 with all the controls and indicators for the applications of this research. The interface allows the settings manipulation of the different electrochemical techniques, choosing the trial, and configuring the proper parameters. Also, it shows the results when they are taken in graphs as current vs. voltage and current vs. time. Hence, the designer can offer a friendly user interface system knowing how to arrange the control and indicators for displaying.

In most of the cases, when a potentiostat application is under development, the following controls and indicators are essential for the techniques contemplated in this investigation:

- Current range control.

- SPS control.
- Electrochemical experiment selector.
- Controls for the experiment according to the technique (Table 9).
- Run trial button.
- Stop trial button.
- Current vs. voltage graph for voltammetric experiments.
- Current vs. time graph for chronoamperometric experiments.
- Error indicator.
- Control to save the data.
- Stop program button.

Furthermore, there are the following controls and indicators not essential, but very useful for this application:

- Messages indicator.
- Indicator for the parameters arrival at the PES.
- Experiment samples indicator.
- Indicator for samples received at the PUIS.
- Control for the WE area.
- Graphs for the current density vs. time and current density vs. voltage.
- Tabulated data indicator.

Also, the designer has to display the controls and indicators logically to keep the interface as friendly as possible. The tab control in LabVIEW allows arranging several pages to show different information just making click on it. Thus, there is a tab control to display the experiment information (Figure 38) and another tab for the trial settings (Figure 39). Hence, the tabs let the designer arrange all the controls and indicators logically just showing the required information. The other controls and indicators outside the tabs are around of the interface. Because the user interface is too wide, a better-quality figure is in Appendix C.

| Current vs Voltage | Current Density vs Voltage | Voltage vs Time | Current vs Time | Current Density vs Time | Tabulated Data |
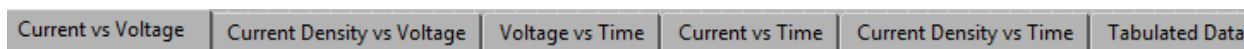
Figure 38. Tab control to display the experiment information.

| Linear Sweep Voltammetry |
| Chronoamperometry |
| Cyclic Voltammetry |
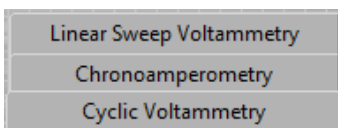
Figure 39. Tab control for the Trial Settings.

3.5.2 User Interface Algorithm

The user interface algorithm from Figure 40 is the most complex as it involves the management of the display system and the control of the PSoC. The program uses a State Machine and a Producer/Consumer design pattern in one of its states. Some states were omitted to simplify the flow chart description in the figure. However, the algorithm still shows the main functionality to handle the LSV, CV, and DSC experiments. Moreover, any device can use this flow chart, not just a computer, because it describes the behavior

of the program. Furthermore, the modifications for a different application involving these techniques are minimum.
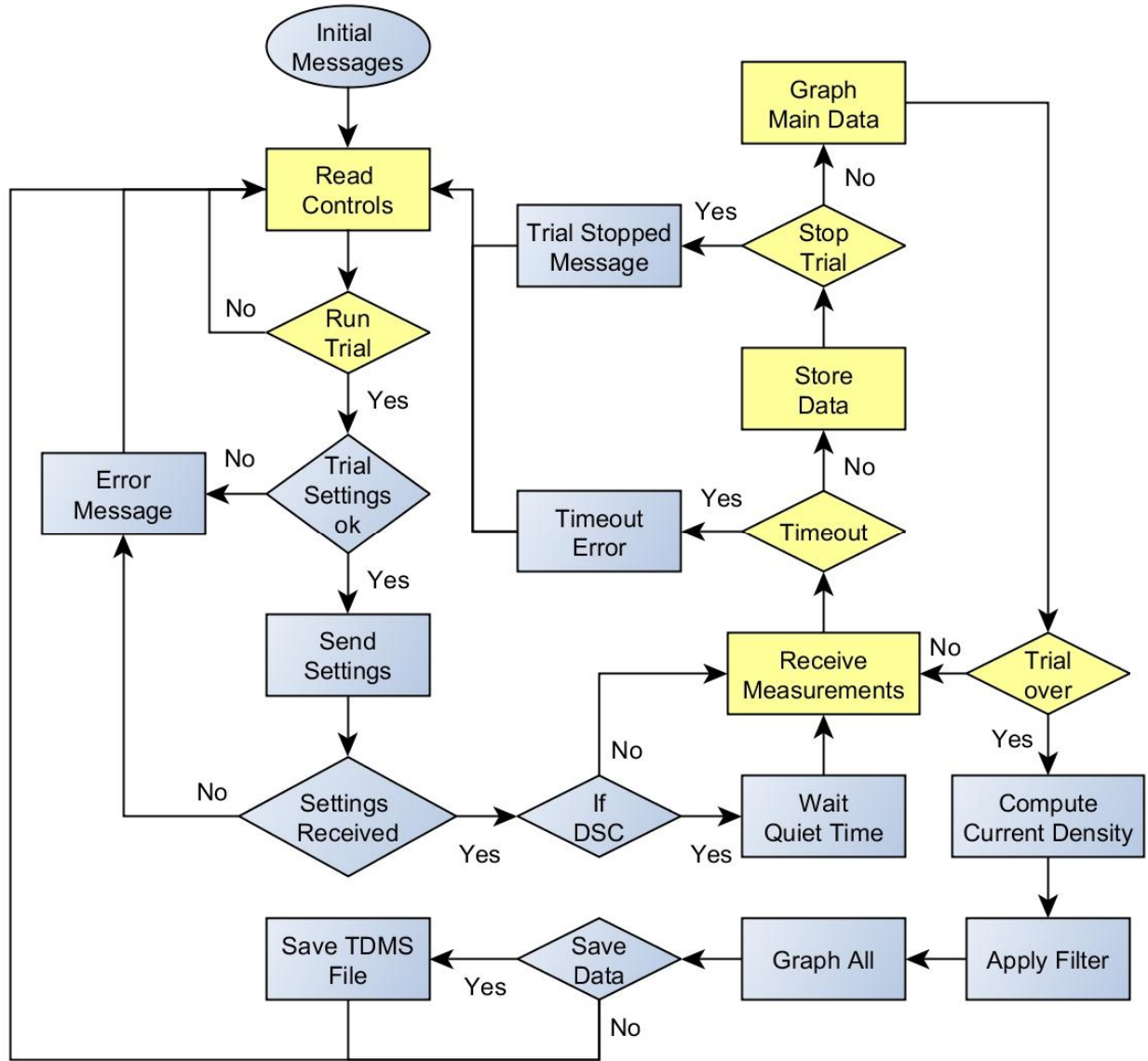
Figure 40. User Interface Algorithm.

The algorithm from Figure 40 needs to meet certain time requirements. The computer performs the blue states as fast as it can. However, some of these processes can take more time than others, and it relies on the amount of data to process. The critical states are the yellow ones where the algorithm executes the loops every 0.1 seconds. This time was selected to refresh the user interface, and it does not seem unresponsive. Hence, the yellow states represent the loops where the user interact with the computer expecting a response back.

The Producer/Consumer design pattern allows separating the work into two loops (two processes) known as a producer and consumer [47]. The pattern takes advantage of the computer multiprocessor system executing both processes at the same time in

different cores if there is no data dependency [83]. Mainly, a producer sends data to the consumer to work with it in a different loop. The communication between processes is by queues ensuring the information consistency. Hence, the producer can continue with its execution while the consumer works in its assignment at its rate.

The algorithm states have several issues to deal. However, the following points describe briefly what is happening in each state:

- **Initial Messages**. In this state, the computer suggests checking some points before to start the experiments as the energy for the PES and the Bluetooth communication between master and slave.
- **Read Controls**. In this state, the computer reads all the controls in the interface to configure a certain electrochemical experiment.
- **Run Trial**. In this state, the computer checks the run trial button. The computer continues with the program flow if the button is on otherwise it goes back to read the controls.
- **Trial Settings ok**. In this state, the computer checks the settings for the electrochemical experiment. The settings are approved if they are inside of the normal parameters otherwise the computer deploys an error message.
- **Error Message**. In this state, the computer deploys an error message explaining the source of the problem. Then, the computer goes back the Read Controls state.
- **Send Settings**. In this state, the computer sends the electrochemical parameters to the PSoC for the waveform creation according to the electrochemical trial selected.
- **Settings Received**. In this state, the computer waits for the PSoC answer. The computer shows an error message if the PSoC does not reply properly otherwise the computer goes to the next state. Also, it notifies which experiment is running.
- **If DSC**. In this state, the computer goes to wait the Quiet Time if the DSC technique was chosen otherwise it goes to receive the measurements.
- **Wait Quiet Time**. In this state, the computer waits the Quiet Time. Then it goes to receive the measurements.
- **Receive Measurements**. In this state, the computer reads its serial buffer. If there are measurements in the buffer, the algorithm stores them in other location to receive more data in that buffer and prevent an overflow.
- **Timeout**. In this state, the computer checks the time waited for new measurements at the computer buffer. An error message is displayed if the time waited is too big otherwise the loop continues to the next state.
- **Timeout Error**. In this state, the computer shows an error because of the missing data in the computer buffer. This error can be for a disconnection of the wireless communication. Thus, the data are never going to arrive.
- **Store Data**. In this state, the computer concatenates the array, where all the data is saved, with the array of the incoming measurements. Hence, the algorithm stores everything in a single array to work with it later.

- **Stop Trial**. In this state, the computer checks the stop trial button. The computer sends a command to stop the experiment if this button is on otherwise the loop continues to the next state.
- **Trial Stopped Message**. In this state, the computer shows a message to the user because the trial is not longer running.
- **Graph Main Data**. In this state, the computer shows the raw data in the Voltage vs. Time, Current vs. Time, and Current vs. Voltage graphs. Also, this state uses a Producer/Consumer design pattern to let another loop to plot the graphs with a decimation process.
- **Trial Over**. In this state, the computer checks the number of samples that have been arrived. The algorithm goes to the Receive Measurements state if this amount is not equal to the samples expected otherwise the algorithm goes to calculate the current density.
- **Compute Current Density**. In this state, the computer calculates the current density and stores it in an array to work with it later.
- **Apply Filter**. In this state, the computer filters all the measurements related to the current saving them in an array.
- **Graph All**. In this state, the computer shows the raw data, the filtered data, and the density current to the user.
- **Save Data**. In this state, the computer reads the control for saving the data. The computer stores the measurements if this control is on otherwise it does not save anything.
- **Save TDMS File**. In this state, the computer performs all the operations related to save the measurements as open, write and close the file.

Some of the states are more complex than others, and they need a major explanation. The most challenging states to develop are:

- Send Settings.
- Receive Measurements.
- Graph Main Data.
- Apply Filter.

The state Send Settings is one of the most important because it contains the communication protocol to send the electrochemical parameters to the PSoC. In this state, the algorithm erases all data from the previous trial to start a new one. Also, there is a function (SubVI) to send the electrochemical settings. It makes the proper variables conversion to match the data types in the PES. The SubVI sends four bytes and then it waits for the slave reply to send the rest of the waveform settings. This sequence is necessary for the PES to understand its task.

The state Receive Measurements reads the computer buffer where all the measurements arrive. The algorithm gets every five bytes (data package) of the buffer until there is no more data to complete a package. The first two bytes of the package are the voltage of the WE, the rest of the bytes represents the current. Also, the algorithm performs the time calculation between samples to show the graphs against this variable. The computer checks the buffer every 0.1 seconds to avoid an overflow. However, this

state reports an error if nothing arrives at the buffer otherwise it reads just a fraction of the whole experiment.

The state Graph Main Data takes more time and computer resources than any other process. Also, the algorithm always executes this state when a trial is running because it is part of a loop. Hence, the task of plot the data is assigned to a consumer process to let the state machine complete the loop in time. Moreover, this state performs a decimation function because the number of samples can go over a million easily. The decimator reduces the data allowing the consumer meet the time requirements. Hence, the Producer/Consumer design pattern and the decimation function allows the proper data displaying.

The state Apply Filter reduces the noise from all the measurements related to the current. This state uses a moving average filter with the following advantages [84]:

- Simplicity (reducing the computing time).
- Reduction of random noise.
- Maintenance of the step response.

The moving average filter performs a convolution to has those features [84]. A more complex algorithm is not necessary because this filter offers a very good relationship between noise reduction and signal sharpness. The main drawback of this filter is the poor performance in the frequency domain. However, this is the price to pay to have a general-purpose filter. Thus, the moving average filter is a good choice to deal with all the electrochemical techniques.

3.6 Prototype Scalability

The section describes the major changes to add more functions to the prototype. These modifications come from the necessities of each researcher to address its goals [10]. The modifications to implement at the PES and PUIS are just an expansion of the code and the user interface functionality. Thus, the hardware capabilities remain equal. Also, the flow charts stay unaltered, and the changes take place in certain states. Moreover, the modifications deal with the addition of more electrochemical techniques.

3.6.1 PES Changes

The designer needs to perform several modifications in different states of the PES. The following point describes these changes.

- The creation of a new command to express a different electrochemical trial (new task).
- The addition of a subroutine to deal with the configuration of the electrochemical experiment.
- The implementation of a new ISR to create the appropriate waveform.

Once made these modifications, the master firmware has to change as well to have a whole prototype with more capabilities.

The creation of a new command is a process that takes place in both systems. As it was expressed in the description of the communication protocol, this variable is 8 bytes.

Thus, the number of different tasks can go up to 256 with this variable. A new command means one more state in the PSoC switch statement. In the master, this means a new option in the electrochemical selector and more controls for the waveform settings. Hence, master and slave must be congruent with the new command number.

The new subroutine is the responsible for setting up the selected trial. Thus, like any other configuration procedure in the PSoC, it has to handle with the reception of the trial settings, the computing of the necessary parameters, the initial waveform value, the proper timers configuration, and the ISRs conditions for the trial. Also, it has to make the proper error notification in case of wrong settings. The program occupies 6.8% of the flash memory with the last three techniques. Thus, the PSoC can store at least 14 more techniques with a similar space memory.

The new ISR has the responsibility to create the new waveform and send the values to the DAC. The complexity of this code relies on the kind of signal to make. The isr_DAC is still responsible for trigger the new ISR. Hence, the designer does not need to make any changes at the Timer_DAC (Figure 34). It is a good idea to make the code as simple as possible because the PSoC is going to execute this code during all the trial. Thus, this is one of the most relevant sections to improve the power consumption.

3.6.2 PUIS Changes

The PUIS modifications take place in the interface and in the algorithm. These changes are more than in the PES. Thus, the designer must have a complete view of the whole system to make it. Furthermore, the actions in the interface are strongly related with the algorithm. An example will be the addition of a control in the interface leading to its reading in the Read Controls state. Hence, the modifications have to be congruent to implement the new electrochemical technique satisfactory.

In the interface system, the user needs more controls to configure the new electrochemical experiment. However, thanks to the tabs (Figure 39), the designer can add a new page to display the proper parameters letting the user configure the new waveform. Also, the electrochemical selector needs to show the new task for the PES, and it deploys the proper tab page. Hence, the proper settings are going to be enabled for its modification when someone chooses a trial.

In the algorithm (Figure 40), the designer needs to modify several states to have a proper incorporation of the new technique. The following points give a brief description of the changes in each state.

- **Read Controls**. This state needs the addition of the proper controls for the new electrochemical technique. Also, the trial settings tab needs to be updated.
- **Trial Settings ok**. This state is where the algorithm checks the proper values of the settings. Thus, a code takes place here if the parameters need a revision otherwise there is nothing to do.
- **Send Settings**. This state gets the major change because it is in charge to make the settings conversion to the proper bytes and send them to the PES. Moreover, it just takes the addition of a new SubVI to accomplish this modification.

- **Settings Received**. In this state, the designer can add a message to show the execution of the new technique to the user.
- **Error Message**. In this state, the designer can add a message to show an error in the settings for the new technique.
- **If DSC**. A code is written here if the technique requires a Quiet Time otherwise there is nothing to do.
- **Save TDMS File**. This state needs the proper modification to save in the file the parameters of the experiment.

With these points in mind, the prototype can have more electrochemical techniques for its execution. Nevertheless, the programmer must have an understanding of the whole program and the prototype functionality in case of debugging.

Chapter 4. Prototype Characterization

A characterization is relevant to know if any adjustments in the analog circuit are necessary to work with the Basic Potetiosntat System of Figure 35. The CY8C5888LTI-LP097 electronic chip from Cypress Semiconductor has the potentiostat design. The idea of the characterization is to probe the electronic modules watching their response to the input variables expecting specific results at the output. The deviation of the calculated values will be the result of the unwanted behaves. The errors will be kept as low as possible compensating all the tested parameters with proper values.

This chapter gives more information about the following points presented in the methodology:

25. Measurement of the reference voltage to make any adjustment necessary. Also, this measurement allows the programmable gain amplifier characterization.
26. Determination of the potentiostat capacity to supply current to a Redox reaction and the potential range.
27. Recording of three LSV waveforms with different parameters in an oscilloscope. Thus, hypothesis one is accepted if the waveforms are consistent with the parameters for this technique.
28. Recording of three CV waveforms with different parameters in an oscilloscope. Thus, hypothesis one is accepted if the waveforms are consistent with the parameters for this technique.
29. Recording of three DSC waveforms with different parameters in an oscilloscope. Thus, hypothesis one is accepted if the waveforms are consistent with the parameters for this technique.
30. Current measurement circuit characterization to know the real resistor values inside of the PSoC and the output offset voltage of the TIA.
31. ADC characterization to compensate its offset voltage and its gain.
32. Measurement of the power consumption of the slave system.
33. Description of all the compensations in the user interface algorithm.

The characterization of the analog circuit of the prototype is according to the polygons of Figure 41. They wrap the following circuits:

- The circuit wrap by the black lines provides the reference voltage.
- The circuit wrap by the orange lines is the potentiostat with the DAC.
- The circuit wrap by the blue lines is the current measurement circuit with the ADC.

A PGA supplies the reference voltage to the potentiostat, the ADC, and the TIA. This voltage is necessary to work with bidirectional potentials in the EC. The PGA has a gain of two and an input of 1.024 V. Hence, the reference voltage value must be of 2.048 V at the PGA output. That value is the middle point of the DAC range (0 to 4.08 V). However, a characterization will describe the real value of that output.

The DAC and the APC represents a single unit for their characterization with a Randles cell. There is no necessity to do it OPAMP by OPAMP because the objective is to introduce a digital signal to get the proper analog value at WE vs. RE. Moreover, the

Randles cell allows us to have a model close to the real cell. Hence, the potentiostat and the DAC characterization increase the accuracy of the waveform generator to have a better control of the potential.

In the same way, the current measurement circuit and the ADC characterization allow us to make the proper correction to have the Redox current values close to the reals. However, the designer cannot consider this circuit as a single unit because the TIA module has several resistors inside of it. Thus, there are three main aspects: the TIA performance without characterization, the TIA with characterization, and the entire performance with the ADC effects.
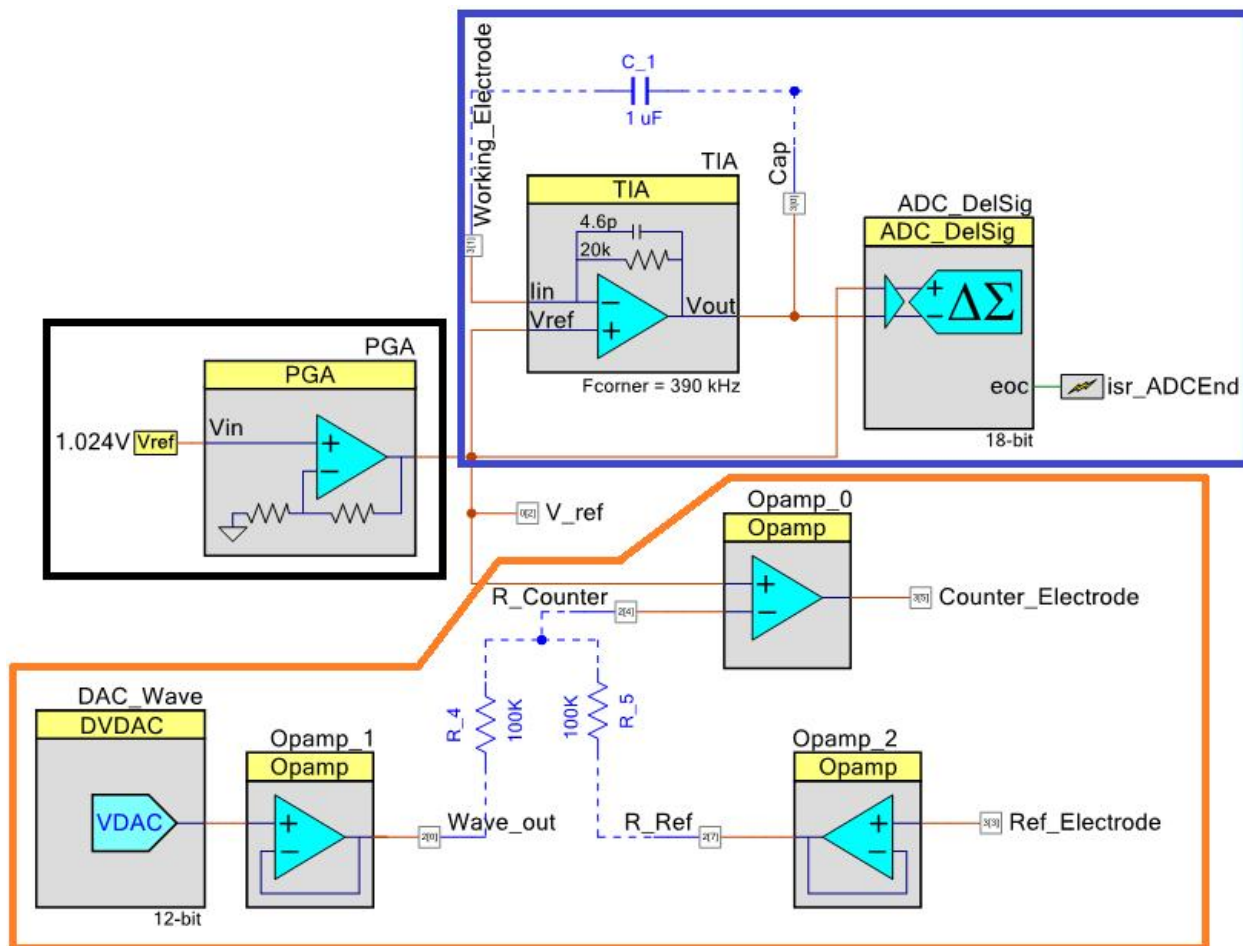
Figure 41. Different Circuits of the analog components of the Prototype.

4.1 Preliminary Tests

The preliminary test has the purpose to determinate the current and the voltage ranges of the potentiostat instrument for the Randles cell. Two major tests are in this section. The first test is about the reference voltage characterization to avoid any permanent offset. The last test studies the device capability to drive Redox reactions in the Randles cell. Also, it explores the linearity of the potentiostat voltage range in a specific current range. Therefore, two subsections are going to take place.

Several instruments as an oscilloscope, a signal generator, a multimeter, and a power source are necessary to perform all the trials in this chapter. Table 10 shows the manufacturer and the model of the instruments to use. With these devices, it is possible to introduce signals to specific circuits and record their response. Hence, a lot of information can be inferred with these instruments to make the proper compensations in the programs. Also, they can determine the working range of the potentiostat.

Table 10. Instruments for the Characterization.

Instrument	Manufacturer and Model
Oscilloscope	Tektronix, TDS 2022B.
Signal Generator	Agilent, 33210A.
Multimeter	BK Precision, 5491A
Power Source	HP, E3630A.

The characterization is going to use the Randles circuit of Figure 9 relying on the values provided by Gamry Instruments [56]. However, the R2 value is going to change in further sections to probe different current levels. Figure 42 shows the labels for the circuit and some fixed values. The electronic components for the Randles cell have a tolerance around of 5%. Table 11 presents the values of the Randles cell elements provided by the manufacturer and the measured values missing R2.
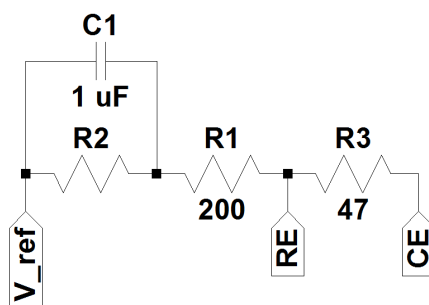
Figure 42. Randles circuit for the potentiostat characterization.

In this section, the PSoC circuit of Figure 35 and the Randles circuit of Figure 42 are connected matching the RE with the RE and the CE with the CE of the respective schematics like Figure 43 shows. The WE is at the reference voltage (V_ref). The main reason to be at the V_ref terminal is that the TIA can introduce uncertainties in the measurements due to its nature. The value of the WE vs. RE voltage in this section express the V_ref vs. RE voltage because the WE and V_ref are on the same node. Thus, the oscilloscope will record this variable for each electrochemical technique in further experiments.

Table 11. Randles circuit values for the potentiostat characterization without R2.

Electronic Component	Label Value	Measured Value
R1	200 Ω	196.93 Ω
R3	47 Ω	46.88 Ω
C1	1 µF	***

4.1.1 Reference Voltage

The reference voltage is an important value because it affects the performance of other circuits. However, in the current measurements, it is not relevant because this value added to the TIA is subtracted in the ADC. Hence, the digital Redox current does not need any adjustment regarding this constant. In the potentiostat, this value can cause a permanent offset. The firmware assumes that the reference voltage is at 2.048 V, but any deviation in the order of millivolts from this value will introduce a permanent error. Therefore, the characterization improves the waveform generator accuracy.

Table 12 provides the conditions for the trials to know the reference voltage. The circuit in the PSoC is according to Figure 35. Henceforth, someone needs to turn the instruments on and wait half hour to get them warm before to make any measurement. The PSoC at its output does not have the Randles cell of Figure 42. The voltage supply for the whole circuit is 5 volts. Therefore, this setup assures that the V_ref value does not deviate due to currents in the Randles cell.

Table 12. Conditions for the Reference Voltage Characterization.

Circuit of Figure 35 in the PSoC	Yes
Randles Cell connected	No
Voltage supply for the PSoC	5V
Turn the instruments on waiting half hour to use them	Yes

A voltmeter, from the multimeter of Table 10, measure the V_ref terminal of Figure 35 against the ground to know the value of the reference voltage. After the instruments get warm, seven measures with the voltmeter will provide the reference voltage values. Table 13 presents those measurements labeled with M1, M2, M3, and so on. The average of those measurements is the value to program in the firmware to compensate any deviation.

Table 13. Reference Voltage measurements.

M1	M2	M3	M4	M5	M6	M7	Average
2.044 V	2.044 V	2.044 V	2.044 V	2.044 V	2.044 V	2.044 V	2.044 V

4.1.2 Current Range and Potentiostat Linearity

The resistors set of the TIA, inside of PSoC, and the voltage range of the Randles cell establish the current range in the preliminary test. The resistor values of the TIA come fixed from the factory. Those values are going to be equal to R2 in the Randles cell of Figure 42 to do the preliminary experiments. When R2 and the TIA resistor are equal, the Randles circuit can deliver suitable currents to the TIA module. Table 14 shows the resistor values of R2, and it also presents the measured. With those resistors, someone can know the potentiostat voltage linearity and the current range of that linearity.

The reference voltage and the DAC range allow us the EC manipulation from -2 V to 2 V approximately. The DAC can go from 0 to 4.08 V taken ground as a reference. However, taken 2.044 V, bidirectional potentials can take place in the EC. The previous subsection declares the permanent offset of the V_ref terminal. However, certain errors can happen due to no linearities. This phenomenon can reduce the potentiostat range to

control the voltage accurately at the electrodes. Thus, a test to probe the linearity is necessary to perform the electrochemical trials in further chapters.

Table 14. R2 values for the Randles cell.

R2 Resistor	Labeled Value	Measured Value
R2.1	20 kΩ	20.374 kΩ
R2.2	30 kΩ	29.624 kΩ
R2.3	40 kΩ	40.026 kΩ
R2.4	80 kΩ	79.23 kΩ
R2.5	120 kΩ	118.75 kΩ
R2.6	250 kΩ	245.92 kΩ
R2.7	500 kΩ	503.95 kΩ
R2.8	1 MΩ	1.0091 MΩ

A LSV experiment with each resistor of Table 14 allows us to know the current range of the potentiostat and its linearity. A waveform voltage from -2 to 2 V with a scan rate of 50 mV/s will provide the information about the current range and the linearity of the system. The conditions for this experiment are in Table 15. The connection between the PSoC and the Randles circuit are according to the Figure 43. An oscilloscope is going to read the WE vs. RE voltage during the LSV experiments. Hence, this setup allows us to know the potentiostat current range and its linearity.

Table 15. Conditions for the Current Range and Linearity Characterization.

Circuit of Figure 35 in the PSoC	Yes
Randles Cell connected	Yes
Voltage supply for the PSoC	5V
Turn the instruments on waiting half hour to use them	Yes

Appendix D shows the LSV graphs for each resistor of Table 14. The previous paragraph describes the experimental conditions for those trials. For each digital value in the waveform generator, there is a unique analog voltage equal to the digital. The goal of Appendix D graphs is to compare the expected values against the measured. Hence, someone can observe the linearity and the congruence between the digital and the analog values. However, numerical values provide a better understanding due to the likeness of several graphs.

Table 16 presents the preliminary results taken with an oscilloscope comparing the errors against the full scale. The full scale of these experiments go from -2 to 2 V. The Mean Error Percent is the average of all absolute errors for a specific LSV experiment. The Maximum Error Percent is the highest error in a given LSV trial. The main disadvantage of the oscilloscope is that this instrument is for visualization instead of measurement precision. However, Table 16 provides an idea of the potentiostat behavior.

In the preliminary experiments the resistor R2, from the Randles circuit of Figure 42, illustrates that the potentiostat has a good response with values above of 30 kΩ. Whit that resistor, the maximum current to detect is ± 66.96 µA according to Table 16. The minimum current of ± 1.98 µA takes place when R2 has a value of 1 MΩ. In this range of

resistors, the potentiostat presents a good linearity having a Mean Error Percent against the full scale of 1.26% with a maximum error of 3.78%. **Thus, the potentiostat can drive currents of ± (1.98 to 67.06) µA in a range of -2 V to 2 V**.
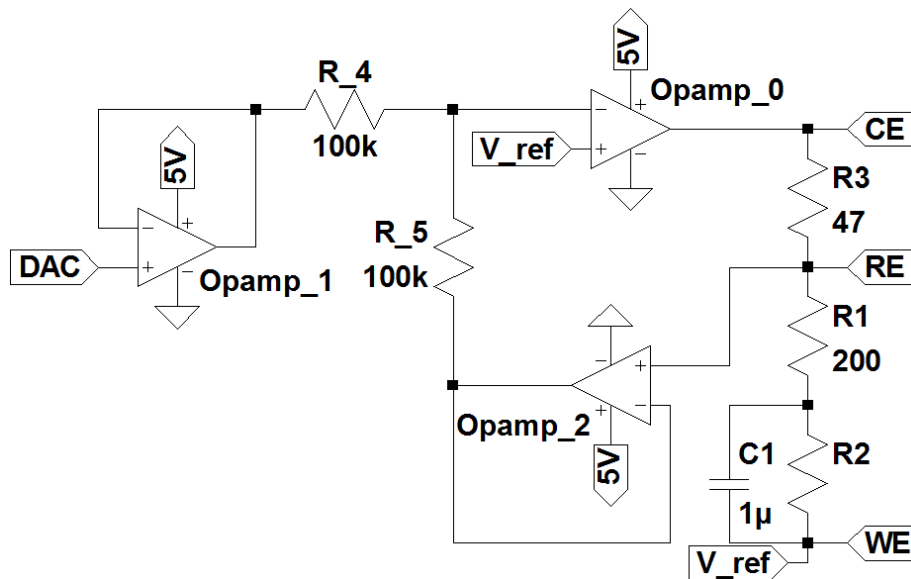
Figure 43. Schematic of PSoC with the Randles Cell.

Table 16. Preliminary results from the LSV experiments.

Resistor	Mean Error Percent vs. Full Scale	Maximum Error Percent vs. Full Scale	Voltage Range	Current Range
R2.1	7.24 %	16.43 %	± 2 V	± 97.21 µA
R2.2	0.98 %	3.03 %	± 2 V	± 67.06 µA
R2.3	1.07 %	3.35 %	± 2 V	± 49.72 µA
R2.4	1.13 %	3.27 %	± 2 V	± 25.18 µA
R2.5	1.16 %	3.48 %	± 2 V	± 16.81 µA
R2.6	1.22 %	3.52 %	± 2 V	± 8.12 µA
R2.7	1.24 %	3.65 %	± 2 V	± 3.97 µA
R2.8	**1.26 %**	**3.78 %**	± 2 V	± 1.98 µA

4.2 Potentiostat Characterization

The potentiostat characterization studies the relationship between the digital values of the waveform generator and the WE vs. RE voltage. In this section, the WE is at the V_ref terminal of Figure 35 to avoid any effects of the TIA as before. This particular section is going to explore the capacity of the waveform generator to deliver signals consistent with the electrochemical trials. The experiments to present are going to be inside of the current and the voltage range found in the last section.

The following subsections will help us to test hypothesis one in the operational range of the potentiostat. The idea is to record all the waveform for each technique to

check the congruence with parameters. The following experiments use the conditions from Table 15, and the connections are according to Figure 43 with an R2 value of 120 kΩ. The value of 120 kΩ is a middle point of the potentiostat resistor range. Therefore, these conditions allow us to test the waveform generator.

4.2.1 LSV Characterization

The LSV characterization allows us to accept or reject hypothesis one just for this technique. Three different trials are going to test this hypothesis for this method according to Table 17. From these experiments, the oscilloscope will record the WE vs. RE voltage, and those values are going to be compared against the expected. It is noteworthy that the LSV and the CV have a quiet time of one second to wait for the voltage settlement before to start a trial. Hence, someone can observe a small constant before the ramp beginning.

Table 17. Parameters for the LSV characterization.

	Test 1	Test 2	Test 3
Initial Voltage	1 V	0	-2
Final Voltage	-2 V	1	0
Scan Rate	100 mV/s	10 mV/s	50 mV/s

Figure 44 shows the congruence between Test 1 from Table 17 and the experimental results. In the vertical axis, each square has a value of one volt while in the horizontal each square represents 5 seconds. The test last 31 seconds and it goes from 1 to -2 V. There is no necessity of a numerical analysis because the oscilloscope is an instrument for visualization. Observing the figure, someone can realize that the oscilloscope measurements agree with the parameters.

Figure 44. Test 1 for the LSV characterization.

Figure 45 shows the congruence between Test 2 from Table 17 and the experimental results. In the vertical axis, each square has a value of 0.5 volts while in the horizontal each square represents 25 seconds. The test lasts 101 seconds, and it goes from 0 to 1 V. As before, there is no necessity of a numerical analysis because the

oscilloscope is an instrument for visualization. Observing the figure, someone can realize that the oscilloscope measurements agree with the parameters.

Figure 45. Test 2 for the LSV characterization.

Figure 46 shows the congruence between Test 3 from Table 17 and the experimental results. In the vertical axis, each square has a value of one volt while in the horizontal each square represents 5 seconds. The test last 41 seconds, and it goes from -2 to 0 V. As before, there is no necessity of a numerical analysis because the oscilloscope is an instrument for visualization. Observing the figure, someone can realize that the oscilloscope measurements agree with the parameters.

Figure 46. Test 3 for the LSV characterization.

Figure 44, Figure 45, and Figure 46 proves that the PSoC can generate LSV waveforms in agreement with the parameters of Table 17. The duration of the LSV experiments may seem incongruent with the table. The quiet time is the responsible of such perception due to a constant value before the ramp. However, the DSC characterization demonstrates the accurately time management by the waveform generator. Regarding the potential, all waveforms show consistency with Table 17.

4.2.2 CV Characterization

The CV characterization allows us to accept or reject hypothesis one just for this technique. Three different trials are going to test this hypothesis for this method according to Table 18. From these experiments, the oscilloscope will record the WE vs. RE voltage, and those values are going to be compared against the expected. It is noteworthy that the LSV and the CV have a quiet time of one second to wait for the voltage settlement before to start a trial. Hence, someone can observe a small constant before the ramp beginning.

Table 18. Parameters for the CV characterization.

	Test 1	Test 2	Test 3
Initial Voltage	0 V	1 V	-0.5 V
Maximum Voltage	0.5 V	1.5 V	0 V
Minimum Voltage	-0.5 V	0.5 V	-2 V
Cycles	3	5	5
Initial Scan Direction	Positive	Negative	Positive
Scan Rate	150 mV/s	250 mV/s	500 mV/s

Figure 47 shows the congruence between Test 1 from Table 18 and the experimental results. In the vertical axis, each square has a value of 0.2 volts while in the horizontal each square represents 5 seconds. The test last 41 seconds. There is no necessity of a numerical analysis because the oscilloscope is an instrument for visualization. Observing the figure, someone can realize that the oscilloscope measurements agree with the parameters.
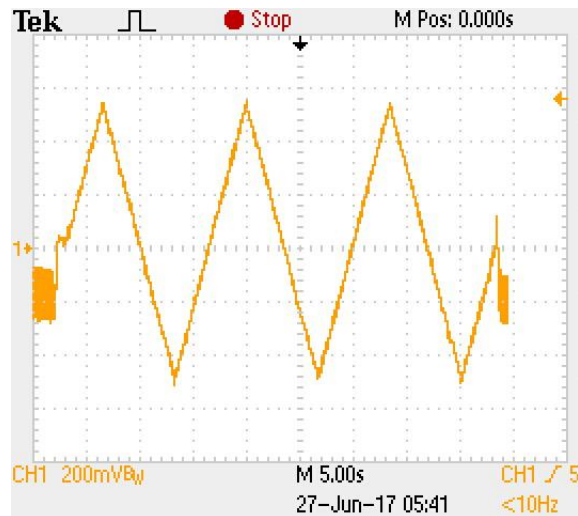
Figure 47. Test 1 for the CV characterization.

Figure 48 shows the congruence between Test 2 from Table 18 and the experimental results. In the vertical axis, each square has a value of 0.5 volts while in the horizontal each square represents 5 seconds. The test last 41 seconds as well. As before, there is no necessity of a numerical analysis because the oscilloscope is an instrument

for visualization. Observing the figure, someone can realize that the oscilloscope measurements agree with the parameters.
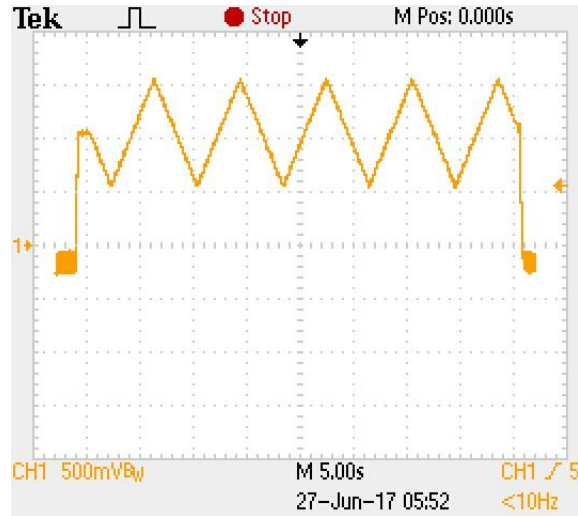
Figure 48. Test 2 for the CV characterization.

Figure 49 shows the congruence between Test 3 from Table 18 and the experimental results. In the vertical axis, each square has a value of one volt while in the horizontal each square represents 5 seconds. The test last 41 seconds as well. As before, there is no necessity of a numerical analysis because the oscilloscope is an instrument for visualization. Observing the figure, someone can realize that the oscilloscope measurements agree with the parameters.
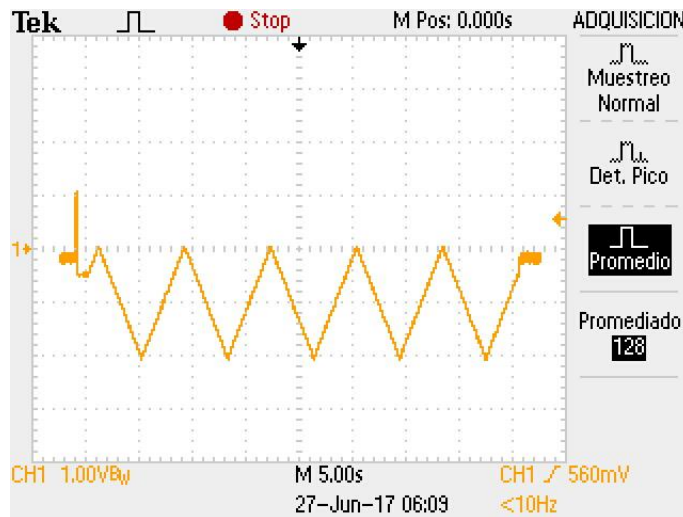
Figure 49. Test 3 for the CV characterization.

Figure 47, Figure 48, and Figure 49 proves that the PSoC can generate CV waveforms in agreement with the parameters of Table 18. The duration of the CV experiments may seem incongruent with the table. The quiet time is the responsible of such perception due to a constant value of one second before the ramps. However, the DSC trials demonstrate the accurately time management by the waveform generator. Regarding the potential, all waveforms show consistency with Table 18.

4.2.3 DSC Characterization

The DSC characterization allows us to accept or reject hypothesis one just for this technique. Three different trials are going to test this hypothesis for this method according to Table 19. From these experiments, the oscilloscope will record the WE vs. RE voltage, and those values are going to be compared against the expected. In this technique, there is an explicit Quiet Time. Hence, a time analysis can be more accurate than the previous electrochemical trials.

Table 19. Parameters for the DSC characterization.

	Test 1	Test 2	Test 3
Last Step	0 V	0 V	1
First Step	-2 V	2	-1.75
Pulse Width	10 s	15 s	25 s
Quiet Time	20 s	10 s	20 s

Figure 50 shows the congruence between Test 1 from Table 19 and the experimental results. In the vertical axis, each square has a value of one volt while in the horizontal each square represents 5 seconds. The test last 20 seconds. There is no necessity of a numerical analysis because the oscilloscope is an instrument for visualization. Observing the figure, someone can realize that the oscilloscope measurements agree with the parameters.
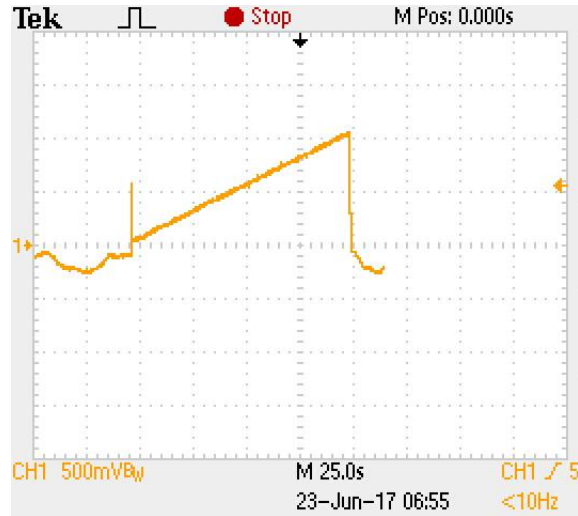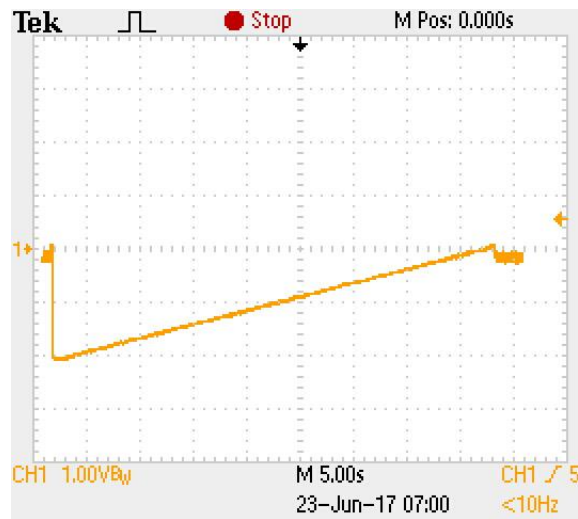

Figure 50. Test 1 for the DSC characterization.

Figure 51 shows the congruence between Test 2 from Table 19 and the experimental results. In the vertical axis, each square has a value of one volt while in the horizontal each square represents 5 seconds as well. The test last 30 seconds. There is no necessity of a numerical analysis because the oscilloscope is an instrument for visualization. This experiment also shows Δt between the two vertical lines giving a value of 15 seconds corresponding to the pulse width. Hence, someone can realize that the oscilloscope measurements agree with the parameters.

Figure 51. Test 2 for the DSC characterization.

Figure 52 shows the congruence between Test 3 from Table 19 and the experimental results. In the vertical axis, each square has a value of one volt while in the horizontal each square represents 10 seconds. The test last 50 seconds. There is no necessity of a numerical analysis because the oscilloscope is an instrument for visualization. This experiment also shows Δt between the two vertical lines giving a value of 50 seconds corresponding to the test duration. Hence, someone can realize that the oscilloscope measurements agree with the parameters.
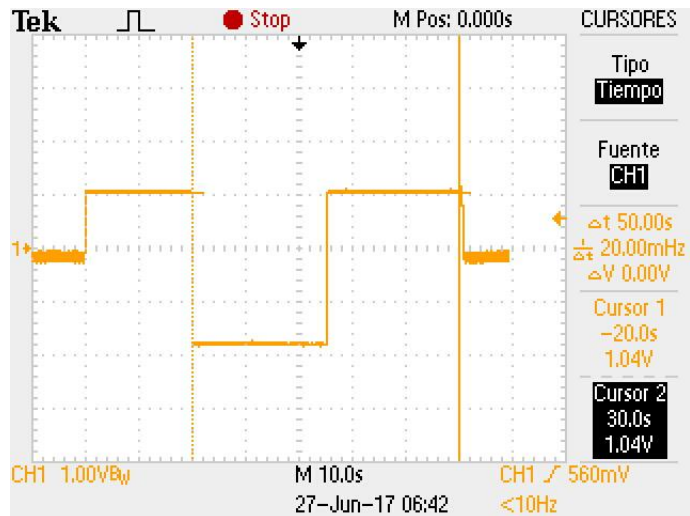
Figure 52. Test 3 for the DSC characterization.

Figure 50, Figure 51, and Figure 52 proves that the PSoC can generate DSC waveforms in agreement with the parameters of Table 19. The last two figures demonstrate that the waveform generator can manage the time of the signals accurately. Regarding the potential, all waveforms show consistency with Table 19. Graphs from Figure 44 to Figure 52 allow us to accept hypothesis one. Therefore, the PSoC can generate several waveforms in a single chip precisely.

4.3 Current Measurements

The current measurement is the circuit wrapped by the blue lines in Figure 41. It has a TIA and it inside of the PSoC 5. Also, it uses a $\Delta\sum$ ADC of 18 bits to make the analog to digital conversion. A characterization of those modules is necessary to get reliable measurements from the prototype. The following subsections describe the real TIA resistors and the offset of the TIA and the ADC. Hence, with all that information, someone can make the appropriate compensations

4.3.1 ADC Offset Voltage

The ADC characterization is about of the ADC offset measurement. The gain does not represent an issue in this converter. Figure 53 shows the schematic to read the ADC error. The idea is to connect both inputs to the same terminal and measure the output voltage. In this case, the V_ref terminal feeds the buffers to avoid any impedance mismatch when the TIA output provides the signal. An average of 40,000 samples gives an ADC offset of **-61.056 µV**. This value may seem low. However, a compensation is necessary because of the management of low currents.
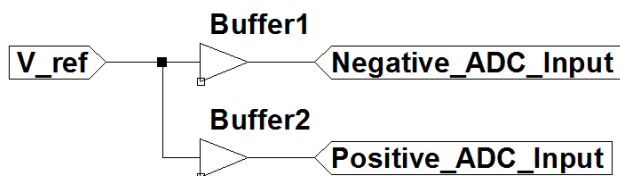
Figure 53. Schematic for the ADC Offset Voltage Characterization.

4.3.2 TIA Resistors Characterization

The TIA resistors characterization helps us to establish the proper gains in the prototype. R2 represents the resistor of the TIA module in Figure 54. Eight values of that resistor are going to be inferred introducing a voltage and reading the output. In each case, R1 is close to R2 to get the input voltage at the output of the circuit (Figure 54). The V1 voltage source is going to take three voltage values for each R2. The first value is zero to know the offset voltage. The second and the third value are ±1.024 V respectively. They are the upper and the lower limit of the ADC input voltage. Table 20 shows the characterization outcome.

Table 20 relies on Equation 4.1 to know the real values of R2, and it takes into account the offset voltage of each resistor. In that table, the Expected R2 has all the values from the manufacturer for all the resistor of the TIA module. V1, R1, and the ADC Measurement are according to the Figure 54. The Calculated R2 is the value that comes from Equation 4.1 considering the offset voltage. The R2 Average is the mean of the upper and the lower values of the ADC input voltage. This average takes place due to no linearities in the circuit. Therefore, the R2 Average column has the most accurate resistor values of the TIA module.
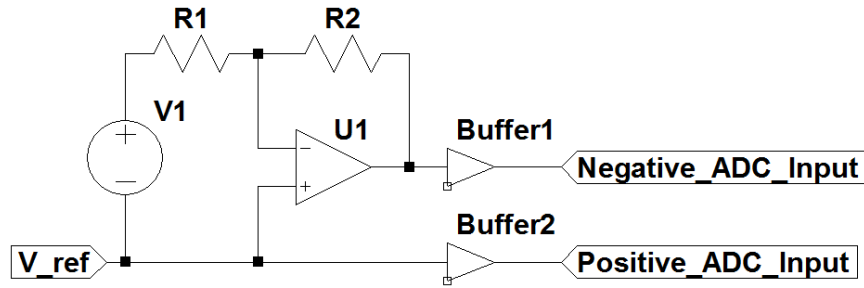
Figure 54. Schematic for the TIA Resistors Characterization.

$$V_{out} = -V_{in} \frac{R2}{R1}$$

4.1

Table 20. TIA Resistors Characterization.

Expected TIA Resistor	V1	R1	ADC Measurement	Calculated R2	R2 Average
20000 Ω	0 V	18985 Ω	-6.13E-03 V		
20000 Ω	1.0244 V	18985 Ω	1.01734 V	18967.85 Ω	**18971.46 Ω**
20000 Ω	-1.0241 V	18985 Ω	-1.0297 V	18975.07 Ω	
30000 Ω	0 V	28633 Ω	-6.19E-03 V		
30000 Ω	1.0244 V	28633 Ω	1.01792 V	28624.97 Ω	**28636.77 Ω**
30000 Ω	-1.024 V	28633 Ω	-1.03075 V	28648.58 Ω	
40000 Ω	0 V	38303 Ω	-6.14E-03 V		
40000 Ω	1.0244 V	38303 Ω	1.01725 V	38265.30 Ω	**38272.14 Ω**
40000 Ω	-1.0241 V	38303 Ω	-1.0296 V	38278.99 Ω	
80000 Ω	0 V	77480 Ω	-6.25E-03 V		
80000 Ω	1.0245 V	77480 Ω	1.01753 V	77425.93 Ω	**77433.47 Ω**
80000 Ω	-1.024 V	77480 Ω	-1.02974 V	77441.02 Ω	
120000 Ω	0 V	116900 Ω	-6.15E-03 V		
120000 Ω	1.0242 V	116900 Ω	1.0173 V	116814.90 Ω	**116828.09 Ω**
120000 Ω	-1.0241 V	116900 Ω	-1.02974 V	116841.27 Ω	
250000 Ω	0 V	244650 Ω	-6.14E-03 V		
250000 Ω	1.0244 V	244650 Ω	1.01776 V	244532.24 Ω	**244583.12 Ω**
250000 Ω	-1.0241 V	244650 Ω	-1.03018 V	244634.00 Ω	
500000 Ω	0 V	489830 Ω	-6.16E-03 V		
500000 Ω	1.0244 V	489830 Ω	1.01922 V	490300.80 Ω	**490370.41 Ω**
500000 Ω	-1.0241 V	489830 Ω	-1.03154 V	490440.02 Ω	
1000000 Ω	0 V	982300 Ω	-6.10E-03 V		
1000000 Ω	1.0244 V	982300 Ω	1.01739 V	981430.46 Ω	**981623.90 Ω**
1000000 Ω	-1.0241 V	982300 Ω	-1.0297 V	981817.33 Ω	

Table 21 shows the errors eliminated through the characterization of the TIA resistors taking the calculated values as the reals. The biggest errors take place at the lower values of these resistors. At high values, the error is minimum. This procedure allows us to compensate all the resistor with more precise values in the PUIS. Moreover, the algorithm eliminates errors as big as 5.42 % with this information. Hence, the calculated values allow us to have a better accuracy when the device is reading the Redox current.

Table 21. Error percent eliminated in the characterization for the TIA resistors.

Resistor	Expected TIA Resistor Values	Value Calculated (R2 Average)	Error Percent Eliminated
R2.1	20000 Ω	18971.46 Ω	**5.42 %**
R2.2	30000 Ω	28636.77 Ω	4.76 %
R2.3	40000 Ω	38272.14 Ω	4.51 %
R2.4	80000 Ω	77433.47 Ω	3.31 %
R2.5	120000 Ω	116828.09 Ω	2.72 %
R2.6	250000 Ω	244583.12 Ω	2.21 %
R2.7	500000 Ω	490370.41 Ω	1.96 %
R2.8	1000000 Ω	981623.90 Ω	1.87 %

4.3.3 TIA Offset Voltage

An equations system is necessary to know the TIA offset voltage. This process is more challenging than the ADC offset voltage. The equations system comes from the offset voltage error of Figure 55. That error follows the Equation 4.2 considering the Vos and the bias current effects from the OPAMP [53]. The letter "E" represents the measurement error of the circuit. Vos is the offset voltage of the OPAMP. The "in" variable represents the current through the TIA inverting input. To make the equations system, R1 needs two values to get two error measurements. Table 22 shows the change of R1 and the error of the entire circuit.

$$E = (1 + \frac{R2}{R1})Vos + ADC_{Vos} + R2 * in \qquad 4.2$$

Table 22. Change of R1 to get two different measurement errors.

R1	R2 Average	E
18975 Ω	18971.5 Ω	-6.15979 mV
10.025 MΩ	18971.5 Ω	-2.80652 mV

Equation 4.3 comes from the equations system neglecting the ADC offset voltage and the bias current. Such consideration takes place because both values remain equal despite the R1 changes. Hence, when one equation subtracts the other, someone can know the Vos value. It is noteworthy that the error values of Table 22 are an average of 40,000 samples. The Equation 4.3 does not take into account the effects of thermal drift, CMRR, PSRR, or the output swing. With the values of Table 22, it turns out that Vos is of **-3.36034 mV** which represents the 0.084 % of the full scale (4.0 V)

$$Vos = \frac{E_1 - E_2}{(1 + \frac{R2}{R1_1}) - (1 + \frac{R2}{R1_2})}$$
4.3
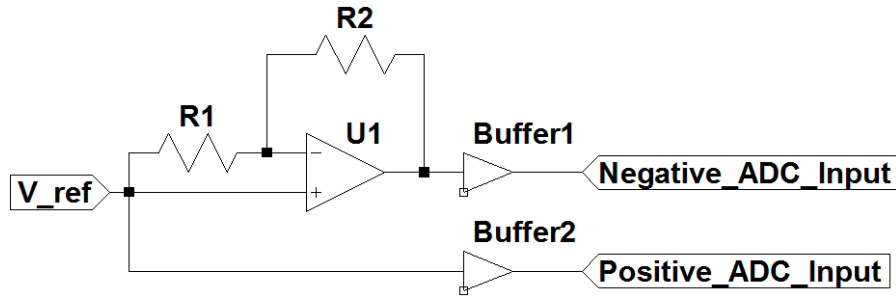
Figure 55. Schematic for the TIA Offset Voltage Characterization.

4.3.4 TIA Bias Current and the TIA Resistor Compensation

The bias current has a strong relationship with the TIA resistor value, and both variables produce an error at the OPAMP output. The bias current is the electron flow that goes inwards at the input terminals of the OPAMP [53]. However, at the non-inverting input of the TIA, there is no resistor. Hence, part of the measurement error comes from the current that goes into the inverting input because it has the TIA resistor connected.

The current through the TIA inverting input relies on the TIA resistor values. Hence, when the resistor changes its values, the current changes as well. Someone can know that current considering the Equation 4.2 from Figure 55. The zero values of V1 from Table 20 help us to use the Equation 4.2. Thus, with the Vos, the ADC offset voltage, the Table 20, and the Equation 4.2, the current through the TIA inverting input is easy to calculate. Table 23 shows the different bias currents for the inverting terminal, and it also compares the accuracy of the calculated and the expected TIA resistor.

Table 23. Inverting Bias Current and the characterization effects.

Expected R2	R2 Calculated	Expected R2 Accuracy	R2 Calculated Accuracy	In
20 kΩ	18971.46 Ω	**97.29 %**	99.99 %	3.40E-08 A
30 kΩ	28636.77 Ω	97.61 %	**99.97 %**	2.06E-08 A
40 kΩ	38272.14 Ω	97.74 %	99.99 %	1.67E-08 A
80 kΩ	77433.47 Ω	98.34 %	99.99 %	6.77E-09 A
120 kΩ	116828.09 Ω	98.64 %	99.99 %	5.35E-09 A
250 kΩ	244583.12 Ω	98.89 %	99.98 %	2.59E-09 A
500 kΩ	490370.41 Ω	99.01 %	99.99 %	1.27E-09 A
1 MΩ	981623.90 Ω	99.06 %	99.99 %	6.89E-10 A

Table 23 shows that the characterization of TIA resistors can reduce the Redox current measurement error from 2.71 to 0.03 %. This table was created using Table 20 replacing the expected and the calculated values of R2 to infer the voltage output of the

circuit (Figure 54). The differences between the calculated values and the measurements give us the accuracy. Also, the ADC offset voltage, the bias current characterization, and the Vos value helps a lot reducing errors. These values are going to be useful in the next section to make the proper compensations reading the digital values from the PES.

4.4 Compensations and Energy Consumption

This section is about the power consumption in the PES and the compensations in the algorithms. The power consumption will describe the battery features that can power the PES. The compensations describe all the changes to do that comes from the characterizations. Those changes increase the accuracy of the entire system. Hence, this section describes the equations and the parameters to know the Redox current and the amount of energy for the PES.

4.4.1 Power Consumption

One important feature of the PES is the energy consumption because that establish the power requirements. In the PES, exists several states that affect directly that consumption. When the PES is waiting for commands, and it is not executing a trial, the PES saves power. That state is called standby. When the PES is working in some trial, the energy consumption increases because it needs to use several circuits to read the Redox current. Table 24 shows the PES power consumption in different states with a source voltage of 5 volts.

Table 24. PES Power Consumption.

PES at:	Stand By	50 SPS	1000 SPS	2000 SPS
Current	27.5 mA	35.5 mA	39.5 mA	41.5 mA
Power Consumption	137.5 mW	177.5 mW	197.5 mW	207.5 mW

The currents of Table 24 where measured connecting an amperemeter between the power source and the PES. The Test 1 from Table 17 is a LSV experiment, and it was used to get the power consumption of Table 24. From those experiments, the standby state consumes 137.5 mW while at the maximum SPS that consumption is of 207.5 mW. Therefore, the energy requirements can go from 137.5 to 207.5 mW for the PES.

4.4.2 PES Compensation

The PES has just one change. That change just removes the voltage offset of the potentiostat output. This adjustment comes from the real reference voltage value because the algorithm ideally takes 2.048 V instead of 2.044 V. The value of 2.048 V comes from the expected value of the PGA output (1.024 V multiplicated by 2). The compensation is in the Miscellaneous.c file inside of the function "Put_DAC_Voltage" where the waveform is subtracted by 4. Hence, with that adjustment, the WE vs. RE voltage has an offset voltage of zero.

4.4.3 PUIS Compensation

The PUIS compensation is an equation that takes into account the bias current lost at the inverting input and the voltage error of the TIA and the ADC. The equation 4.4 describes the Redox current for each TIA resistor replacing the "X" of R2 for one value of Table 25. It is noteworthy that this equation is true for the circuit wrap by the blue lines in Figure 41. The ADC value represents the digital voltage of the TIA output. The offset voltage of the ADC and the OPAMP is in the previous section. Therefore, this equation needs to be contemplated in the code of the PUIS to have the most accurate results.

$$i_{R2.X} = \frac{ADC - ADC_{Vos} - (1 + \frac{R2.X}{R1})Vos - R2.X * in_{R2.X}}{R2.X} + in_{R2.X} \qquad 4.4$$

Table 25. Values to use to reduce the Error.

TIA Resistors (R2.X)	Resistors Value	Bias Current (inverting input)
R2.1	18971.46 Ω	3.40E-08 A
R2.2	28636.77 Ω	2.06E-08 A
R2.3	38272.14 Ω	1.67E-08 A
R2.4	77433.47 Ω	6.77E-09 A
R2.5	116828.09 Ω	5.35E-09 A
R2.6	244583.12 Ω	2.59E-09 A
R2.7	490370.41 Ω	1.27E-09 A
R2.8	981623.90 Ω	6.89E-10 A

Chapter 5. Electrochemical Experiments.

Chapter 5 performs the experiments to approve or reject hypothesis two, three, six, and seven. Therefore, it is going to present the results of the electrochemical experiment from the prototype and the commercial potentiostat system. The idea for these tests is to compare results and watch how much they alike. A good performance of the prototype system takes place if both results are congruent. In general, that congruence allows us to accept the hypothesis for each electrochemical method.

This chapter gives more information about the following points presented in the methodology:

34. Description of the electrochemical cell design, the analyte, the electrolyte, and the electrodes for the Redox experiments.
35. Description of the materials, solutions, and procedures for the Redox experiments.
36. Experimental design to evaluate the potentiostat performance. Also, this design has some experiments where the wireless data traffic is as high as possible to probe hypothesis seven.
37. Presentation of the electrochemical result comparing the prototype with a commercial potentiostat system like some researchers has been done [2], [10], [20]. This comparison allows us to probe hypothesis two and six.
38. Analysis of the electrochemical results taken as reference the current values from the commercial instrument. This comparison will describe in a quantitative way how far is the prototype measurements from that instrument.

The conclusions of the results are in the following chapter, and it explains a particular issue.

5.1 EC Design, Analyte, Electrolyte, and Electrodes.

The EC design fulfills the small A/V conditions with the three-electrodes cell (Figure 7). Those conditions state that the WE area should be small compared with the solution volume (electrode of several millimeters and down to 10 mL in the solution) [85]. The small A/V conditions allow us to get comparable data because the Redox reaction does not modify the analyte concentration in bulk. The three-electrodes cell is more accurate than the two-electrode configuration because RE keeps a stable voltage in the solution. Also, the cell is of plastic, and it has a capacity of 20 mL. Hence, the following experiments are going to be with this setup.

Scientist and engineers wildly use Potassium Ferricyanide (PF) to test the performance of many potentiostat systems [1], [86]–[88]. They largely use this analyte due to be electrochemically active, and because it has a reversible behavior [89], [90]. $K_3[Fe(CN)_6]$ is the molecular formula of PF. Ferricyanide ($Fe(CN)_6^{3-}$) ions from PF can be reduced to Ferrocyanide ($Fe(CN)_6^{4-}$) as Equation 5.1 shows. Likewise, Ferrocyanide ions can be oxidized to Ferricyanide as Equation 5.2 shows. However, someone can achieve those Redox reactions, driving the proper potential at the electrodes. Hence, PF is going to be the analyte in the following experiments.

$$Fe(CN)_6^{3-} + e \rightarrow Fe(CN)_6^{4-} \qquad\qquad 5.1$$
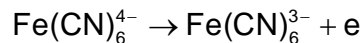
$$Fe(CN)_6^{4-} \rightarrow Fe(CN)_6^{3-} + e \qquad\qquad 5.2$$

Potassium Chloride (PC) has an excellent conductivity to support the Redox current from the reaction in the EC [91]. It is an electrolyte with a conductivity of 0.11/(ohm*cm) at a concentration of 1.05 M in water as a solvent. KCL is the molecular formula for PC. Furthermore, PC is widely used in several investigations like this one to allow that current flow [1], [86], [87]. Also, the Ag/AgCL electrode uses PC as an electrolyte for its polarization [79]. Hence, PC is going to be the electrolyte in the following experiments.

The silver/silver chloride electrode (Ag/AgCL) is one of the most common reference electrodes in electrochemistry [79]. This electrode can work with PC as a supporting electrolyte in a solution. Usually, the silver wire of the electrode is inside of the glass capillary with some silver chloride. The electrode area in contact with the solution is not relevant because there is no current flow through it. Therefore, the potential measurement at this electrode is precise. Hence, Ag/AgCL is going to be the RE in the following experiments

Scientist and engineers use the platinum wire in the three-electrode system as a CE because it reacts uneasily [50]. Also, they can use silver, but this material has more chances to react than those from platinum. The CE has to supply the current for the Redox reaction in the three-electrode cell [92]. Therefore, the electron-transfer is fast with this material for many reactions. Also, the potential for the platinum oxidation is relatively high while the potential for the platinum reduction is a little more limited [93]. However, platinum wire is going to be the CE in the following experiments because it has better features than other electrodes.

One of the most popular carbon electrodes to perform Redox reactions is the Glassy Carbon Electrode (GCE) [93]. This electrode is also known as vitreous carbon. The GCE is hard, highly conductive, resistant to chemical attacks, isotropic, and impermeable to gasses [94]. Those properties are highly desirable in an electrode to be suitable for many applications, especially in non-aqueous solvents. Hence, the GCE is going to be the WE in the following experiments.

5.2 Materials, Solutions, and Procedures.

The prototype results will be compared against to the Electrochemical Analyzer-Workstation (EAW), model 700E series, from CH Instruments. The electrochemical techniques to perform are LSV, CV, and DSC. The materials and suppliers for the experiments are in Table 26. The idea is to switch between potentiostats systems without modifying the other variables. Thus, the results are going to be comparable when someone performs the same trial under the same conditions. Therefore, that allows a level abstraction above the electrochemistry, and the electronic issues of the potentiostat prototype system will be more clear.

The Randles-Sevcik equation relates the analyte concentration and the current peak from a CV experiment in a reversible reaction [95]. Table 27 shows the parameters of the equation and the current result. The issue is that Zaib et al. report the diffusion coefficient of the PF in 0.1 M of PC and this value is different in our trials [96]. Also, the

peak measure in a CV involves making graphical arrangement for it [79]. Moreover, the concentration of the sample can have a certain inaccuracy. Therefore, the results of the following experiments can be different from the Randles-Sevcik equation.

Table 26. Materials and Suppliers for the Experiments.

Material.	Supplier.
Potassium Ferricyanide.	Sigma-Aldrich, CAS: 13746-66-2.
Potassium Chloride.	Fermont, presentation no. 24842.
Working Electrode.	BASi model MF-2012, ϕ=3 mm.
Reference Electrode.	BASi model MF-2052.
Counter Electrode.	BASi model MW-4130.

Before to start each experiment the working electrode has to be clean. It is noteworthy that the geometric area of the WE is always a circle for all the trials. The cleaning of this electrode cannot be mechanical due to the risk of damage the electrode surface [93]. In this case, the electrode surface is submerged in a solution with 30% of hydrogen peroxide around ten seconds. The rest of that solution is double distilled water. This procedure allows us to start each experiment without impurities.

Table 27. Solution concentration and expected current from CV experiments.

	Solution 1	Solution 2
PF Concentration	1 mM	10 mM
PC Concentration	0.5 M	
Solvent	Double distilled water	
Diffusion Coefficient	7.6 µcm^2/s [96]	
Scan Rate	10 mV/s	
Temperature	25 ºC	
Electrode Diameter	3 mm	
Randles-Sevcik Peak	5.23 µA	52.3 µA

After the cleaning, the electrode activation is the next step. This procedure is necessary to prepare the electrode surface for interchanging electrons in the EC [93]. Table 28 describes the experiments and the sequence to execute them goes from one to four. The solution to make the activation was 0.5 M of PC in double distilled water. After the activation, the EC is ready to work with an analyte. Thus, each electrochemical experiment has to have its proper cleaning and electrode activation before to start a Redox reaction.

5.3 Experimental Design.

It is noteworthy that all the following voltage values, in tables or graphs from this section until the end of the chapter, are versus the RE potential. The setup of the following experiments is according to the previous sections descriptions. Henceforth, if a potential value has no reference, it is referenced to the RE voltage. Also, each experimental

condition makes reference to one trial. Therefore, the number of experimental conditions is the number of electrochemical experiments.

Table 28. Electrode activation experiments.

	Experiment 1	Experiment 2	Experiment 3	Experiment 4
Scan Rate	500 mV/s	250 mV/s	100 mV/s	50 mV/s
Cycles	50	25	10	5
Method	Cyclic Voltammetry			
Initial Voltage	0.25 V			
Maximum Voltage	0.65 V			
Minimum Voltage	-0.15 V			
Initial Scan Direction	Positive			

Table 29 describes the conditions for the CV experiments. The conditions rely on the previous investigation where similar values were used [10], [12]. The only changes between conditions are the scan rate value. According to the Randles-Sevcik equation, that changes will have a different current response [95]. Hence, those conditions allow us to evaluate the behavior of the potentiostat prototype system at different currents levels and watch the performance.

Table 29. Cyclic Voltammetry conditions for the experiments.

	Conditions 1	Conditions 2	Conditions 3	Conditions 4
Scan Rate	10 mV/s	100 mV/s	250 mV/s	500 mV/s
Initial Voltage	0.25 V			
Minimum Voltage	-0.15 V			
Maximum Voltage	0.65 V			
Cycle	Fifth			
Initial Scan Direction	Positive			
Analyte	$Fe(CN)6$, 1 mM			
Electrolyte	KCL, 0.5 M			
Working Electrode	Glassy Carbon Electrode			
Reference Electrode	Silver/silver chloride electrode			
Counter Electrode	Platinum Wire			

Table 30 describes the conditions (cond.) for the DSC experiments. The small changes between the First and the Last Step allow us to explore the current prototype Lowest Limit of Detection. The Pulse Width was set to 62 seconds because the current gets close to the steady-state response at that time. The Last Step is practically the OPC. For the Solution 1 of Table 27, the OPC value is of 0.308 V. Therefore, those conditions allow us to know the working range of the PES.

Table 31 describes the conditions for the LSV experiments. The conditions rely on the previous investigation where similar values were used [10], [12]. The changes are the scan rate value and the direction of this variable. These experiments are very similar to

those performing a CV. Thus, they also allow us to evaluate the behavior of the potentiostat prototype system at different currents levels and watch the performance.

Table 30 DSC conditions for the experiments.

	Cond. 5	Cond. 6	Cond. 7	Cond. 8	Cond. 9
First Step	0.325 V	0.315 V	0.305 V	0.295 V	0.195 V
Last Step	0.310 V				
Pulse Width	62 seconds				
Quite Time	62 seconds				
Analyte	Fe(CN)6, 1 mM				
Electrolyte	KCL, 0.5 M				
Working Electrode	Glassy Carbon Electrode				
Reference Electrode	Silver/silver chloride electrode				
Counter Electrode	Platinum Wire				

Conditions 16 from Table 32 allow us to explore the highest limit of detection of the prototype. The main change in these conditions is a higher concentration of the analyte using the Solution 2 from Table 27. A minor change is the use of a homemade silver to be the CE. However, this electrode reduces the Maximum Voltage because above that value the electrode can react [97]. Thus, the disadvantages of this electrode are notable.

Table 31. LSV conditions for the experiments.

	Cond. 10	Cond. 11	Cond. 12	Cond. 13	Cond. 14	Cond. 15
Initial Voltage	0.65 V	-0.15 V	0.65 V	-0.15 V	0.65 V	-0.15 V
Final Voltage	-0.15 V	0.65 V	-0.15 V	0.65 V	-0.15 V	0.65 V
Scan Rate	10 mV/s	10 mV/s	100 mV/s	100 mV/s	500 mV/s	500 mV/s
Analyte	Fe(CN)6, 1 mM					
Electrolyte	KCL, 0.5 M					
WE	Glassy Carbon Electrode					
RE	Silver/silver chloride electrode					
CE	Platinum Wire					

Conditions 17 from Table 32 allow us to know the effect of the noise without a proper filter in the prototype. These conditions also change the circuit from Figure 35 where capacitor value is reduced to 4.6 pF. All the previous conditions use the indicated capacitor value of the circuit. With this, someone can realize of the relevance of a filter in a prototype system. Thus, the resulting graph could show a noisy signal.

Table 33 shows the experimental conditions to probe or reject hypothesis seven. The idea is to send many data wirelessly to stress the Bluetooth communications between the PES and PUIS. According to the table, those conditions take 2000 SPS, and this is the maximum value for that variable. The other conditions are not relevant because they do not probe the wireless communication as those from the table. Hence, the communication system has to keep the congruency of the data when it arrives at the PUIS to be accepted.

Table 32. Conditions to explore the highest limit of detection and the prototype noise.

	Conditions 16	Conditions 17
Scan Rate	10 mV/s	10 mV/s
Initial Voltage	0.40 V	0.262 V
Minimum Voltage	-0.10 V	-0.10 V
Maximum Voltage	0.53 V	0.50 V
Cycle	Fifth	Fifth
Initial Scan Direction	Positive	Positive
Analyte	Fe(CN)6, 10 mM	Fe(CN)6, 1 mM
Electrolyte	KCL, 0.5 M	
Working Electrode	Glassy Carbon Electrode	
Reference Electrode	Silver/silver chloride electrode	
Counter Electrode	Silver	

Table 33. Conditions with the maximum samples per second.

	Samples Per Second
Conditions 3	2000
Conditions 4	2000
Conditions 14	2000
Conditions 15	2000

5.4 Electrochemical Results

The results of the trials with the proper experimental conditions are in the graphs from Figure 56 until Figure 75. The PSoC Current makes reference to the current measured with the potentiostat prototype system. In the LSV and CV, the voltage values are versus the RE voltage, and it is indicated as EREF. Unexpectedly, the main problem of the prototype takes place at high currents as Figure 71 shows. However, the results from the prototype are congruent with the EAW in most of the graphs considering a proper range to work.

A minor drawback of the potentiostat prototype is the filter. This capacitor introduces a shift phase, and it shows up when the scan rate is fast as Figure 59 shows. However, its presences is justified because much noise will be in the measurements without it as Figure 72 illustrates. This filter helps a lot where the current is very small and more sensitive to the noise as Figure 61 describes. Thus, this component allows us to lower the detection limits sacrificing a little of the potentiostat prototype bandwidth.

Figure 73, Figure 74, and Figure 75 presents the information of all Cycle and Linear Sweep Voltammetries from the prototype in the respective graphs. With this, someone can see the effects of the scan rate easily. The DSC is not in these graphs because there is no such a variable in this technique. However, part of the prototype instrument performance can be observed in those figures.
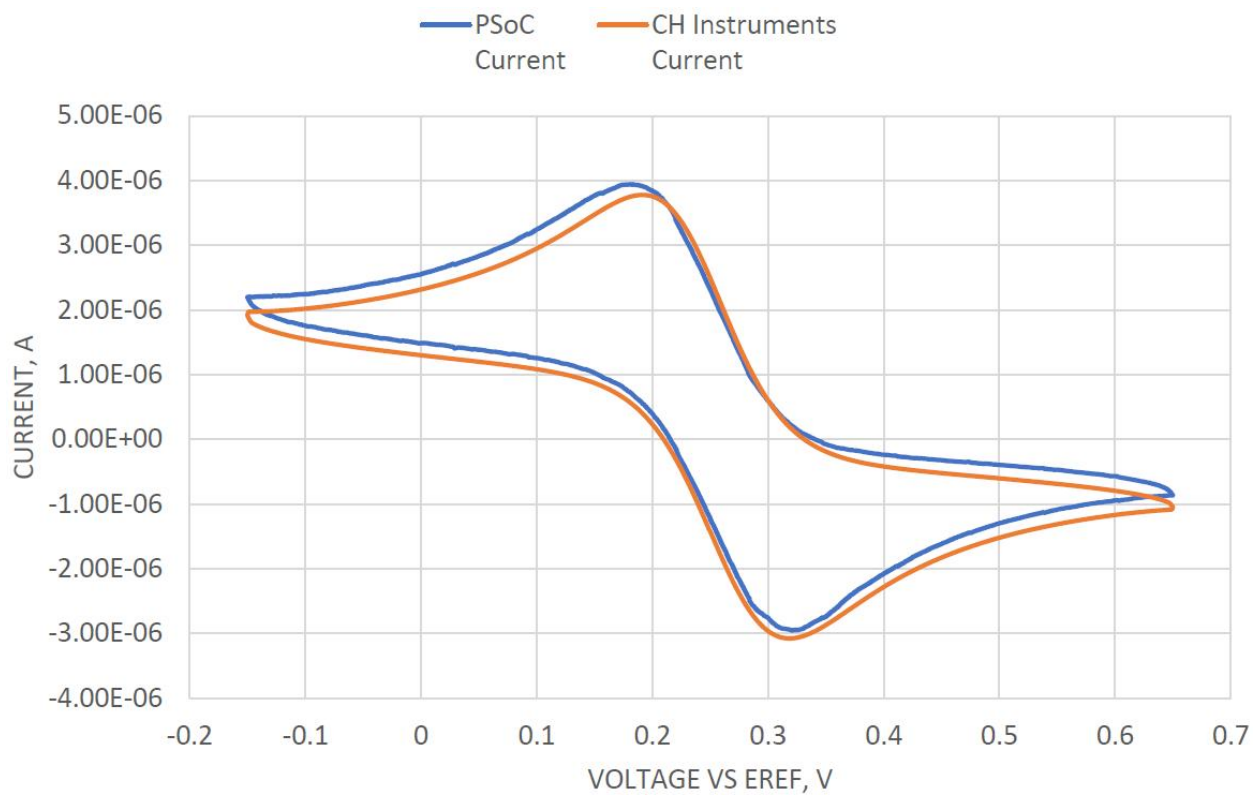
Figure 56. Cyclic voltammetry experiment under the conditions 1.
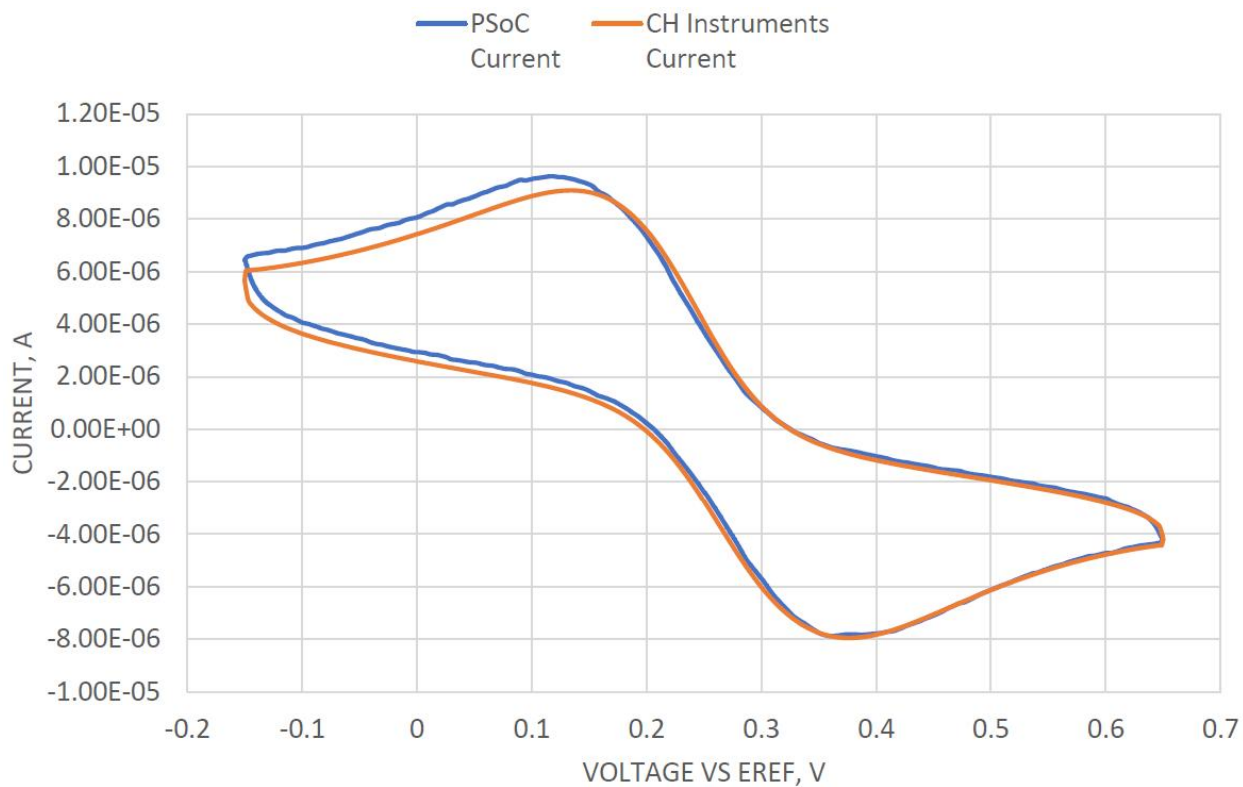
Figure 57. Cyclic voltammetry experiment under the conditions 2.
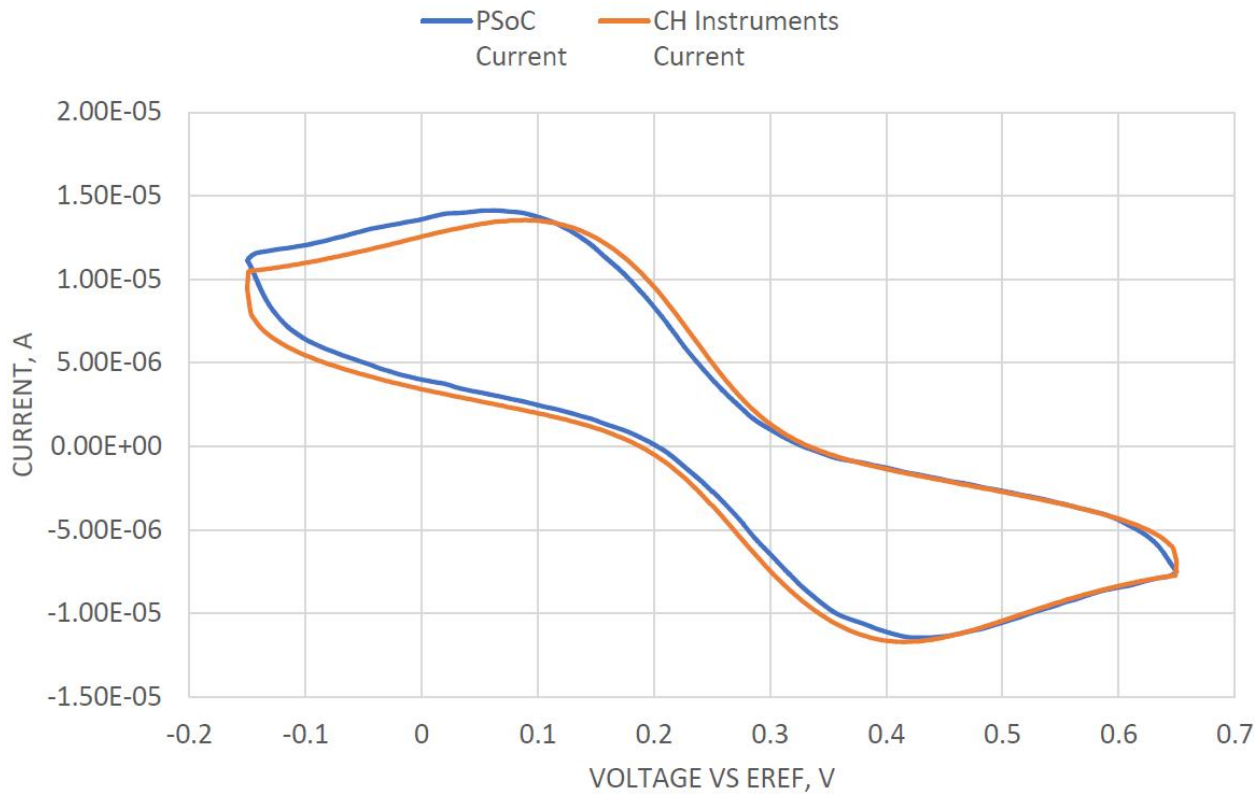
Figure 58. Cyclic voltammetry experiment under the conditions 3.
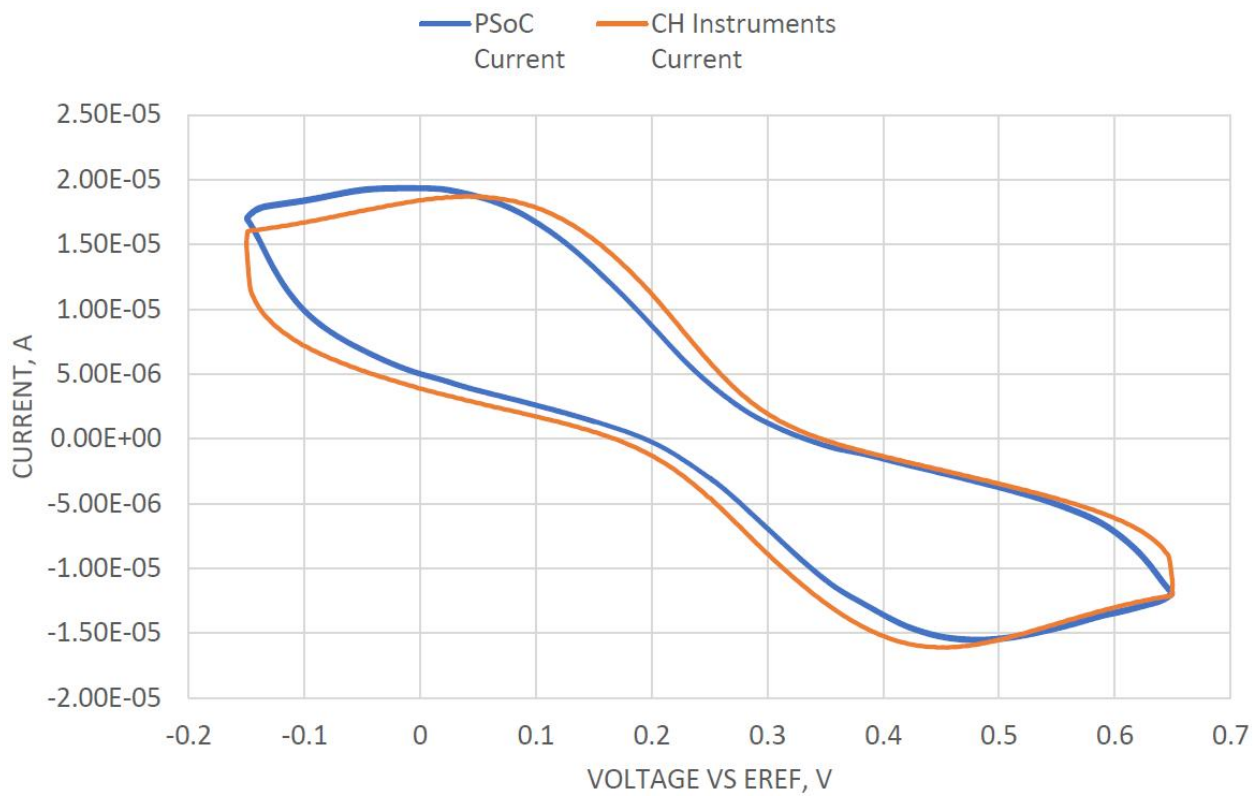
Figure 59. Cyclic voltammetry experiment under the conditions 4.
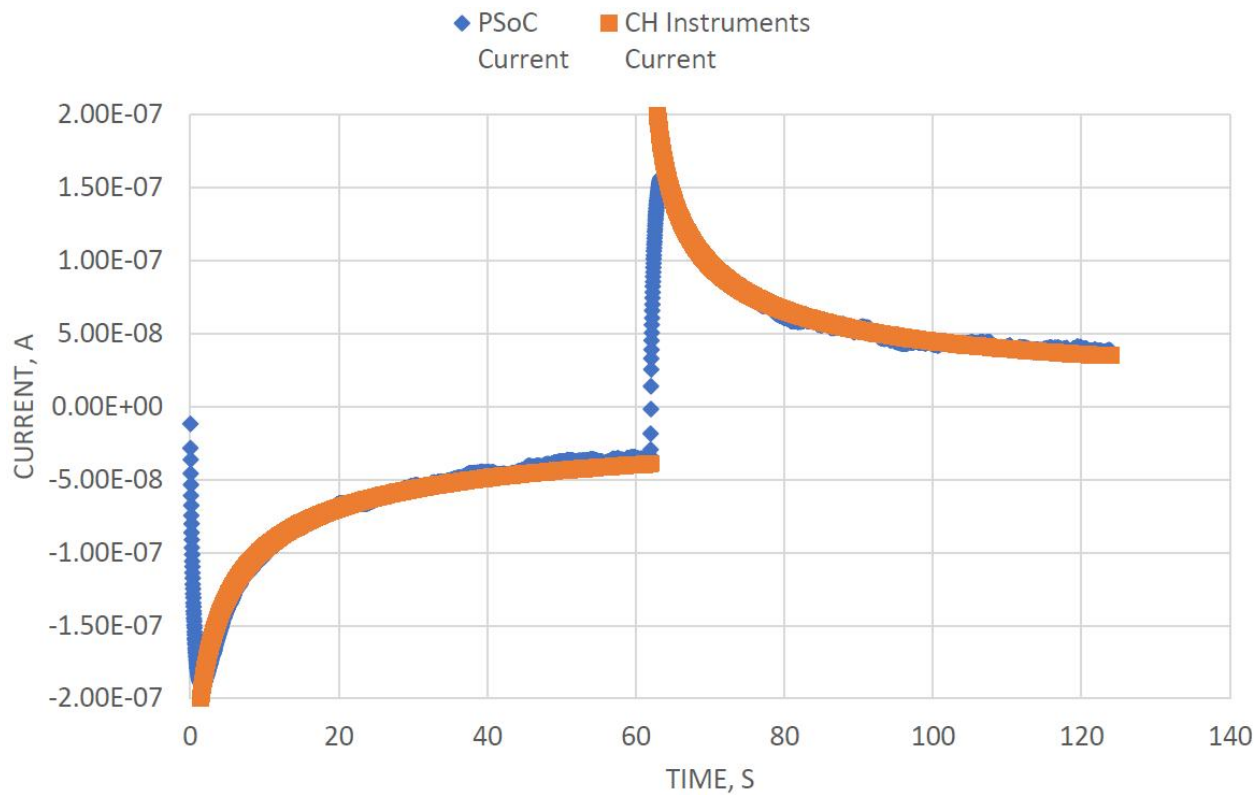
Figure 60. DSC experiment under the conditions 5.
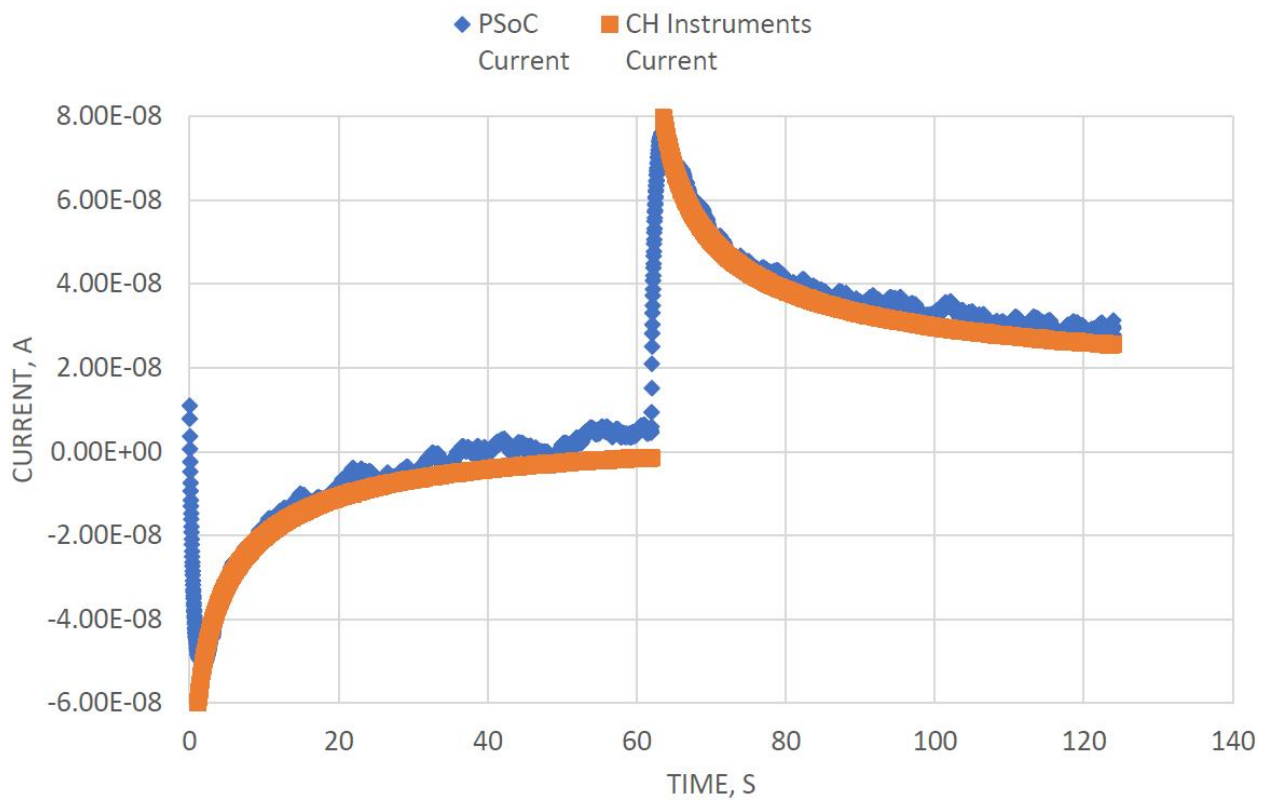
Figure 61. DSC experiment under the conditions 6.
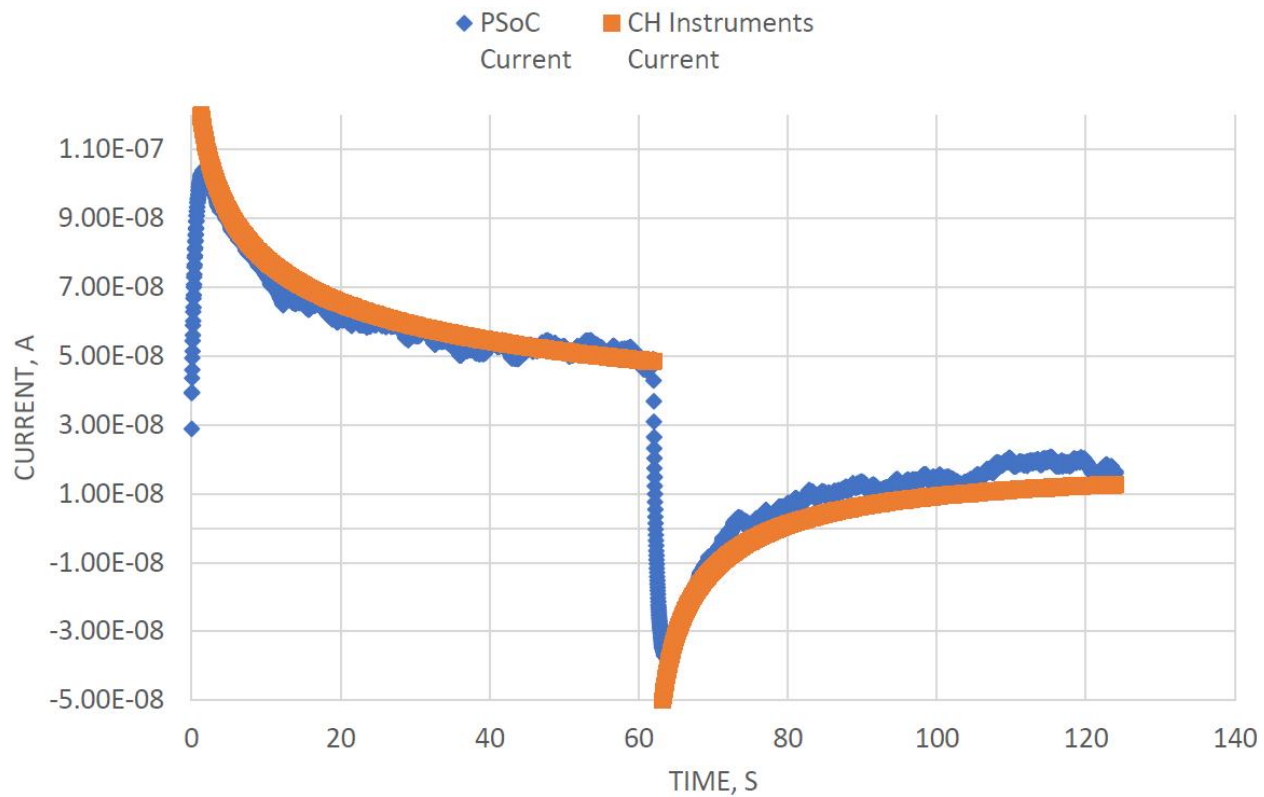
Figure 62. DSC experiment under the conditions 7.
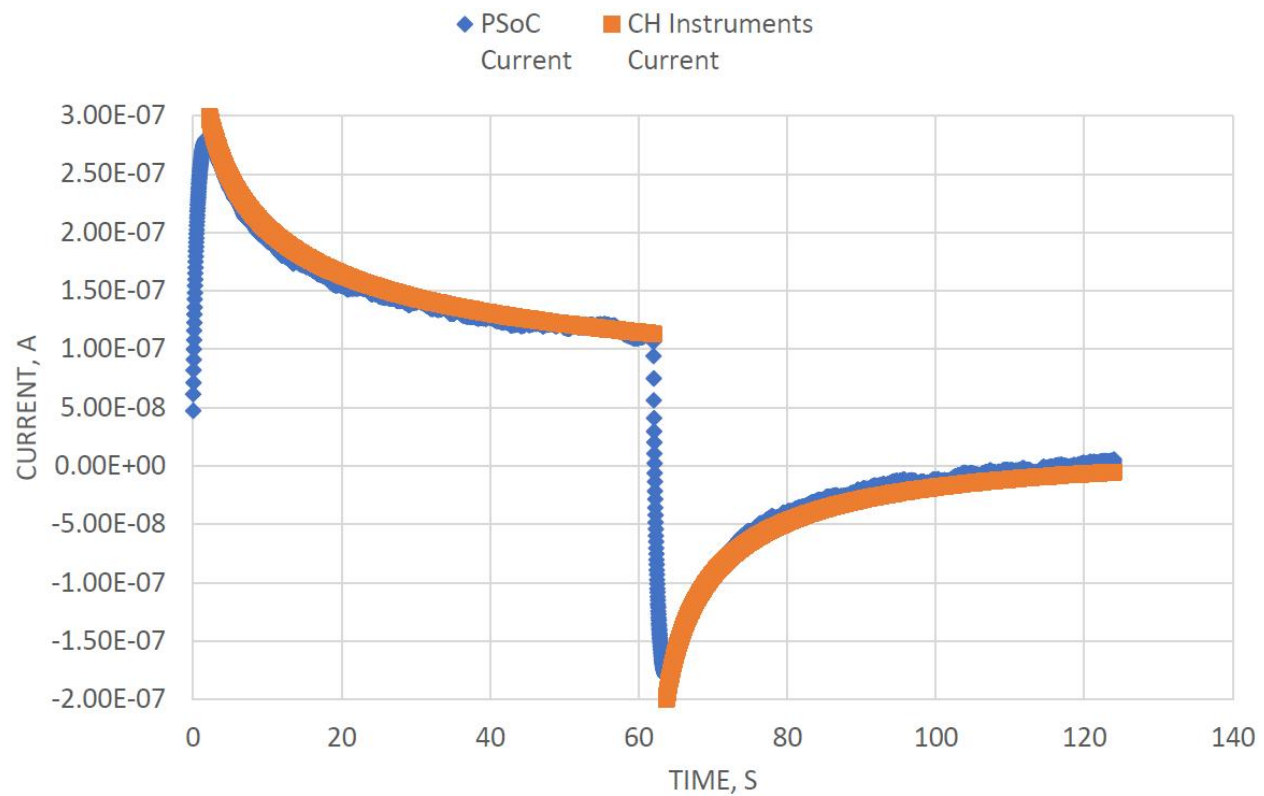
Figure 63. DSC experiment under the conditions 8.
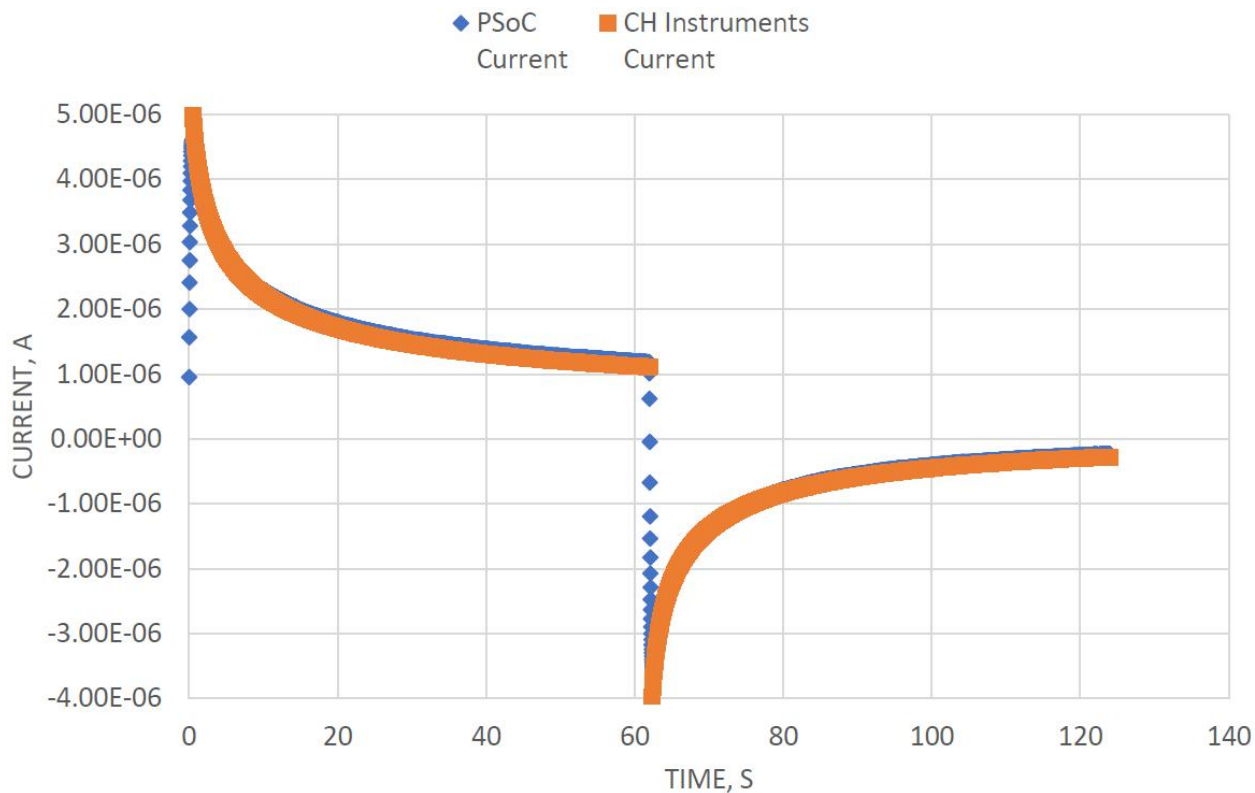
Figure 64. DSC experiment under the conditions 9.
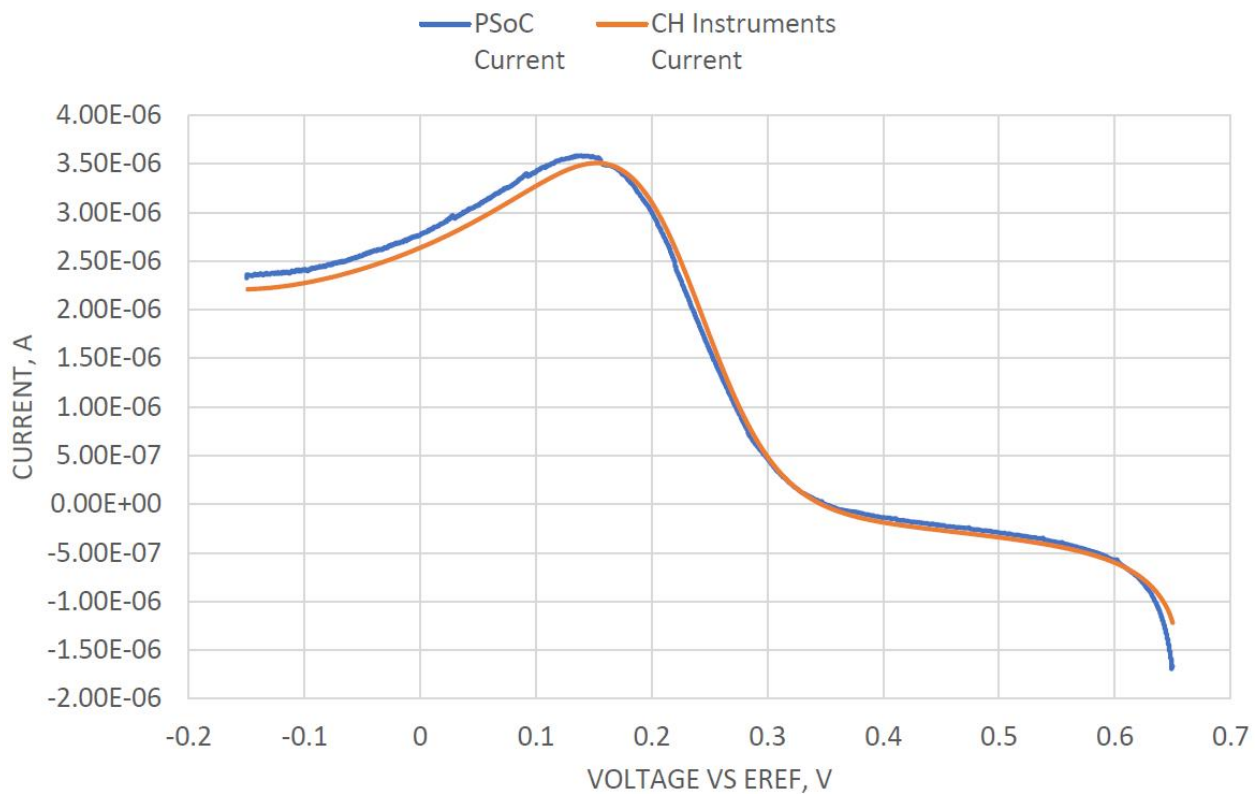
Figure 65. LSV experiment under the conditions 10.

87
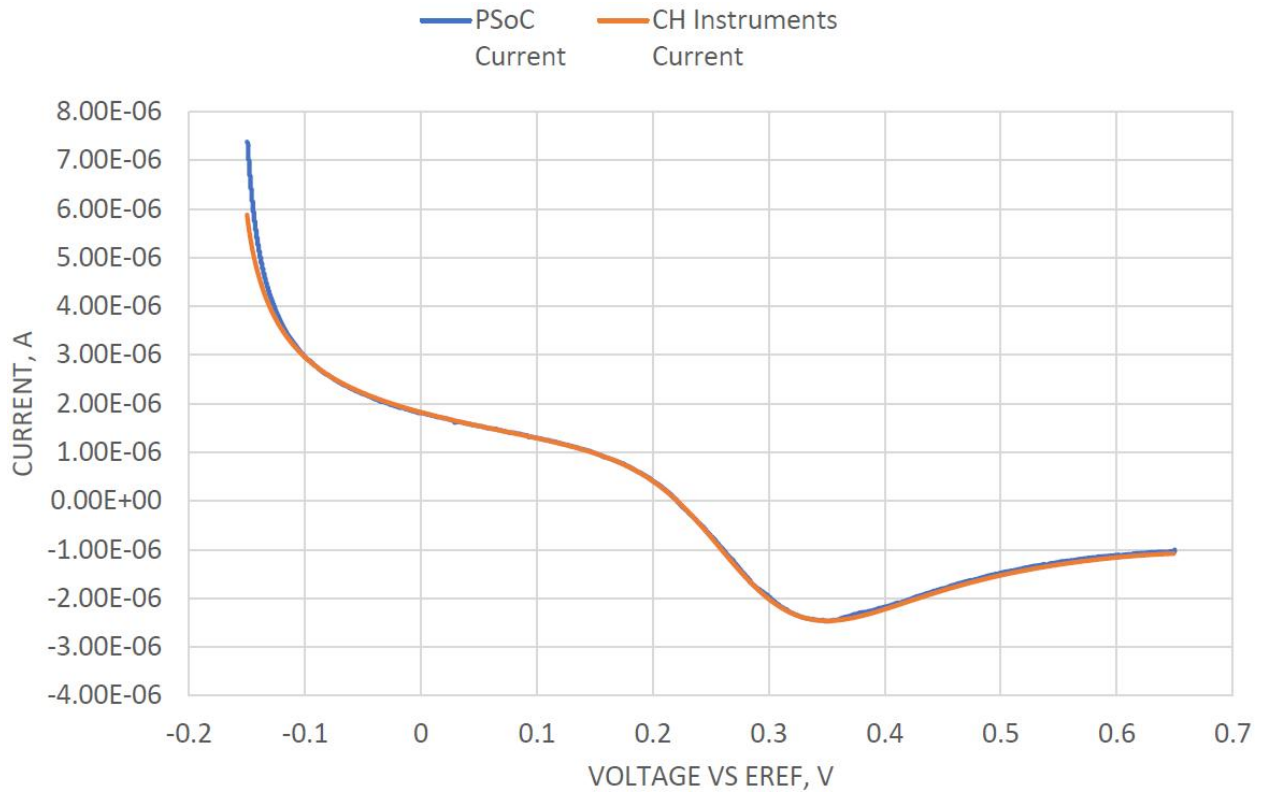
Figure 66. LSV experiment under the conditions 11.
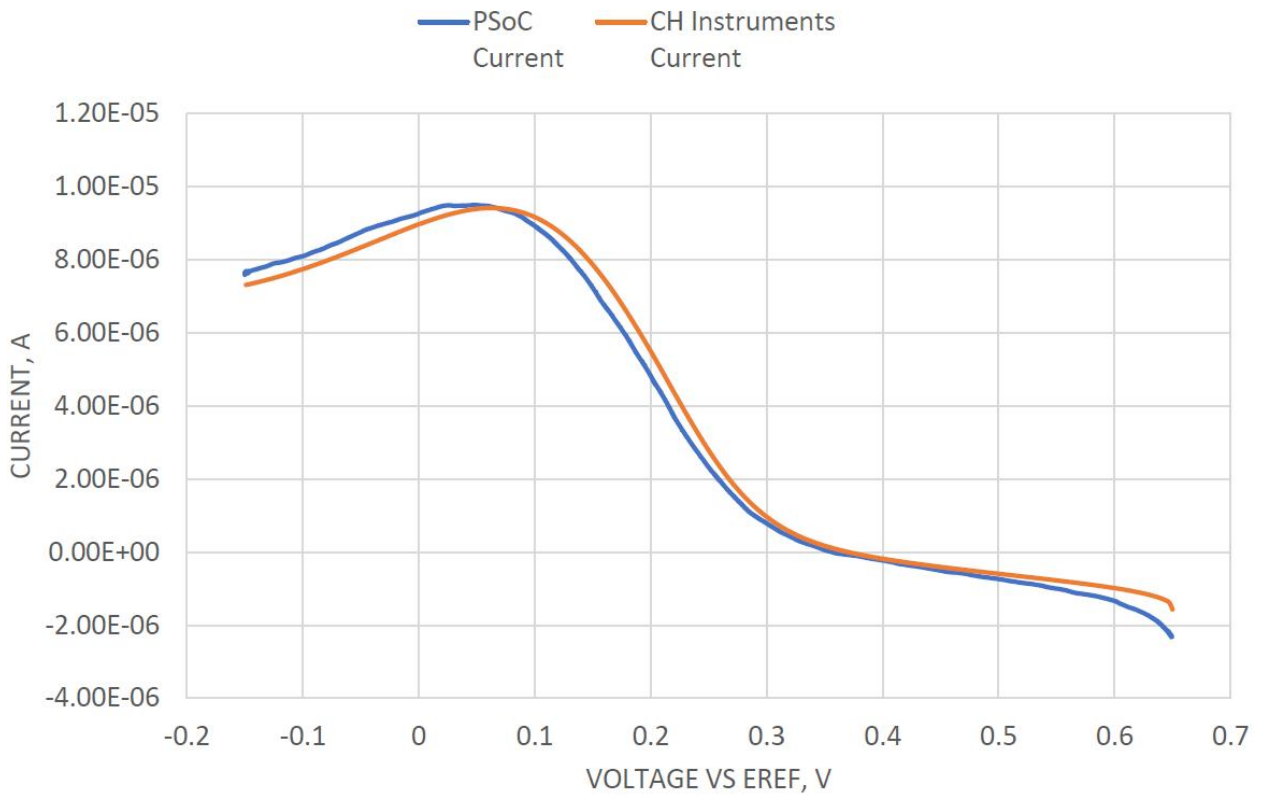
Figure 67. LSV experiment under the conditions 12.
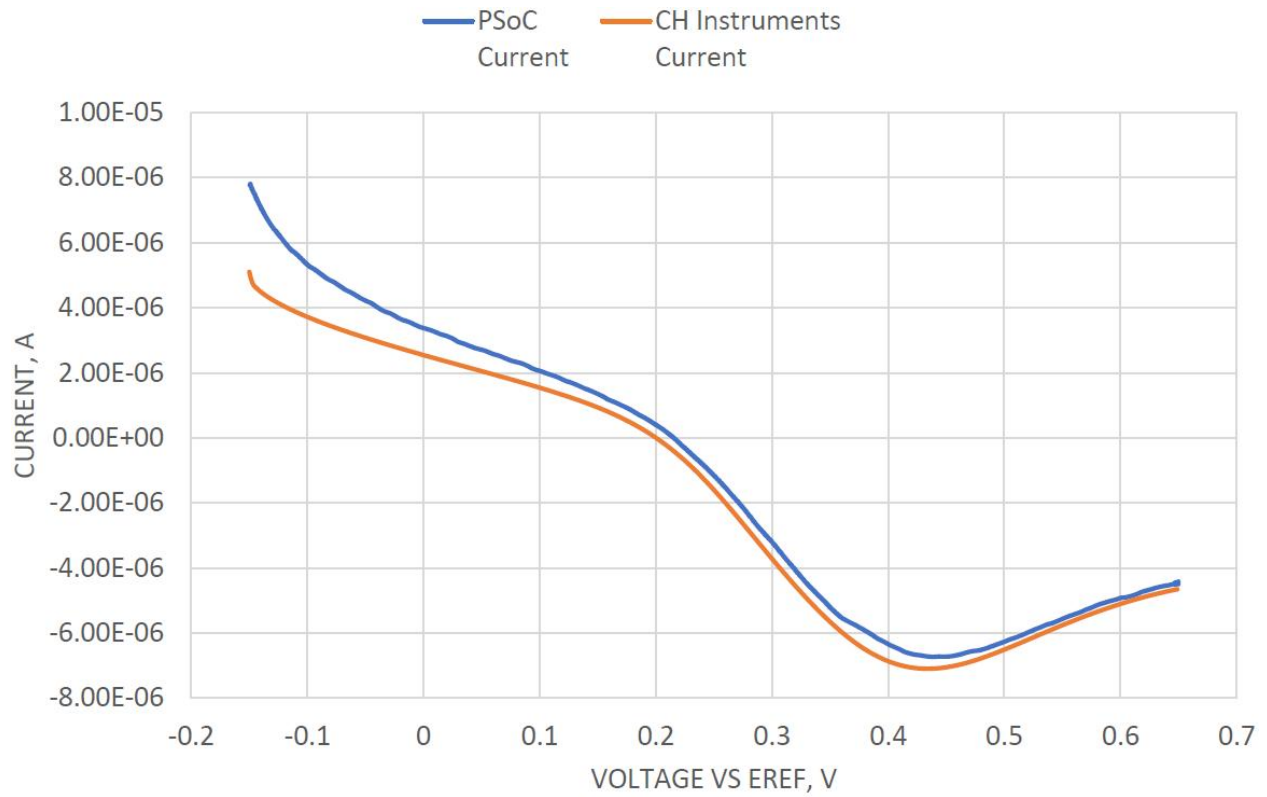
Figure 68. LSV experiment under the conditions 13.
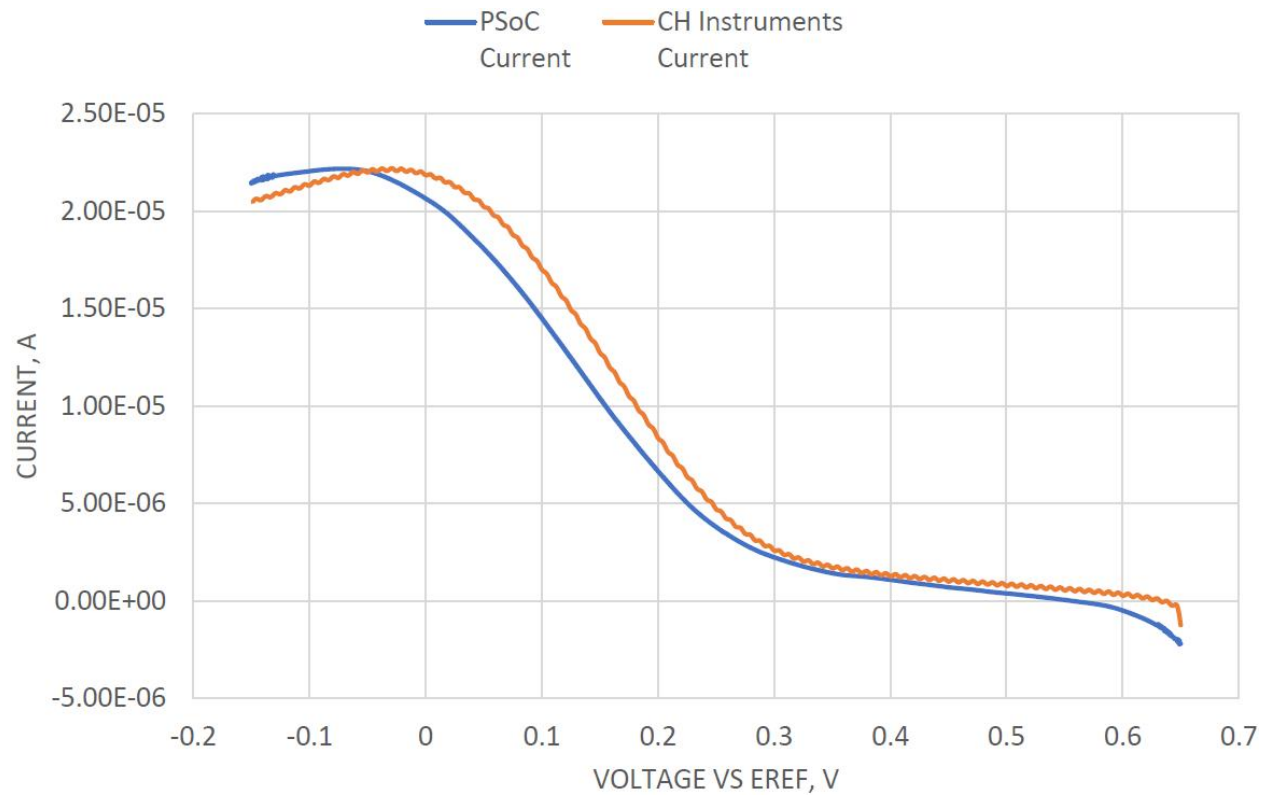
Figure 69. LSV experiment under the conditions 14.

89
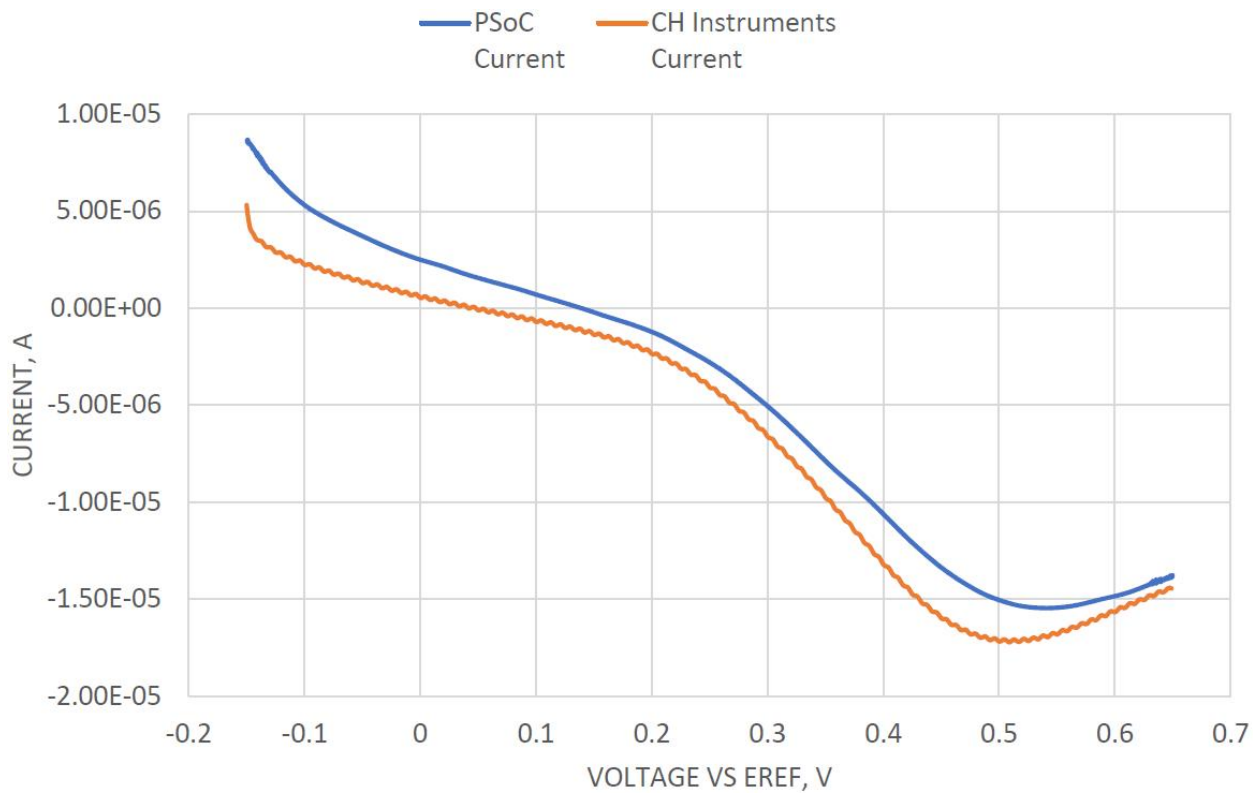
Figure 70. LSV experiment under the conditions 15.
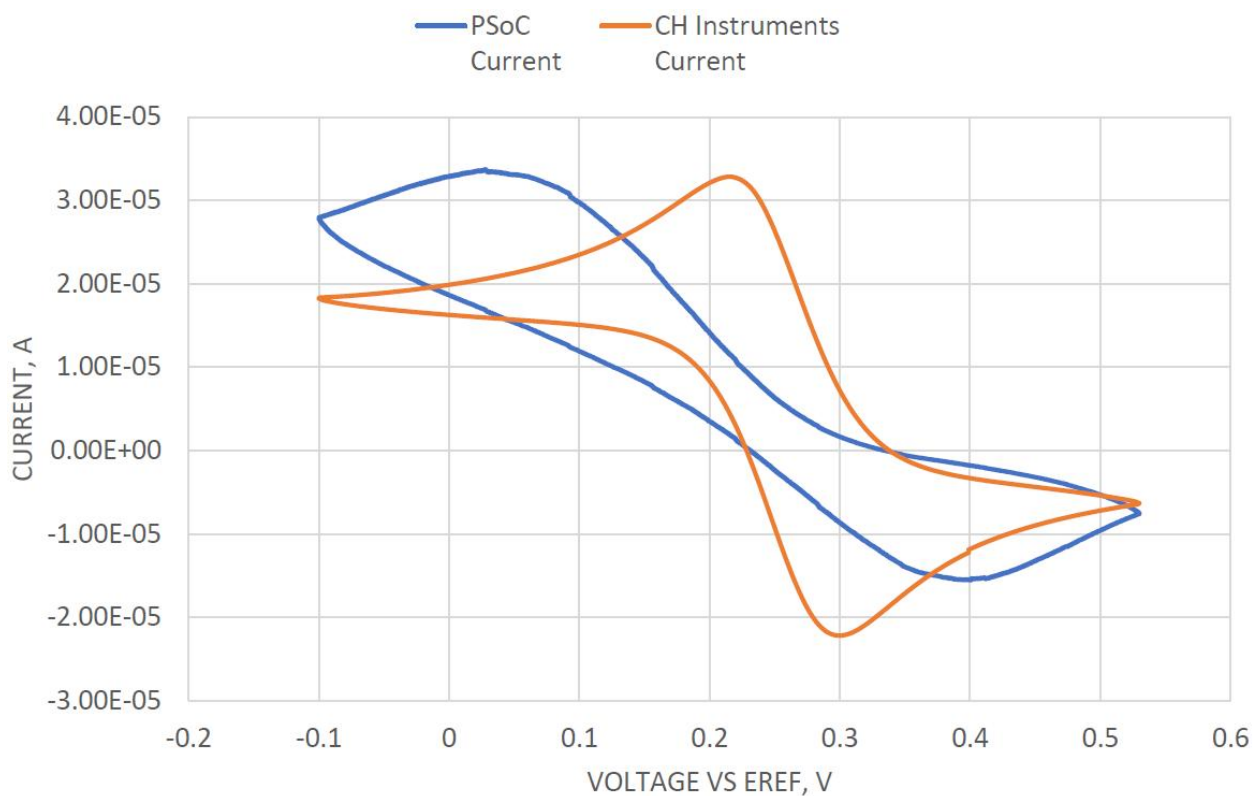
Figure 71. Cyclic voltammetry experiment under the conditions 16.
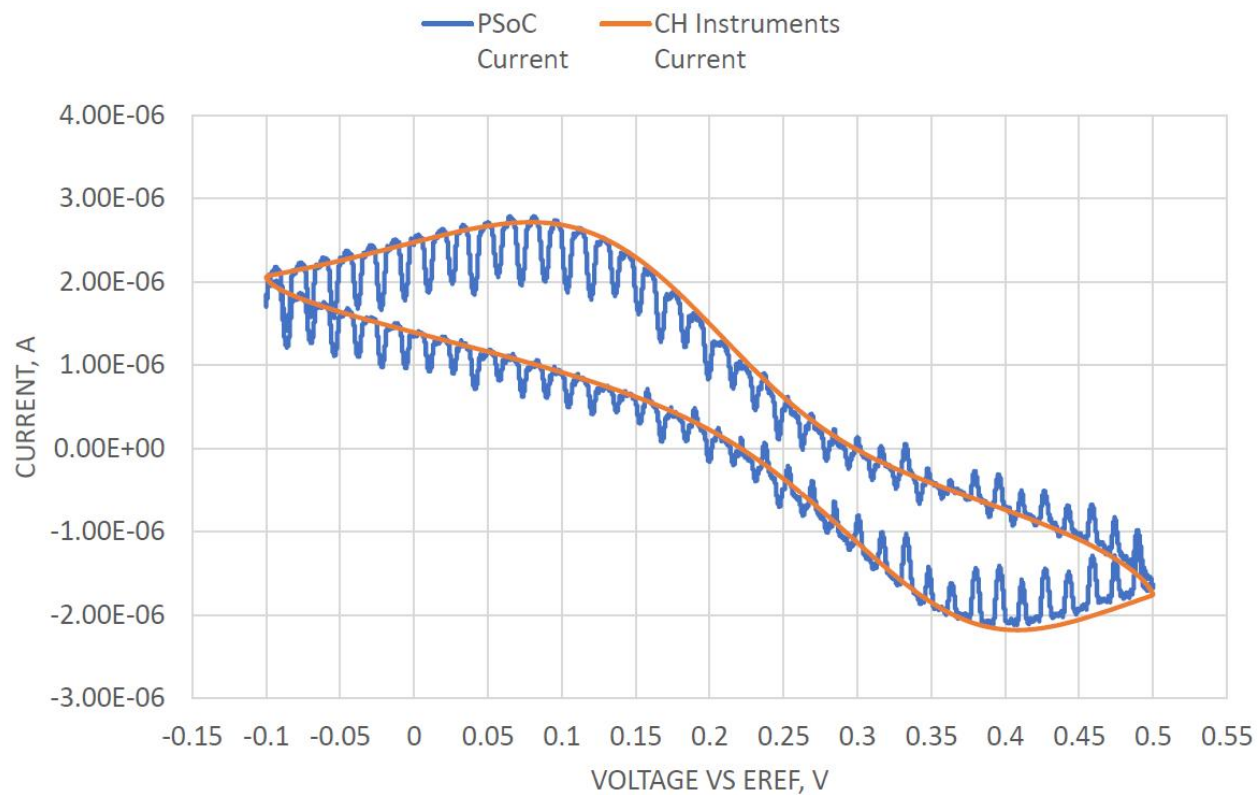
Figure 72. Cyclic voltammetry experiment under the conditions 17.
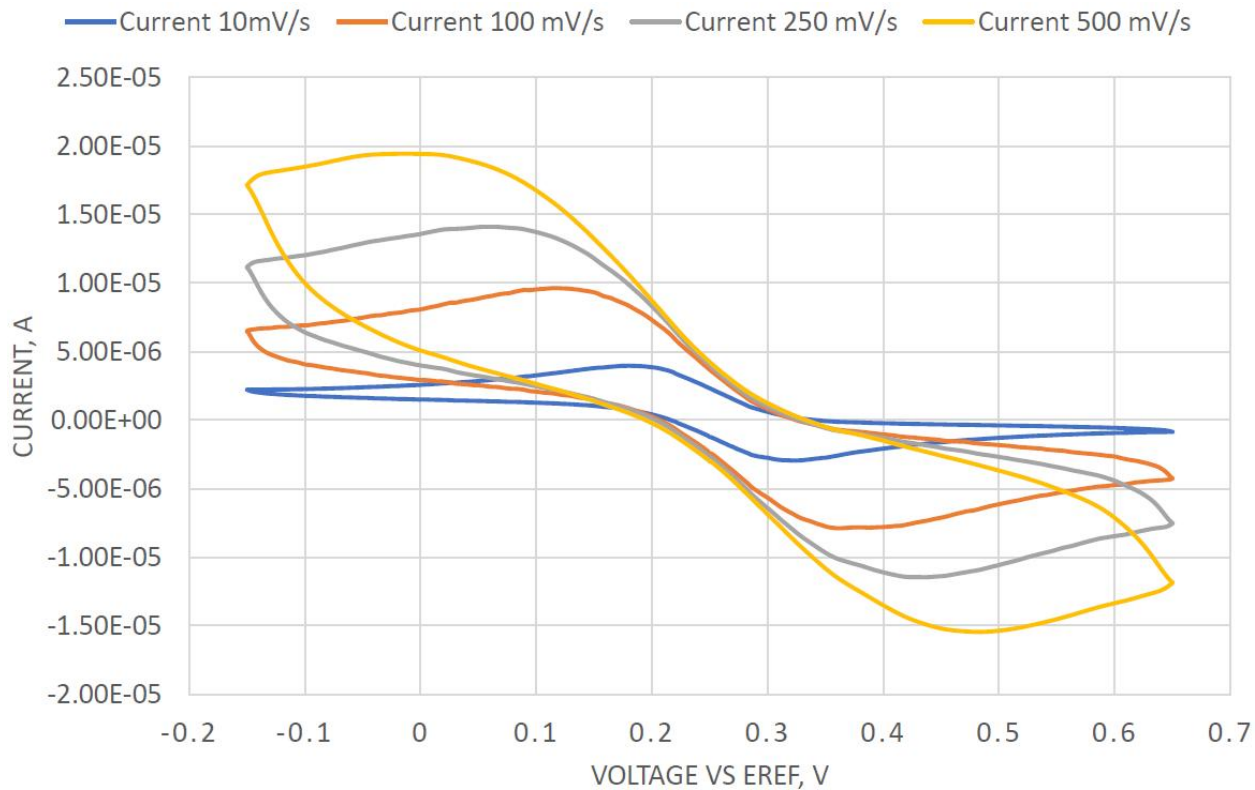
Figure 73. All Cycle Voltammetries from the PSoC with different scan rates. Blue line, CV experiment under the conditions 1. Orange line, CV experiment under the conditions 2. Gray line, CV experiment under the conditions 3. Yellow line, CV experiment under the conditions 4.
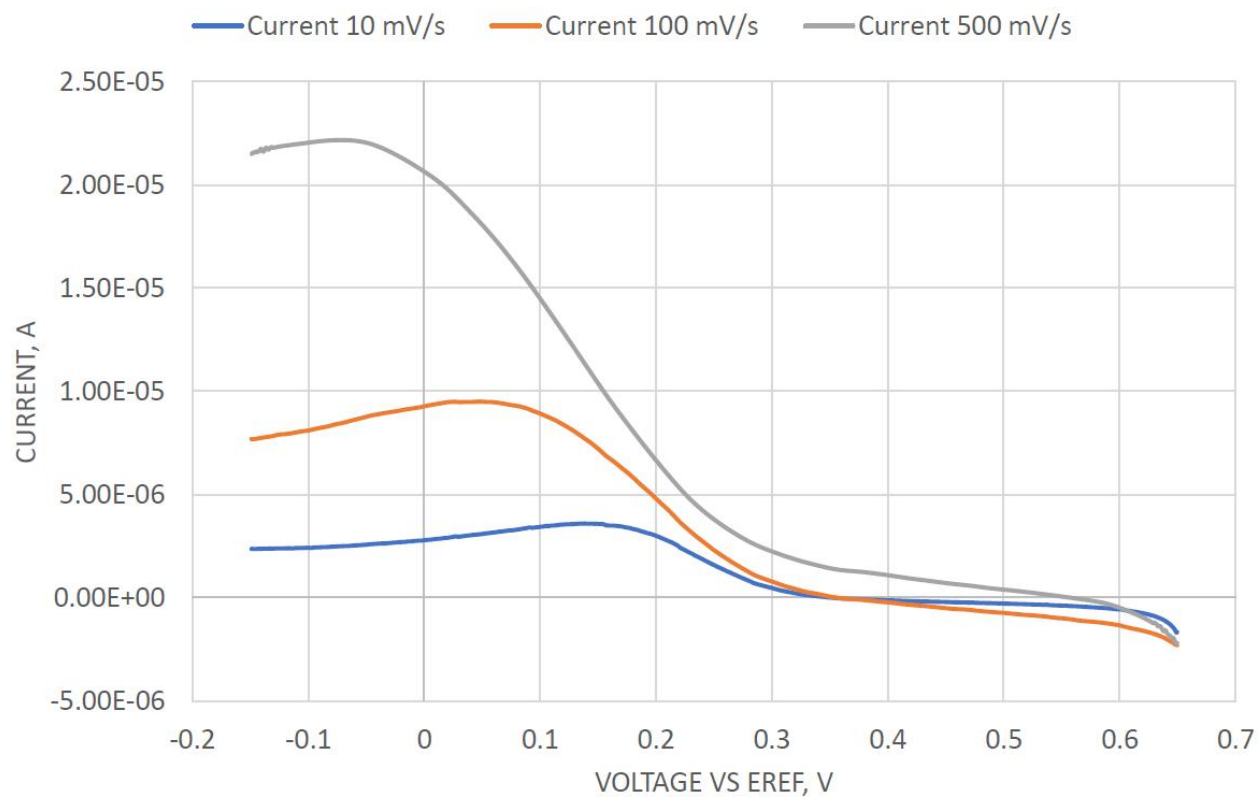
Figure 74. All Linear Sweep Voltammetries from the PSoC with a negative scan direction. Blue line, LSV experiment under the conditions 10. Orange line, LSV experiment under the conditions 12. Gray line, LSV experiment under the conditions 14.
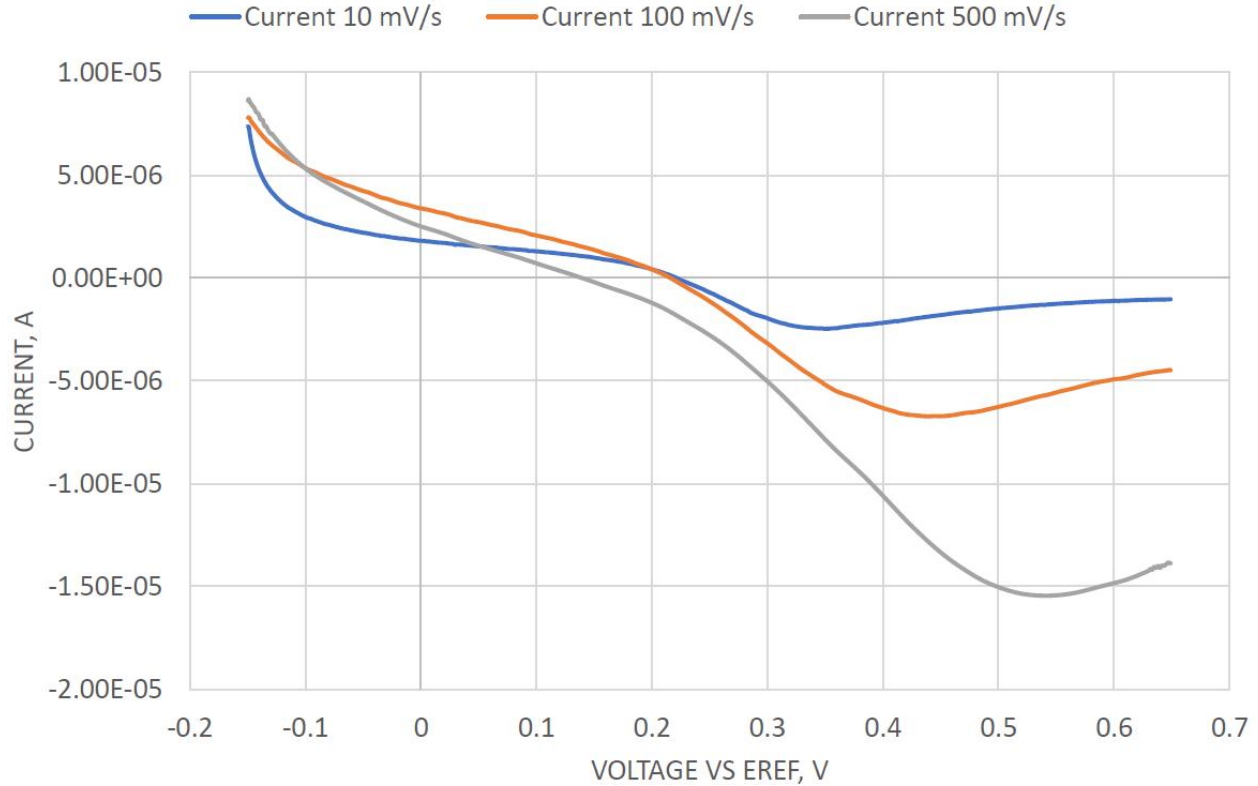
Figure 75. All Linear Sweep Voltammetries from the PSoC with a positive scan direction. Blue line, LSV experiment under the conditions 11. Orange line, LSV experiment under the conditions 13. Gray line, LSV experiment under the conditions 15.

5.5 Results Analysis

An error analysis will show the differences between both devices for each experiment quantitatively. The absolute error express how far is the measured value of the real as Equation 5.3 shows. In these experiments, the real values are from the EAW while the measured values are from the prototype. The mean error makes reference to the average of the absolute errors in an experiment as Equation 5.4 describes. The highest error is a value very close to the maximum error because it comes from the standard deviation of the absolute errors as Equation 5.5 illustrates. Thus, someone can have an idea of the prototype performance knowing well the measurement scale.

$$\text{Absolute Error} = ||\,Value_{Measured}\,| - |\,Value_{Real}\,|| \qquad 5.3$$

$$\text{Mean Error} = \frac{\sum_{i=1}^{Samples\ Number} \text{Absolute Error}_i}{\text{Samples Number}} \qquad 5.4$$

$$\text{Highest Error} = 3\sigma + \text{Mean Error} \qquad 5.5$$

The previous equations do not have any reference to describe the error and someone cannot have a clear idea of how bad is that error. Thus, the full scale will be the reference with a value according to the peak to peak amplitude of the Redox current

signal from the EAW. The Mean Error Percent (MEP) describes how big the mean error against the peak to peak amplitude is as Equation 5.6 illustrates. The Highest Error Percent (HEP) describes how big this highest error against the peak to peak amplitude is as Equation 5.7 shows. Hence, these indicators will describe the error of the prototype measurements with a solid reference.

$$\text{Mean Error Percent} = \frac{\text{Mean Error}}{\text{Peak to Peak Amplitude}} * 100 \qquad 5.6$$

$$\text{Highest Error Percent} = \frac{\text{Highest Error}}{\text{Peak to Peak Amplitude}} * 100 \qquad 5.7$$

Table 34 presents the most relevant indicators for the error analysis. The MEP describes the error percent to expect in given measure. The HEP describes maximum error percent to expect in an electrochemical trial. The CV errors are higher than those from the DSC, and that can come from two factors: the full scale and the scan rate. However, it is difficult to know which of both has more weight because they are related. The LSV experiments are not entire trustful because the conditions before to start the trial are unknown. However, this drawback is not present in the DSC and the CV because the quiet time and the fifth cycle allow each device to start the trial from a known point.

Table 34. Error analysis summary.

Experiment under the:	MEP, %	HEP, %	Mean Error, A	Highest Error, A	Full Scale, A	Method
Conditions 1	2.887	5.226	1.98E-07	3.58E-07	6.852E-06	CV
Conditions 2	1.691	5.721	2.88E-07	9.75E-07	1.704E-05	CV
Conditions 3	2.226	7.653	5.62E-07	1.93E-06	2.527E-05	CV
Conditions 4	**3.397**	**11.178**	1.18E-06	3.89E-06	3.481E-05	CV
Conditions 5	0.319	5.185	5.35E-09	8.69E-08	1.676E-06	DSC
Conditions 6	0.587	5.386	**3.6E-09**	3.30E-08	**6.134E-07**	DSC
Conditions 7	**0.780**	5.480	**5.04E-09**	3.54E-08	**6.461E-07**	DSC
Conditions 8	0.562	**6.169**	1.03E-08	1.13E-07	1.827E-06	DSC
Conditions 9	0.414	4.758	7.73E-08	8.87E-07	1.865E-05	DSC
Conditions 10	2.019	5.994	9.55E-08	2.83E-07	4.728E-06	LSV
Conditions 11	0.585	5.464	4.88E-08	4.56E-07	8.341E-06	LSV
Conditions 12	2.837	8.429	3.12E-07	9.26E-07	1.098E-05	LSV
Conditions 13	5.081	17.825	6.2E-07	2.18E-06	1.220E-05	LSV
Conditions 14	4.243	14.483	9.94E-07	3.39E-06	2.342E-05	LSV
Conditions 15	**7.655**	**19.173**	1.72E-06	4.32E-06	2.252E-05	LSV

The experimental conditions six and seven allows knowing the Lower Limit of Detection (LLD) because in these trials the prototype measured the smallest signal value. From those experiments, the 5% of the mean error of is the LLD to have an expected accuracy of 95% in an electrochemical trial compared with the EAW. With that criterion,

the prototype can handle currents above 86.44 nA and below of -86.44 nA, as Table 35 shows, to have an accuracy above of the 95%.

Table 35. Lower Limit of Detection analysis.

	Mean Error, A	LLD from 5% of the Mean Error, A
Conditions 6	3.6E-09	***
Conditions 7	5.04E-09	***
Conditions Average	4.32E-09	86.44E-09

The Higher Limit of Detection comes from the current values of experimental conditions one because conditions sixteen shows how the prototype cannot handle much current. The main difference between experimental conditions 1 and 16 is the amount of analyte. Therefore, the current levels are different as well. However, the prototype has no congruency with the EAW at high currents as Figure 71 shows. Thus, **the conditions one provides the Higher Limit of Detection of ±3 μA** according to the lowest signal value of Figure 56 because it was the last conditions working properly. However, trials with analyte concentration between 1 and 10 mM could prove a greater current range.

Chapter 6. Conclusions.

The chapter describes the objectives accomplished in this research and the most relevant results. It also describes the possible applications for the PES where someone can use the information given. Moreover, the chapter gives a cost and size estimation to visualize the potential of this research in certain fields. Furthermore, it makes a review of the hypothesis and the objectives achieved. Thus, the chapter provides an understanding of the research outcome and its capacity to solve the problematic situation explained in chapter 1.

Chapter six analyze a specific issue from the last chapter, and it suggests possible paths to make more investigations. Mainly, there is a concern about the Higher Limit of Detection. This value is a little low compared with the ideal capacity of the PSoC. Hence, the following subsection gives more details about it. Moreover, this chapter provides some ideas to enhance the actual hardware features, and it also encourages to use this device in some applications. Therefore, this chapter finishes the whole dissertation.

This chapter gives more information about the following points presented in the methodology:

39. Explanation of the electrochemical results to establish the limitations of the prototype system.
40. Description of the possible size of the embedded system to review applications for the prototype system to probe hypothesis four.
41. Description of the cost of the embedded system to review applications for the prototype system to probe hypothesis five.
42. Description of the possible applications for the prototype system.
43. Review of the objectives.
44. Review of the hypothesis.
45. Description of the enhancements to the prototype and future work.

6.1 Conclusions from the Electrochemical Experiments

From the electrochemical experiments, someone can summaries the coverage of these trials and the most relevant electric features for the PES. Also, there is a subsection with an analysis of the Higher Limit of Detection. This analysis takes place because this limit shows an uncommon behavior. Thus, this sections presents all the electrochemical ranges tested in Chapter 5 and the electrical features that come with these results and those from Chapter 4.

6.1.1 Electrochemical Experiment Summary

Table 36 presents the electrochemical conditions where the prototype was congruent with the EAW. This table is a summary of the experiments to appreciate the capacity of the embedded system. There is just one analyte concentration due to the prototype capacity. However, this concentration gives information about the voltage and the current range in the EC. It also helps us to probe the scan rate and the SPS range of the potentiostat system. Furthermore, this concentration allows us to test the DSC

technique changing some parameters for that. Thus, this table provides a clear idea of the PES skills.

Out of the ranges of Table 36, the behavior of the PES is erratic or unknown. The potentiostat loses the voltage control with analyte concentrations above 10 mM. Between 1 to 10 mM of ferricyanide, there is no information to evaluate the prototype. Inside of this concentration, someone can test the PES to get more information in future work. However, the PES capacity established in this research allows us to have several applications as the next section will explain.

Table 36. Electrochemical conditions evaluated.

	CV	LSV	DSC
Analyte Concentration	Fe(CN)6, 1 mM	Fe(CN)6, 1 mM	Fe(CN)6, 1 mM
Voltage Range	-0.15 to 0.65 V	-0.15 to 0.65 V	0.195 to 0.325 V
Peak Current Range	-3.0 to 4.0 µA	-2.5 to 3.5 µA	***
Maximum Step	***	***	0.310 to 0.195 V
Minimum Step	***	***	0.310 to 0.315 V
Maximum Current at 62 seconds	***	***	1.2 µA
Minimum Current at 62 seconds	***	***	43.22 nA
Scan Rate Range	10 to 500 mV/s	10 to 500 mV/s	***
SPS Range	50 to 2000 SPS	50 to 2000 SPS	50 to 2000 SPS

6.1.2 Technical Summary of the PES

Table 37 presents the principal features of the PES for this investigation. The PES has a capacity of ± 2 volts to control the voltage. However, the electrodes available for this research do not have the capacity to explore the whole voltage range. The current range was established from the electrochemical experiments of Chapter 5. The number of SPS comes from the ADC selected in the PSoC. The scan rate range relies on the architecture of the PSoC and the algorithm that controls the waveform generator. Whit all these ranges in Table 37, the PSoC is a suitable device to make a potentiostat system.

Table 37. Principal electric features of the PES

Voltage Range: **± 2 V**	SPS: **50 to 2000**
Current Range: **± 3 µA**	Scan Rate: **10 to 500 mV/s**

Table 38 and Table 39 give information about the power consumption and the values to compensate for having more accurate results. The offset voltages come from Chapter 4, and they are in the algorithms to infer the Redox current. The resistor values calculated in that chapter help to reduce errors as Table 21 shows. The bias current at the inverting input allows us to establish the minimum current to read in the device. The power consumption provides a clear idea of the battery requirements. Hence, in future works, all this data is relevant to make modifications in the PES.

Table 38. Aditional features of the PES with a source voltage of 5 volts.

ADC Offset Voltage: **-61.056 µV**	PES consumption at Stand By: **137.5 mW**
TIA Offset Voltage: **-3.36034 mV**	PES consumption at 2000 SPS: **207.5 mW**

Table 39. TIA resistor calculated and bias current at the inverting input.

TIA Resistors	Value Calculated	Bias Current at the inverting input
R1	18971.46 Ω	3.40E-08 A
R2	28636.77 Ω	2.06E-08 A
R3	38272.14 Ω	1.67E-08 A
R4	77433.47 Ω	6.77E-09 A
R5	116828.09 Ω	5.35E-09 A
R6	244583.12 Ω	2.59E-09 A
R7	490370.41 Ω	1.27E-09 A
R8	981623.90 Ω	6.89E-10 A

6.1.3 Higher Limit of Detection

From the last chapter, all the results make sense except for the Higher Limit of Detection. The PSoC has the capacity to measure currents until 50 µA according to the manufacturer [74]. However, the prototype can deal just with Redox currents inside of ±3 µA. In the experiment of Figure 71, it is obvious that the PES fails with a current of 20 µA approximately. Figure 76 shows that the connection between the WE and the TIA has a resistance high enough to introduce errors. Thus, that impedance establishes the Higher Limit of Detection.
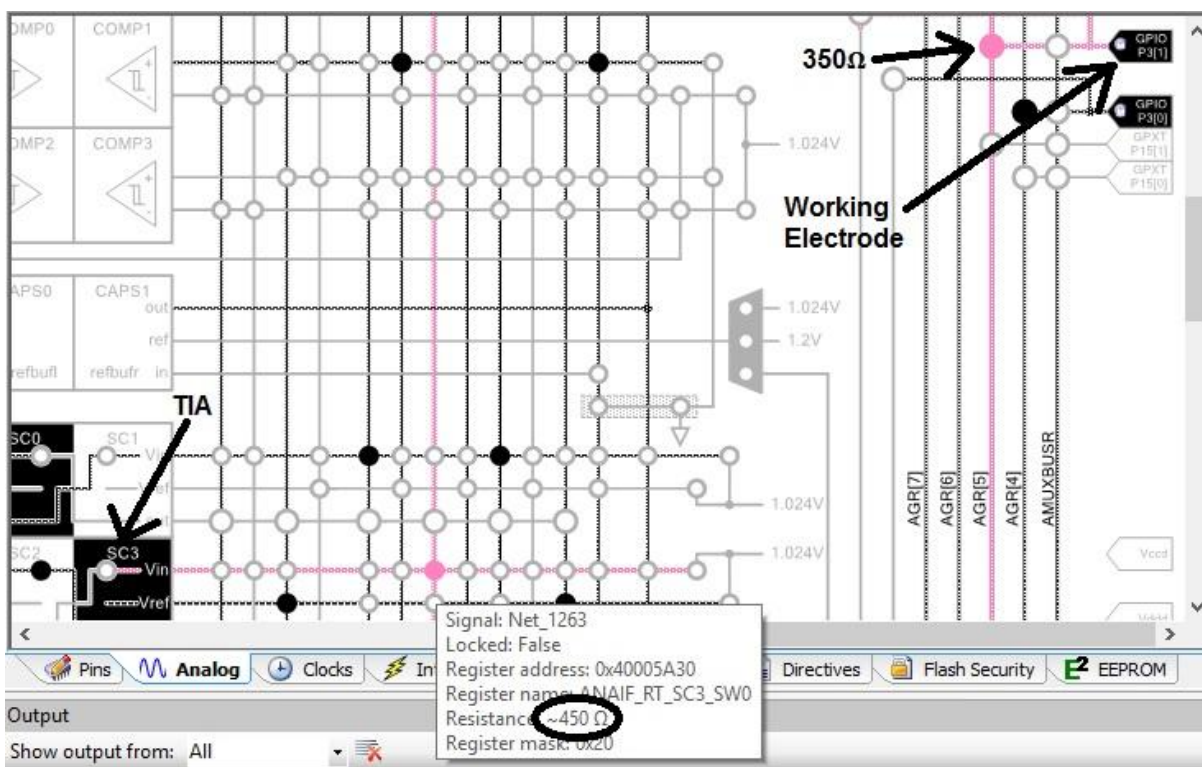
Figure 76. Routing inside of the PSoC.

The pink points of Figure 76 represent the analog multiplexers, and they should have a very low resistance to make the proper connections inside the PSoC. However, the Redox current finds two resistors before to reach the TIA. Those resistors together make a value of 800 Ω approximately. The circuit of Figure 77 illustrates the connection between the WE and the TIA. When the current is high, the potentiostat lost the voltage control in the EC because of the tension at R3. Thus, the resistance in the multiplexers will produce a measurement error in the EC at high Redox currents.
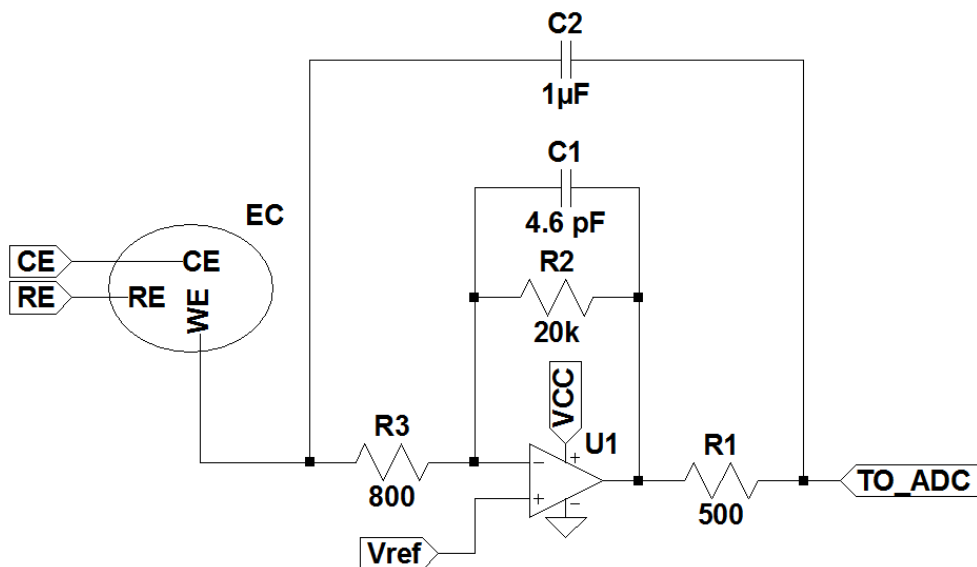
Figure 77. TIA (U1) connections inside of the PSoC.

6.2 Area, Cost, and Applications of the PES

The PES has several features and applications which allow us to accept or reject some of the hypothesis established. The area is an important characteristic when someone tries to develop small devices. The price gives a chance to the people to get this kind of technology to improve their lives. The applications are the results of the design of the whole Potentiostat System. Therefore, this section describes with more details the achievements obtained in this dissertation.

6.2.1 PES Area

The PES area is an important feature to be in small places. The objective of this thesis never was to create a PCB because it just tries to prove that a PSoC can have and a potentiostat inside. With this in mind, the prototype area is of 29.06 cm^2. However, Figure 33 shows that someone can reduce this area in a future work changing the components distribution. Table 40 has an approximation of the components area and the routing that it will take. Thus, an optimization of the PES area can throw, as a result, a circuit of 5 cm^2 approximately.

The PES developed in this research can be in applications like Lab-on-a-Disc, POCT, and wearable monitoring systems. Table 41 shows some investigations where the potentiostat system can fit taking the area as a metric. In this table, potentiostat

instruments constitute the section of POCT applications. Table 41 probes that hypothesis four is true. Hence, the PRoC and the PSoC are a good choice to be embedded in this kind of applications and have a potentiostat system inside.

Table 40. PES components area and routing.

Main Components	Area
PSoC chip	0.81 cm^2
PRoC chip	0.64 cm^2
Resistors	0.28 cm^2
Capacitors	1.00 cm^2
Routing	1.00 cm^2
Antenna	1.00 cm^2

Table 41. Applications where the Potentiostat System can fit.

Reference	Application	Area
Höfflin et al. [4]	Lab-on-a-Disc	19.63 cm^2
Abi-Samra et al. [5]	Lab-on-a-Disc	120.76 cm^2
Sayad et al. [98]	Lab-on-a-Disc	213.82 cm^2
Dorta-Quinones et al. [15]	POCT	8.93 cm^2
Dryden et al. [10]	POCT	64.00 cm^2
Sun et al. [2]	POCT	6.32 cm^2
Majumder et al. [99]	Wearable	16.00 cm^2
Miao et al. [100]	Wearable	29.00 cm^2
Haghi et al. [101]	Wearable	21.00 cm^2

6.2.2 PES Cost

The PES has few components turn it into an affordable device. This fact is convenient for people who need special health care equipment in the house or wears monitoring devices. Table 42 is a cost estimation just for the PES, and it does not show the PUIS cost because a smartphone or another device can take its place. With this information, the PES has an expected value of 30.08 dollars. However, this price is just for a single unit, and it can drop making several instruments. Compared with other instruments, the cost of the PES is good.

Table 42. Price of the PES components.

Main Components	Price (USD)	Reference
PSoC chip	$ 19.78	Mouser Electronics [102]
PRoC chip	$ 8.80	Mouser Electronics [102]
Resistors	$ 0.20	Mouser Electronics [102]
Capacitors	$ 0.30	Mouser Electronics [102]
PCB	$ 1.00	PCBWay [103]

Table 43 compares similar potentiostat systems to approve or reject hypothesis five. The first device of the table is on the market while the following two are homemade. The last device comes from this document. In the table, someone can see that the commercial device is the most expensive. Inside of the homemade potentiostat, the one from this dissertation is the cheapest. These instruments are alike in some points and are different in others. Therefore, it is not possible to establish which of them is better. However, someone can accept hypothesis five because the PES is the most affordable of the table and it has a competitive price with competitive features.

Table 43. Comparison of homemade and commercial potentiostat systems.

Device	Price	Price (USD)
EmStat 3+Embedded / OEM [10]	$ 1000.00 EUR	$ 1161.95
Dryden [10]	$ 120.00 CAD	$ 94.00
CheapStat [10]	$ 60.00 CAD	$ 47.00
PES from this dissertation	$ 30.08 USD	$ 30.08

6.2.3 Applications

One of the applications of this prototype can be the detection of glucose. According to Periasamy et al., someone can use their biosensor in a linear concentration range of 6.3 to 20.09 mM [104]. Moreover, that concentration can go from 2 to 22 mM in humans beings [105]. Therefore, it is suitable for monitoring the glucose level in a patient. The biosensor has a sensitivity of 2.47 µA/(mM cm^2) following the fabrication method of that research. Also, the output current range of the biosensor with a fixed area of 2 mm x 2 mm is of 0.62 to 1.98 µA. Hence, this prototype can handle that sensor because the PES input current is wider than the biosensor output.

Anyone can find many glucose biosensors in the market, but Accu-Check sells a suitable one for the prototype [106]. That biosensor is the Performa glucose test-strips number 06454011, and it has a sensitivity of 62.155 nA/mM with an offset of 10.993 nA [107]. Steinberg et al. characterized the biosensor in range of 0.1 to 10 mM. However, with the device developed in this research, we cannot detect 0.1 mM of glucose because the current is too low. The actual range of the prototype system with that biosensor is of 1.5 to 10 mM, and it can be greater making the proper characterization. However, that range is still relevant for glucose detection according to Steinberg.

Another application of the prototype system is the detection of melatonin. Doctors usually prescribe this active element to threat sleep disorders [108]. Apetrei et al. developed a sensor with a sensitivity of 37.1 nA/µM with an area of 0.8674 cm^2 in a linear range of 1-300 µM. Considering the input current range of the PES developed the melatonin detection range is around of 2.5-80.0 µM. However, this range is enough to detect a melatonin concentration of 43 µM making the appropriate dissolution of the pills. Thus, someone can use the PES with that sensor for quality control in pharmaceuticals industries or look for counterfeit medication.

Another application of the prototype system is the detection of hydrogen peroxide. That component can be toxic relying on the concentration [109], [110]. In an amount of 10-200 µM, it can provoke a senescence-like state if a human cell gets in contact with it.

Chen et al. developed a sensor in 2016 with a sensitivity of 35 mA/(M cm^2) for this analyte [111]. Thus, in a fixed area of 7.2mm x 7.2mm, the prototype developed can make the detection of the component in a range of 5-165 μM. A higher analyte concentration will lead to apoptosis in the cell. Hence, the instrument is capable enough to describe the lowest degree of hydrogen peroxide toxicity.

Today, researchers relate the nitrite (NO2-) with some health problems as a methemoglobinemia [112]. Also, it is common to find this component in ordinary stuff. Therefore, Jaiswal et al. developed a biosensor for the determination of this analyte. He found two linear ranges of 0.1 to 1 μM and 1 to 1000 μM having two different sensitivities of 1.25 μA/(μM cm^2) and 0.005 μA/(μM cm^2) respectively. The developed device could make the nitrite detection in a range of 0.1 to 833 μM with and an electrode area of 0.72 cm^2 considering the two slopes in this range. Thus, the prototype, with that biosensor, can be useful detecting nitrite.

El Harrad et al. developed a biosensor to study the potential of medicinal plants to treat gout [113]. In his research, he made an infusion from several plants, and he detected the concentration of xanthine oxidase. This enzyme blocks the production of uric acid to treat this disease. His biosensor has a sensitivity of 0.6 A/(M cm^2) in a linear range of 5 to 45 μM for that enzyme. The prototype created can cover all that detection range with an electrode area of 0.111 cm^2. Hence, someone can use this device to study more medicinal plants to treat gout.

All the applications from this subsection allow us to accept hypothesis three. It may seem that the input current range of PES is not wider. However, engineers and researchers can play with the biosensor area to match the output current of the transducer with the input current of the PES. Someone can find more examples of applications in the literature where the instrument can handle the Redox current. However, the applications explained prove that this instrument can play a relevant role in the field.

6.3 Hypothesis Review

The thesis has, as a result, the acceptation of all the hypothesis established. It means that all the initials ideas and suppositions are true. Hence, this document proves that the PSoC and the PRoC can hold all the hardware and software necessary to work as potentiostat system. It also shows that the SoC technology can bring to the potentiostat new features and new capabilities. Therefore, this is information is one of the principal contributions to the scientific community.

The following subsection describes the acceptation of the hypothesis and the information to make such conclusion.

6.3.1 Hypothesis Review from One to Seven

Hypothesis one declares that the PSoC can generate several waveforms in a single chip. It is very helpful to keep the PES size and the cost low. Chapter 4, section 2 allow us to accept the hypothesis one. The different signals recorded for each electrochemical trial agrees with the parameters to create them. It means that the PSoC

can generate all the electrochemical waveforms properly to do the respective experiments in the EC.

Hypothesis two declares that a state machine is a good approach to develop efficient firmware for potentiostat systems. The criterion to accept or reject this hypothesis relies on the results consistency between the EAW and the PES from this dissertation. In the working range established, the EAW and the PES throw similar graphs. Someone can observe this congruency from Figure 56 to Figure 70. Therefore, hypothesis two is true due to the likeness of the Redox currents from both instruments.

Hypothesis three declares that the PSoC can reach limits of detection in the nanoampere range where relevant applications can be developed. Section 5.5 explains that the PES can handle negative and positive Redox currents in the range of 86.44 to 3000 nA. Hence, the prototype has the proper working range. Regarding the applications, subsection 6.2.3 describes some biosensors where someone can use the PES of this thesis. Therefore, hypothesis three is true.

Hypothesis four declares that the PSoC and the PRoC can hold a small potentiostat system. Applications like Lab-on-a-Disc, POCT, and wearable monitoring systems establish the space limitation. Someone can redesign the PES of this dissertation to fit in an area of 5 cm^2 approximately as Table 40 shows. Table 41 shows the space available in some applications. Taking into account those applications, hypothesis four is true because the PES fits in those areas.

Hypothesis five declares that the potentiostat system can be affordable for people who need special equipment in the house or wear monitoring devices. SoC technology is a good option to save money because in a single chip someone can have several components. As a result, the PES of this thesis can have a price of 30.08 dollars according to the estimation of Table 42. This PES cost is reasonable compared with those instruments from Table 43. Thus, this fact allows us to accept hypothesis five.

Hypothesis six declares that a State Machine and a Producer/Consumer design pattern is a good approach to develop a user interface for potentiostat systems. The criterion to accept or reject this hypothesis relies on the results consistency between the EAW and the PES from this dissertation. In the working range established, the EAW and the PES throw similar graphs. Someone can observe this congruency from Figure 56 to Figure 70. Therefore, hypothesis six is true because both user interfaces have Redox current values very close.

Hypothesis seven declares that the PRoC technology can deal with the all the data traffic from the PSoC to the computer. This hypothesis tries to probe capacity of the system to send all the data from the experiments. The experimental conditions 3, 4, 14, and 15 use 2000 SPS to generate as much data as possible. Figure 58, Figure 59, Figure 69, and Figure 70 shows that the results from the EAW and the PES are similar. Therefore, hypothesis seven is true.

6.4 Objectives Review

One of the objectives of this research is to explore new technology with the capacity of being reconfigurable. A PSoC and a PRoC from Cypress Semiconductor have

proven to be a good choice to make a potentiostat system. It has as advantages the use of few components, schematic simplification, modest hardware performance, excellent software features, and a reasonable cost. Thus, this dissertation proof that PSoC and PRoC technology are useful in potentiostat systems.

Another objective is to provide information to researchers about the creation of a complete potentiostat system. Also, this document presents a potentiostat system configuration highly scalable to add more features. In this sense, a State Machine is a key to power the prototype with such capacity. In this investigation, the PES can carry out DSC, CV, and LSV trials as part of the thesis goals. With the information of this document, it is clear that researchers and engineers can take this tool to attend their specific need.

One concern of this investigations is to reduce the potentiostat systems size. With the PRoC and the PSoC, the prototype could reach an area of 5 cm^2 approximately as subsection 6.2.1 explains. That brings to the table the possibility to have this work in applications like Lab-on-a-Disc, POCT, and wearable monitoring systems. The main objective of the investigation always was to provide the bases for a small potentiostat system. Therefore, with all the data presented, the tools to make that happen are given.

The specific objectives accomplished in the dissertation are in the following points:

1. This thesis provides a low cost (30.08 dollars approximately) and Io size (5 cm^2 approximately) hardware design for a potentiostat system.
2. Chapter 3 explains about the potentiostat system components.
3. Chapter 2 describes the electronic circuits for a potentiostat system.
4. The section 5.5 establish that the device has a sensitivity in the nA scale for the Redox current measurements.
5. Section 3.3 explains about the waveform of the electrochemical techniques to develop algorithms for the function generator.
6. The PUIS has a data logger for the electrochemical experiments, and it gives, as a result, an Excel file.
7. Figure 78 shows an intuitive user interface for this dissertation.
8. The PES uses Bluetooth to communicate wirelessly with the PUIS and vice versa.
9. A moving average filter and an analog filter helps to clean the signal as Figure 72 shows.
10. Chapter 5 focus on the detection of some analyte to prove the hardware, software, and wireless functionality of the PES.
11. Section 5.4 compares the electrochemical results against a commercial potentiostat.
12. Section 5.5 declares the working range of the potentiostat developed.
13. Section 6.2 explains the PES feasibility to be used in embedded applications like Lab-on-a-Disc, POCT, and wearable monitoring systems.
14. Subsection 6.2.3 describes some applications for the prototype.

6.5 Future Work

This investigation encourages new works to improve the prototype performance and to use this work in embedded applications. Additional futures for this device will be

the capacity to measure the open circuit potential and make ohmic compensations. Those features involve the development of new hardware. Also, this document recommends taking this work into applications like Lab-on-a-Disc, POCT, and wearable monitoring systems. Those applications will give more relevance to technologies like SoC, PRoC, and PSoC. Therefore, any person will have a research opportunity in these fields.

Add to this prototype the capacity to make ohmic compensation and measure the open circuit potential, will have as a consequence hardware modification. Thus, this addition is just for those applications where these features are necessary. The integration of more components to the hardware design will increase the PCB size if the PSoC cannot provide such elements. Therefore, this document suggests a careful evaluation of the application needs to create the potentiostat system.

The integration of this work in applications like Lab-on-a-Disc, POCT, and wearable monitoring is one of the most promising paths. This research provides the hardware and the software design to have an embedded potentiostat system. With that information, someone can give solutions to several applications with small space requirements. Therefore, this document suggests the creation of small PCB according to the application needs.

Appendix A: Abbreviations and Acronyms

A

ADC: Analog to Digital Converter.
APC: Advance Potentiostat Circuit.

B

BLE: Bluetooth Low Energy.

C

Cond: Conditions.
CV: Cyclic Voltammetry.

D

DAC: Digital to Analog Converter.
DSC: Double Step Chronoamperometry.

E

EAW: Electrochemical
    Analyzer/Workstation.
EC: Electrochemical Cell.
EIS: Electrochemical Impedance
    Spectroscopy.

F

FPC: Follower Potentiostat Circuit.

G

GCB: Glassy Carbon Electrode.

H

HEP: Highest Error Percent.

I

I/O: Input and Output.
IC: Integrated Circuit.
IDE: Integrated Design Environment.
ISR: Interrupt Service Routine.

L

LLD: Lower Limit of Detection.
LSB: Least Significant Bit.
LSV: Linear Sweep Voltammetry.

M

MEP: Mean Error Percent.

O

OCP: Open Circuit Potential.
OPAMP: Operational Amplifier.

P

PC: Potassium Chloride.
PCB: Printed Circuit Board.
PES: Potentiostat Embedded System.
PF: Potassium Ferricyanide.
PGA: Programmable gain amplifier.
POCT: Point Of Care Technologies.
PSoC: Programmable-System-on-a-
    Chip.
PUIS: Potentiostat User Interface
    System.
PWM: Pulse-Width Modulation.

R

Rc: Compensated Resistor, Ω.
Redox: Reduction-Oxidation.
Ru: Uncompensated Resistor, Ω.

S

SNR: Signal-to-Noise Ratio.
SoC: System-on-a-Chip.
SPP: Serial Port Profile.
SPS: Samples Per Second.
SWD: Serial Wire Debug.

T

TIA: Transimpedance Amplifier.

U

UART: Universal Asynchronous Receiver-Transmitter.

V

V_ref: Reference Voltage, V.
Vcs: Control Signal Voltage, V.

Voff: Offset Voltage, V.
Vos: Input Offset Voltage, V.
Vre: Reference Electrode Voltage, V.
Vwe: Working Electrode Voltage, V.

Z

Zc: Impedance at the CE, Ω.
Zwk: Impedance at the WE, Ω.

Δ

$\Delta\Sigma$: Delta-Sigma.

Appendix B: PSoC Firmware

The PSoC firmware has eight files to implement the program. Between them are the following:

- main.c
- main.h
- Miscellaneus.c
- Voltametria_Lineal.c
- Voltametria_Ciclica.c
- Cronoamperometria.c
- Selector_Ganancia.c
- Interrupcion_UART.c

In the following subsections, someone can observe the code to verify the flowcharts presented in previous chapters. This code relies on a State Machine design pattern. It is noteworthy that all the files help to the main.c file for execute the firmware and it is divided in this way to have a better understanding of what is going on. Furthermore, with this program, as a reference, someone can add more states to have more techniques in this chip.

main.c

```
#include <main.h>
int main()
{
  CyDelay(1000);
  CyGlobalIntEnable;
  UART_Start();
  isr_ADCEnd_StartEx(Interrupcion_ADCEnd);
  UART_ClearRxBuffer();
  Cnt_Puntos=0;
  while(1)
  {
    CyPmAltAct(PM_ALT_ACT_TIME_NONE, PM_ALT_ACT_SRC_INTERRUPT);
    CyDelay(1);
    int8 RxByteSer=UART_GetRxBufferSize();

    if(RxByteSer==4)
    {
      Potenciostato_Start();
      UART_PutChar(1);
      Ganancia(UART_ReadRxData());
      sps=(UART_ReadRxData()<<8)|UART_ReadRxData();
      Period_ADC=24000000/sps;
```

```
        CyDelay(200);
        switch(UART_ReadRxData())
        {
            case 1:
                Voltametria_Lineal();
                break;
            case 2:
                Voltametria_Ciclica();
                break;
            case 3:
                Cronoamperometria();
                break;
            default:
                UART_PutChar(251);
                Fin_Voltametria();
        }
    }
    else
    {
        if(RxByteSer==1)
        {
            if(UART_ReadRxData()==255&&Cnt_Puntos!=0)
            {
                Fin_Voltametria();
            }
        }
        if(RxByteSer>4){UART_ClearRxBuffer();}
    }
  }
}
```

main.h

```
#include <device.h>
#include <Timer_VC.h>

volatile uint16 Voltage_Maximo, Voltage_Minimo, Pendiente;
volatile char Ciclos;
volatile int Signo;

volatile uint16 Voltage_Inicial, Voltage_Final;

volatile uint32 Periodo2, Cnt_CR, Quiet_Time;

volatile int Puntos_ADC, Cnt_Puntos, t1mV;
volatile uint16 Voltage_DAC, sps;
```

```
volatile uint32 Period_ADC;

void Voltametria_Ciclica(void);
void Voltametria_Lineal(void);
void Cronoamperometria(void);
void Potenciostato_Start(void);
void Potenciostato_Stop(void);
void Ganancia(char caso);
void Print_DAC_Voltage(uint16 Voltage_Dac);
void Print_ADC_Current(int Resultado_ADC);
void Put_DAC_Voltage(uint16 Voltage_Dac);
void Fin_Voltametria(void);

CY_ISR_PROTO(Interrupcion_ADC);
CY_ISR_PROTO(Interrupcion_ADCEnd);
CY_ISR_PROTO(Interrupcion_DAC_VL);
CY_ISR_PROTO(Interrupcion_DAC_VC);
CY_ISR_PROTO(Interrupcion_DAC_CR);
CY_ISR_PROTO(Interrupcion_UART);
```

Miscellaneus.c

```c
#include <main.h>

void Print_DAC_Voltage(uint16 Voltage_Dac)
{
    UART_WriteTxData((char)(Voltage_Dac>>8));
    UART_WriteTxData((char)Voltage_Dac);
}

void Print_ADC_Current(int Resultado_ADC)
{
    UART_WriteTxData((char)(Resultado_ADC>>16));
    UART_WriteTxData((char)(Resultado_ADC>>8));
    UART_WriteTxData((char)(Resultado_ADC));
}

void Put_DAC_Voltage(uint16 Voltage_Dac)
{
    DAC_Wave_SetValue(Voltage_Dac - 4);
}

CY_ISR(Interrupcion_ADCEnd)
{
    Print_ADC_Current(ADC_DelSig_GetResult32());
}
```

```
CY_ISR(Interrupcion_ADC)
{
   Print_DAC_Voltage(Voltage_DAC);
   if(Cnt_Puntos<Puntos_ADC)
   {
      ADC_DelSig_StartConvert();
      Cnt_Puntos++;
   }
   else
   {
      Fin_Voltametria();
   }
}

void Fin_Voltametria(void)
{
   Cnt_Puntos=0;
   TIA_SetResFB(TIA_RES_FEEDBACK_20K);

   Timer_ADC_Stop();
   Timer_DAC_Stop();

   isr_DAC_Stop();
   isr_ADC_Stop();

   Potenciostato_Stop();
}

void Potenciostato_Start(void)
{
   PGA_Start();
   DAC_Wave_Start();
   Opamp_0_Start();
   Opamp_1_Start();
   Opamp_2_Start();
   TIA_Start();
   ADC_DelSig_Start();
}

void Potenciostato_Stop(void)
{
   PGA_Stop();
   DAC_Wave_Stop();
   Opamp_0_Stop();
   Opamp_1_Stop();
```

```
    Opamp_2_Stop();
    TIA_Stop();
    ADC_DelSig_Stop();
}
```

Voltametria_Lineal.c

```
#include <main.h>
#include <math.h>
#include <stdlib.h>

void Voltametria_Lineal(void)
{
    if(UART_GetRxBufferSize()==6)
    {
        uint8 i, VL_Param[6];
        UART_PutChar(1);

        for(i=0;i<6;i++)
        {
            VL_Param[i]=UART_ReadRxData();
        }

        Voltage_Inicial=(VL_Param[0]<<8)|VL_Param[1];
        Voltage_Final=(VL_Param[2]<<8)|VL_Param[3];
        Pendiente=(VL_Param[4]<<8)|VL_Param[5];

        Signo=Voltage_Final-Voltage_Inicial;
        t1mV=24000000/Pendiente;
        Puntos_ADC=sps*abs(Signo)/Pendiente;

        Cnt_Puntos=0;
        Voltage_DAC=Voltage_Inicial;
        Put_DAC_Voltage(Voltage_DAC);
        CyDelay(1000);

        isr_DAC_StartEx(Interrupcion_DAC_VL);
        isr_ADC_StartEx(Interrupcion_ADC);

        Timer_DAC_Init();
        Timer_ADC_Init();

        Timer_DAC_WritePeriod(t1mV);
        Timer_ADC_WritePeriod(Period_ADC);

        Timer_DAC_Enable();
```

```
    Timer_ADC_Enable();
  }
  else
  {
    UART_PutChar(254);
    Fin_Voltametria();
  }
}

CY_ISR(Interrupcion_DAC_VL)
{
  if(Signo>0)
  {
    Voltage_DAC++;
  }
  else
  {
    Voltage_DAC--;
  }
  Put_DAC_Voltage(Voltage_DAC);
}
```

Voltametria_Ciclica.c

```
#include <main.h>

void Voltametria_Ciclica(void)
{
  if(UART_GetRxBufferSize()==10)
  {
    uint8 i, VC_Param[10];
    UART_PutChar(2);

    for(i=0;i<10;i++)
    {
      VC_Param[i]=UART_ReadRxData();
    }

    Voltage_DAC=(VC_Param[0]<<8)|VC_Param[1];
    Voltage_Maximo=(VC_Param[2]<<8)|VC_Param[3];
    Voltage_Minimo=(VC_Param[4]<<8)|VC_Param[5];
    Ciclos=VC_Param[6];
    Signo=VC_Param[7]-1;
    Pendiente=(VC_Param[8]<<8)|VC_Param[9];

    Puntos_ADC=(Voltage_Maximo-Voltage_Minimo)*2*Ciclos*sps/Pendiente;
```

```
        t1mV=24000000/Pendiente;

        Cnt_Puntos=0;
        Put_DAC_Voltage(Voltage_DAC);
        CyDelay(1000);

        isr_DAC_StartEx(Interrupcion_DAC_VC);
        isr_ADC_StartEx(Interrupcion_ADC);

        Timer_DAC_Init();
        Timer_ADC_Init();

        Timer_DAC_WritePeriod(t1mV);
        Timer_ADC_WritePeriod(Period_ADC);

        Timer_DAC_Enable();
        Timer_ADC_Enable();

    }
    else
    {
        UART_PutChar(253);
        Fin_Voltametria();
    }
}

CY_ISR(Interrupcion_DAC_VC)
{
    if(Signo)
    {
        Voltage_DAC++;
        if(Voltage_DAC>=Voltage_Maximo){Signo=0;}
    }
    else
    {
        Voltage_DAC--;
        if(Voltage_DAC<=Voltage_Minimo){Signo=1;}
    }
    Put_DAC_Voltage(Voltage_DAC);
}
```

Cronoamperometria.c

```
#include <main.h>

void Cronoamperometria(void)
```

```c
{
    if(UART_GetRxBufferSize()==12)
    {
        uint8 i, CR_Param[12];
        UART_PutChar(3);

        for(i=0;i<12;i++)
        {
            CR_Param[i]=UART_ReadRxData();
        }

        Voltage_Inicial=(CR_Param[0]<<8)|CR_Param[1];
        Voltage_Final=(CR_Param[2]<<8)|CR_Param[3];

Periodo2=(CR_Param[4]<<24)|(CR_Param[5]<<16)|(CR_Param[6]<<8)|CR_Param[7];

Quiet_Time=(CR_Param[8]<<24)|(CR_Param[9]<<16)|(CR_Param[10]<<8)|CR_Param[11];
        Puntos_ADC=sps*2*Periodo2/(1000);

        Cnt_CR=0;
        Cnt_Puntos=0;
        Voltage_DAC=Voltage_Inicial;
        Put_DAC_Voltage(Voltage_DAC);
        CyDelay(Quiet_Time);

        isr_DAC_StartEx(Interrupcion_DAC_CR);
        isr_ADC_StartEx(Interrupcion_ADC);

        Timer_DAC_Init();
        Timer_ADC_Init();

        Timer_DAC_WritePeriod(24000);
        Timer_ADC_WritePeriod(Period_ADC);

        Timer_DAC_Enable();
        Timer_ADC_Enable();

        Voltage_DAC=Voltage_Final;
        Put_DAC_Voltage(Voltage_DAC);
    }
    else
    {
        UART_PutChar(252);
        Fin_Voltametria();
    }
```

```c
}

CY_ISR(Interrupcion_DAC_CR)
{
   Cnt_CR++;
   if(Cnt_CR>=Periodo2)
   {
      Voltage_DAC=Voltage_Inicial;
      Put_DAC_Voltage(Voltage_DAC);
   }
}
```

Selector_Ganancia.c

```c
#include <main.h>

void Ganancia(char caso)
{
   switch(caso)
   {
      case 1:
         TIA_SetResFB(TIA_RES_FEEDBACK_20K);
         break;

      case 2:
         TIA_SetResFB(TIA_RES_FEEDBACK_30K);
         break;

      case 3:
         TIA_SetResFB(TIA_RES_FEEDBACK_40K);
         break;

      case 4:
         TIA_SetResFB(TIA_RES_FEEDBACK_80K);
         break;

      case 5:
         TIA_SetResFB(TIA_RES_FEEDBACK_120K);
         break;

      case 6:
         TIA_SetResFB(TIA_RES_FEEDBACK_250K);
         break;

      case 7:
         TIA_SetResFB(TIA_RES_FEEDBACK_500K);
```

```
        break;

    case 8:
        TIA_SetResFB(TIA_RES_FEEDBACK_1000K);
        break;

    default:
        UART_PutChar(255);
        Fin_Voltametria();
    }
}
```

Interrupcion_UART.c

```
#include <main.h>

CY_ISR(Interrupcion_UART)
{

}
```

Appendix C: User Interface

The user interface of Figure 78 manages the electrochemical reactions in LabVIEW. The code of this algorithm is not in this document because it will take several images to make a complete documentation. However, Chapter 3 explains the logic of the PUIS. With that description, someone can recreate this work or move forward to another language as java for mobile applications. Figure 78 has the basic functionality to get data for LSV, DSC, and CV. Thus, when someone is developing a similar application, all those controls and indicators have to be in the user interface somehow.
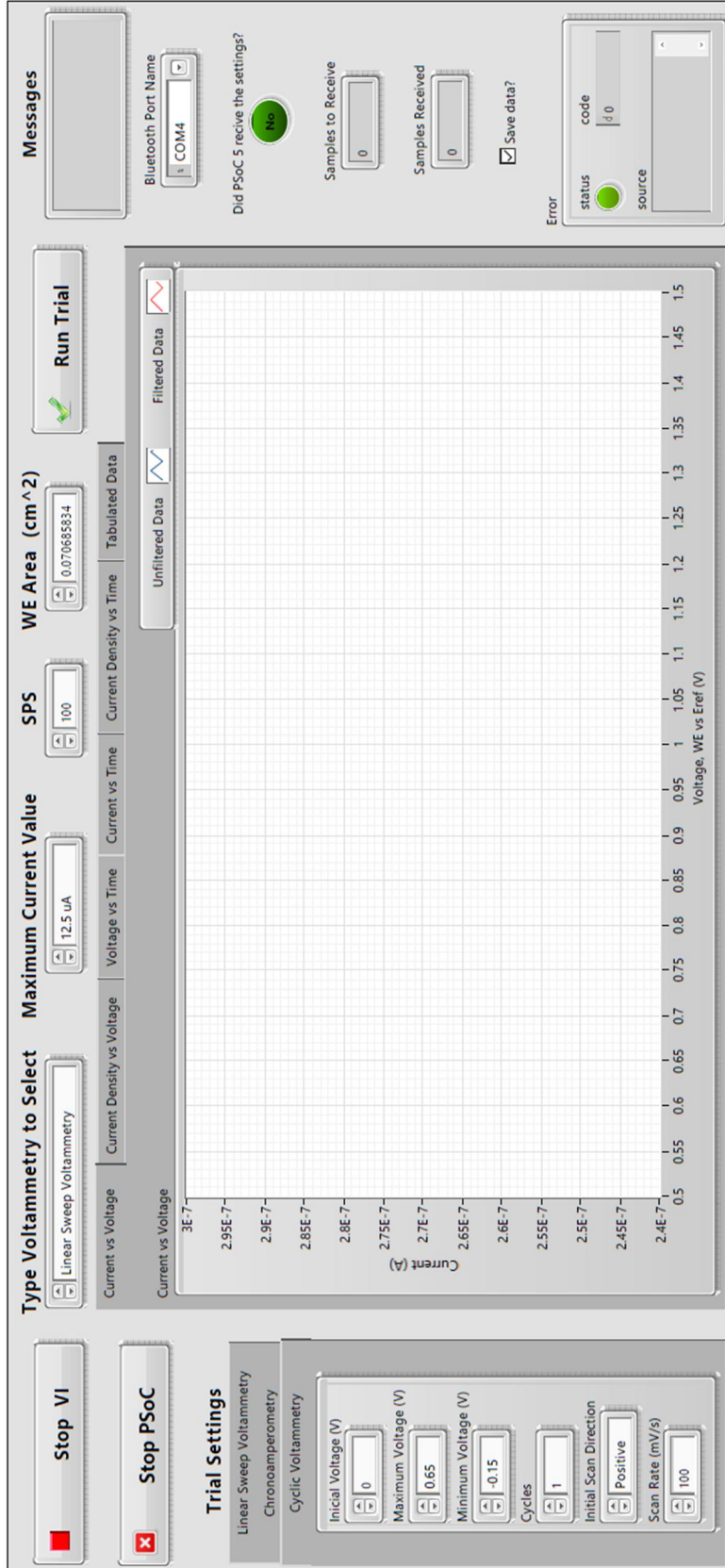
Figure 78. User Interface.

120

Appendix D: Potentiostat Linearity Graphs

The graphs of this appendix present the LSV experiments from -2 to 2 V with a scan rate of 50 mV/s. The conditions of these trials are in Table 15. The connections are according to Figure 43. The values of R2 for the Randles cell are in Table 14. With these graphs, someone can observe the potentiostat linearity at different current levels.
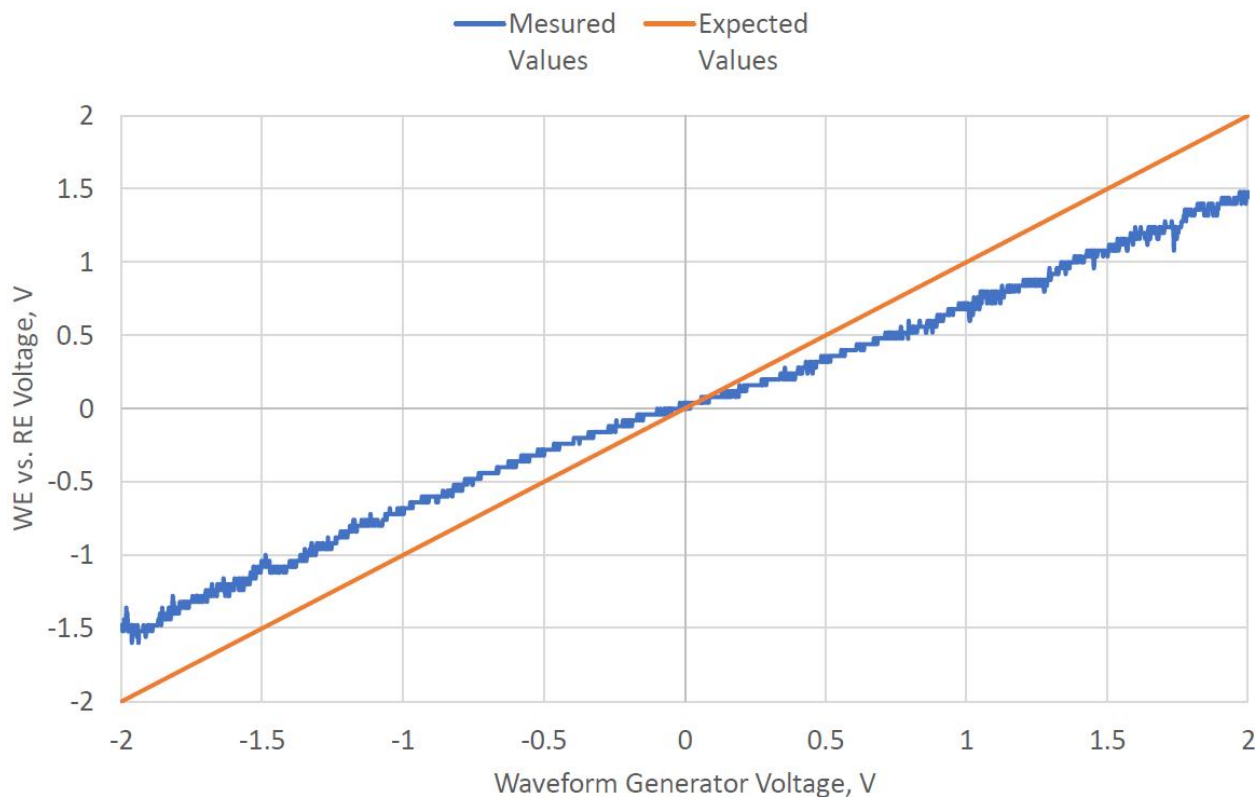
Figure 79. LSV experiment with R2.1 from Table 14.
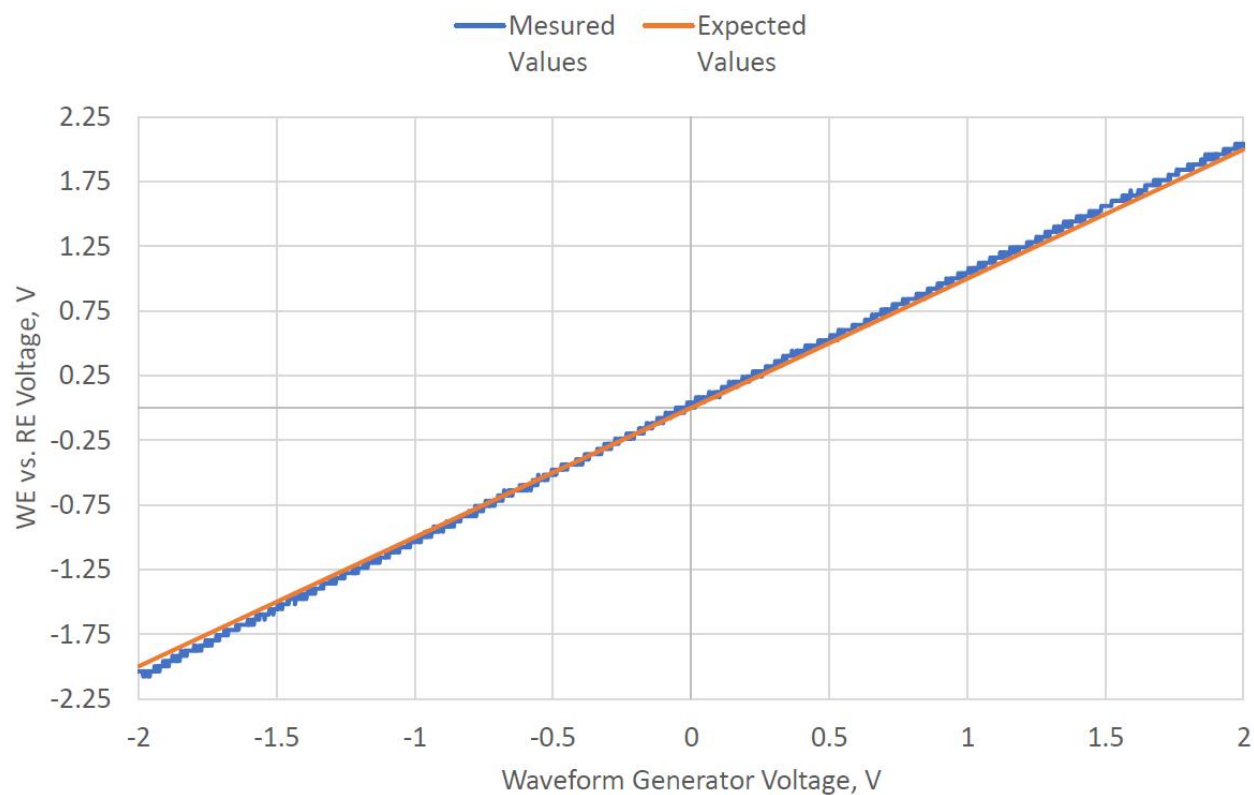
Figure 80. LSV experiment with R2.2 from Table 14.
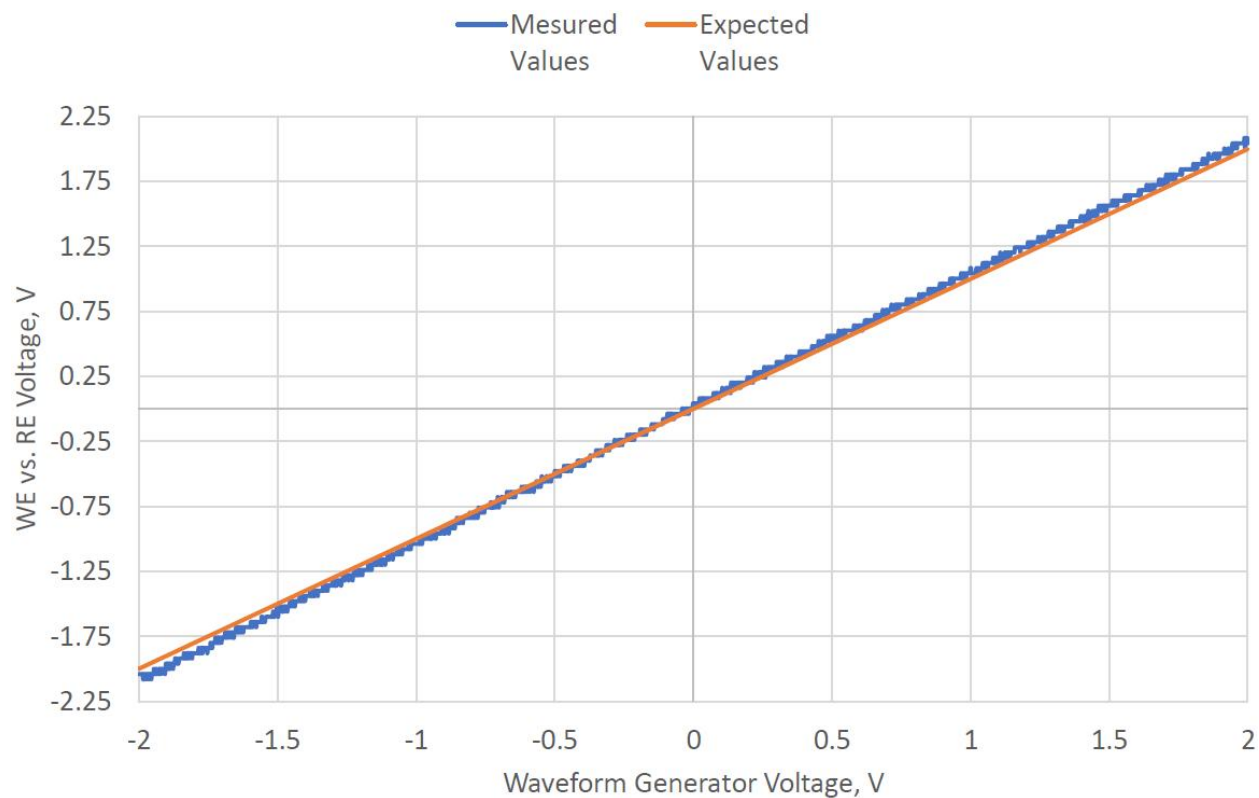
Figure 81. LSV experiment with R2.3 from Table 14.
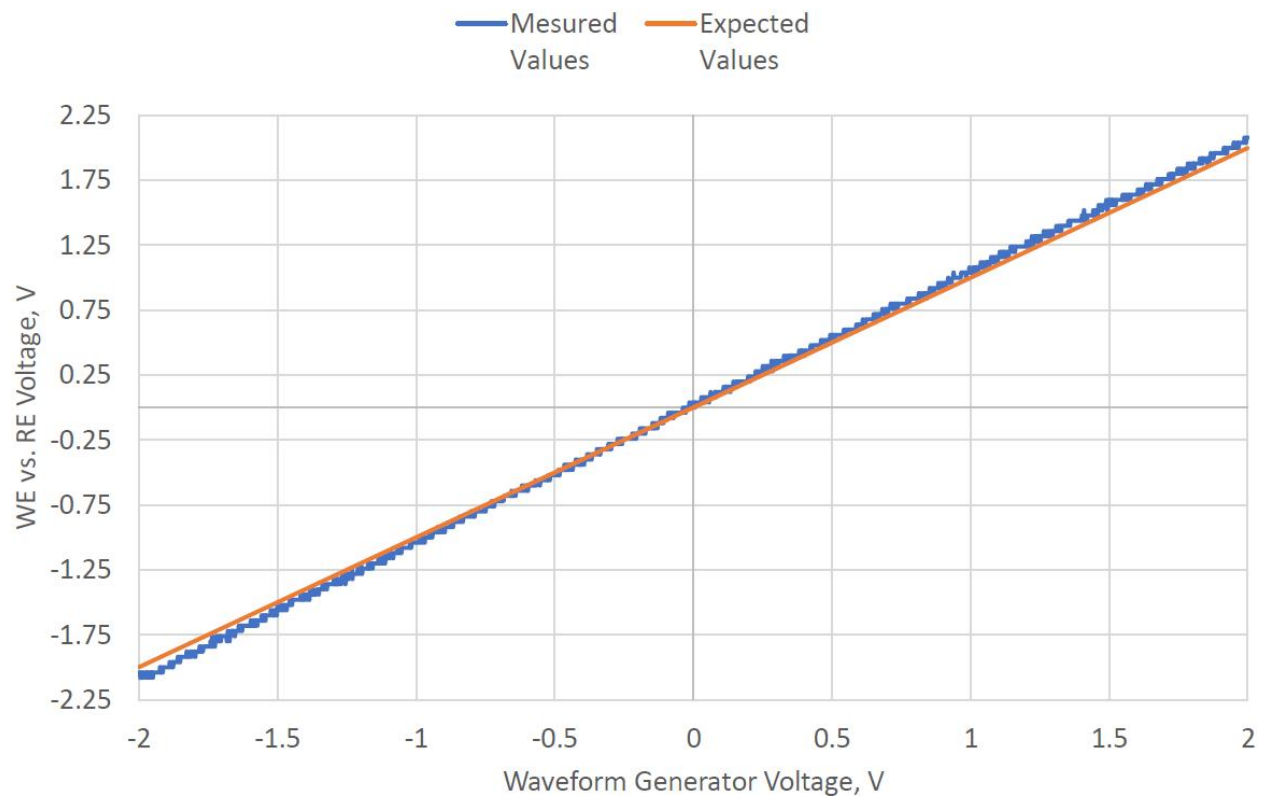
Figure 82. LSV experiment with R2.4 from Table 14.
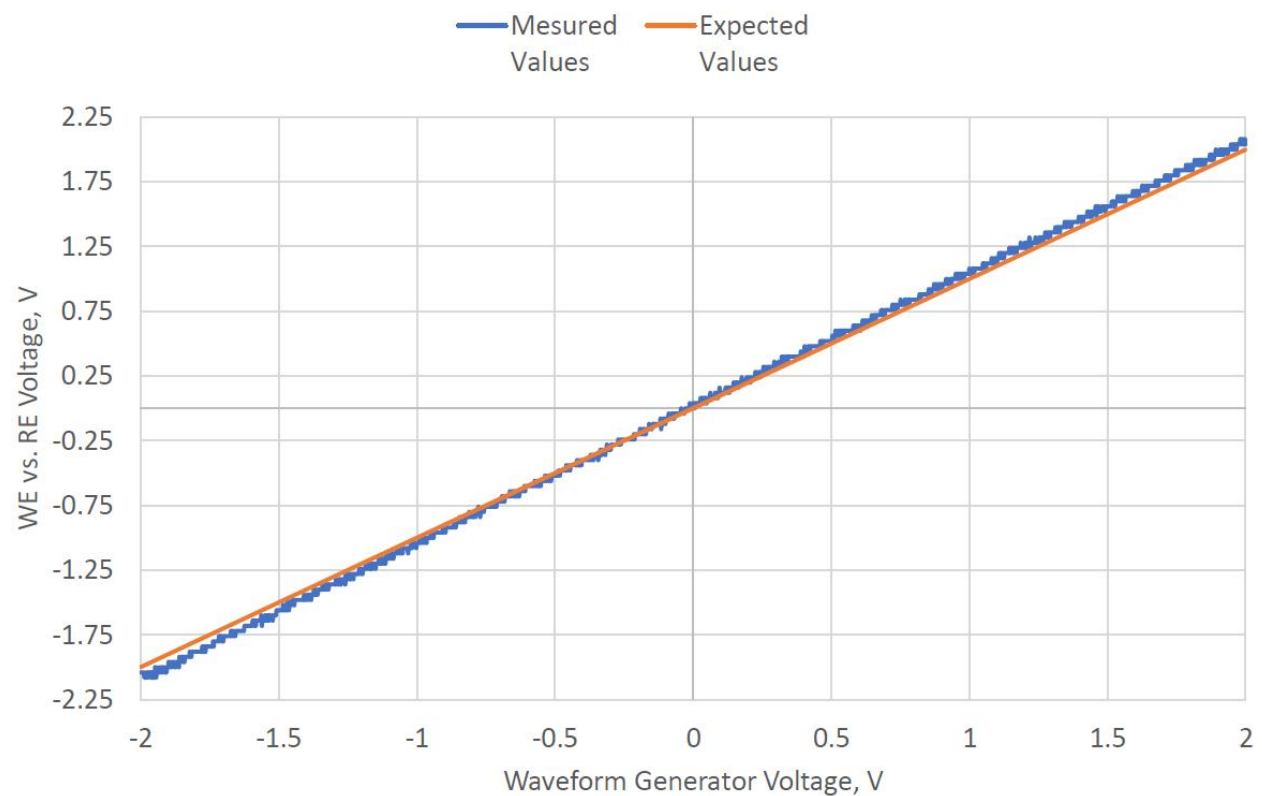
Figure 83. LSV experiment with R2.5 from Table 14.

Figure 84. LSV experiment with R2.6 from Table 14.

Figure 85. LSV experiment with R2.7 from Table 14.

Figure 86. LSV experiment with R2.8 from Table 14.

Bibliography

[1]   T. Luo, H. Wang, H. Song, and J. B. Christen, "CMOS potentiostat for chemical sensing applications," in *IEEE SENSORS 2013 - Proceedings*, 2013, pp. 1–4.

[2]   A. Sun, A. G. Venkatesh, and D. A. Hall, "A Multi-Technique Reconfigurable Electrochemical Biosensor: Enabling Personal Health Monitoring in Mobile Devices," *IEEE Trans. Biomed. Circuits Syst.*, pp. 1–10, 2016.

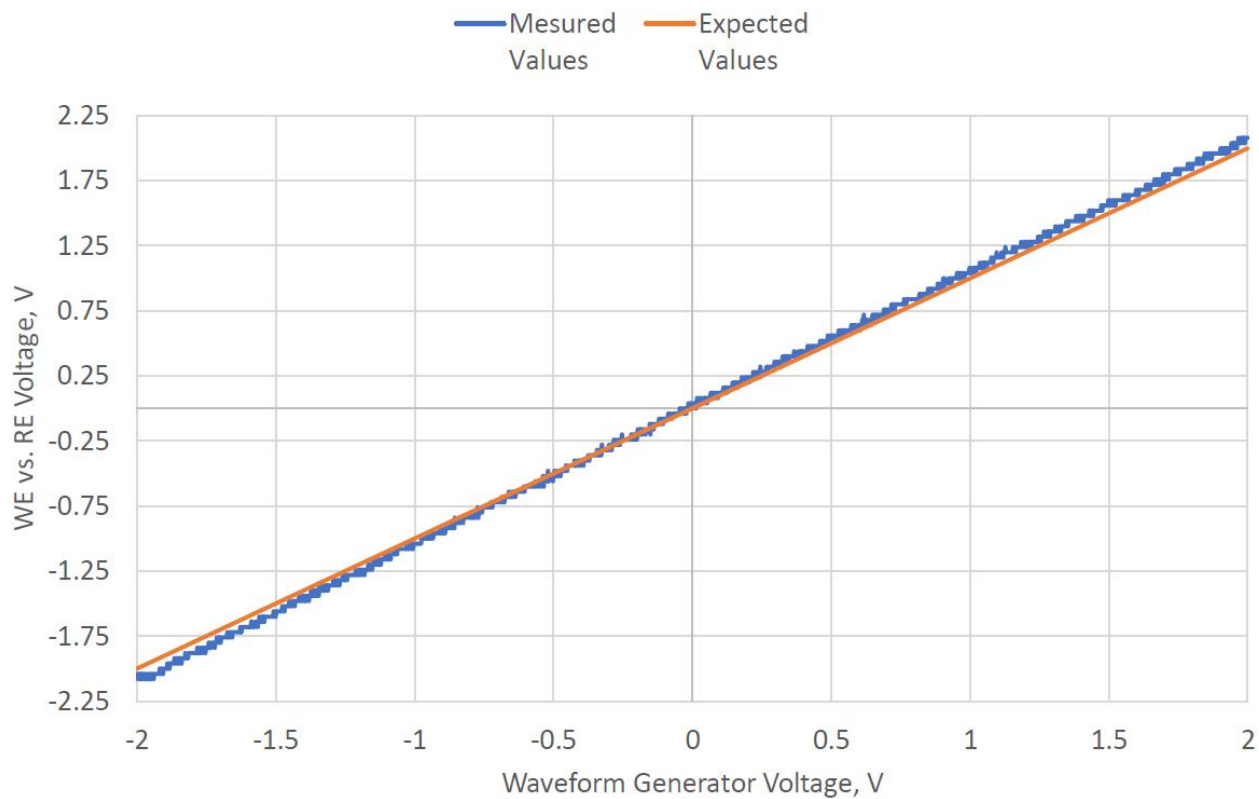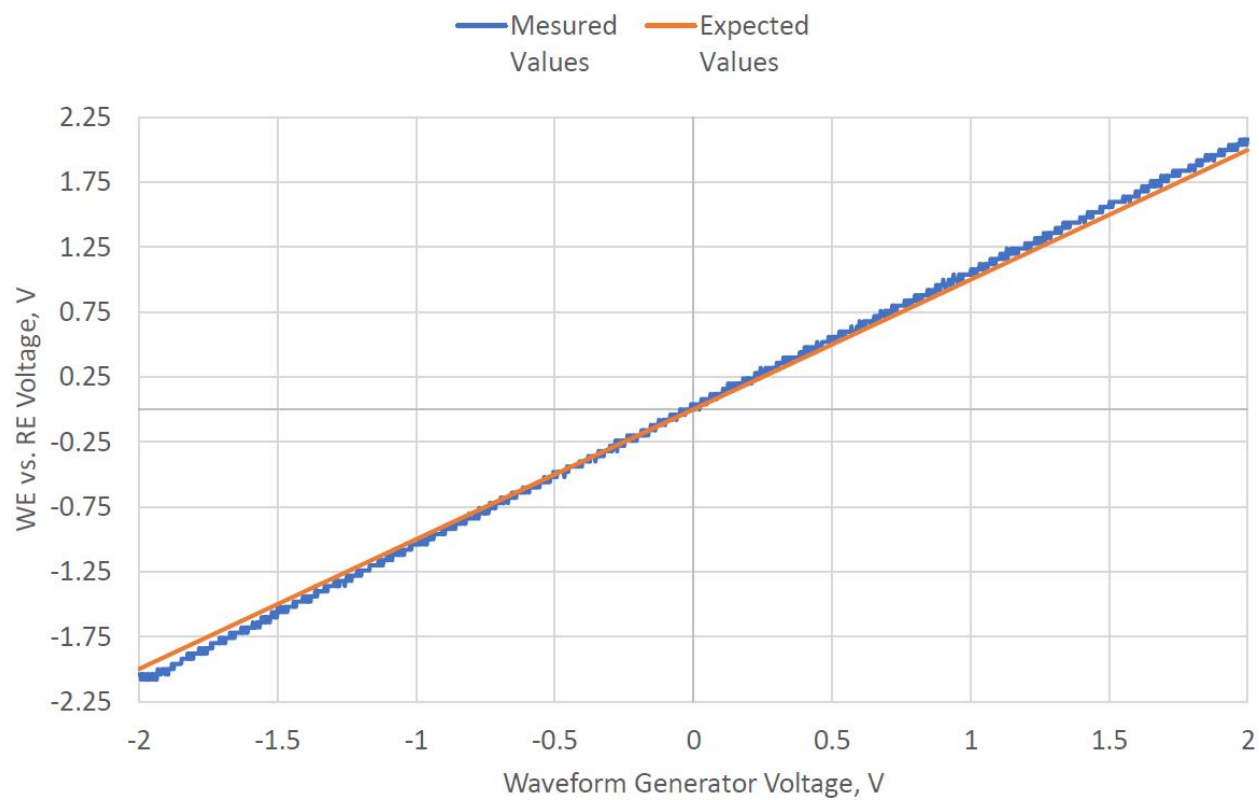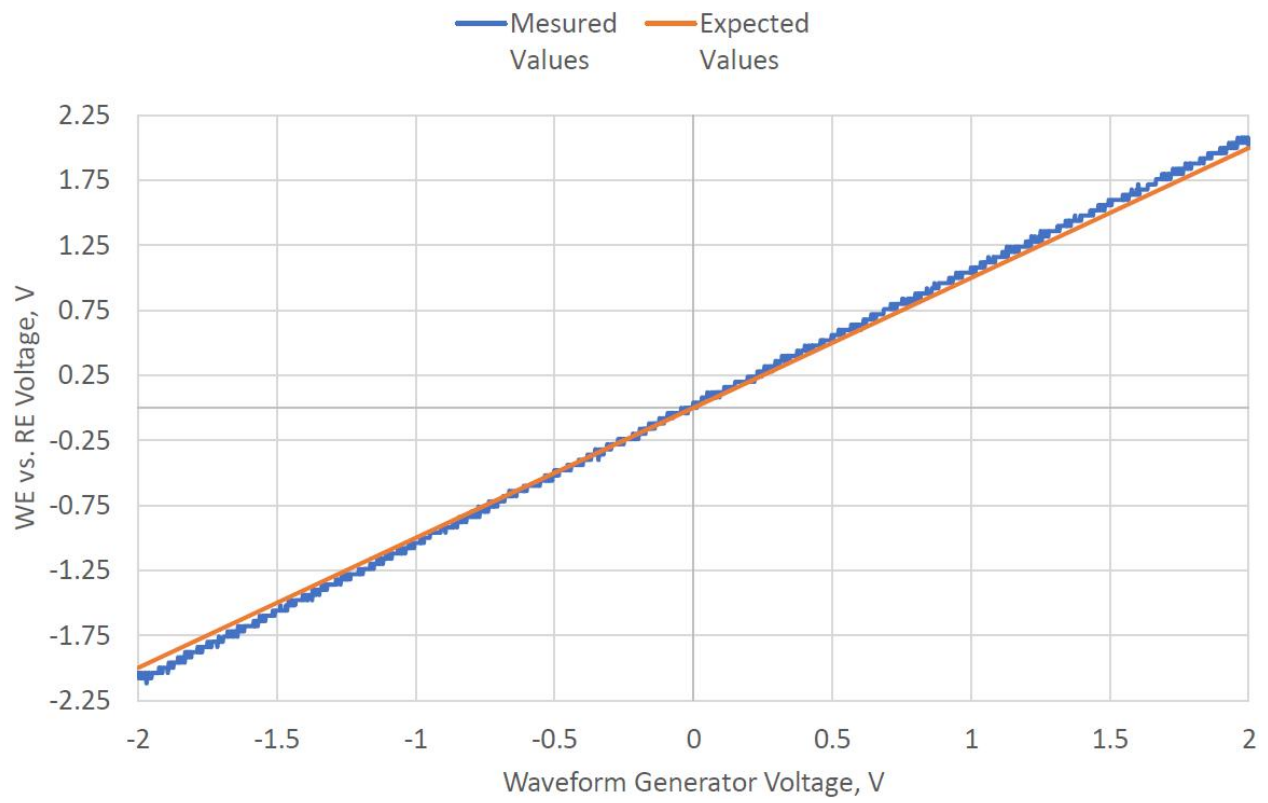[3]   L. Lombardo, S. Generelli, N. Tscharner, D. Migliorelli, and N. Donato, "A compact electronic interface for electrochemical sensors," in *2016 IEEE Sensors Applications Symposium (SAS)*, 2016, pp. 1–4.

[4]   J. Höfflin, S. M. Torres Delgado, F. Suárez Sandoval, J. G. Korvink, and D. Mager, "Electrifying the disk: a modular rotating platform for wireless power and data transmission for Lab on a disk application.," *Lab Chip*, vol. 15, no. 12, pp. 2584–7, 2015.

[5]   K. Abi-Samra, T.-H. Kim, D.-K. Park, N. Kim, J. Kim, H. Kim, Y.-K. Cho, and M. Madou, "Electrochemical velocimetry on centrifugal microfluidic platforms.," *Lab Chip*, vol. 13, no. 16, pp. 3253–60, Aug. 2013.

[6]   C. E. Nwankire, A. Venkatanarayanan, T. Glennon, T. E. Keyes, R. J. Forster, and J. Ducrée, "Label-free impedance detection of cancer cells from whole blood on an integrated centrifugal microfluidic platform," *Biosens. Bioelectron.*, vol. 68, pp. 382–389, 2015.

[7]   J. Colomer-Farrarons, P. Miribel-Català, I. Rodríguez-Villarreal, and J. Samitier, "Portable Bio-Devices: Design of electrochemical instruments from miniaturized to implantable devices," *New Perspect. Biosens. Technol. Appl.*, pp. 1–458, Jul. 2011.

[8]   E. Juanola-Feliu, P. L. Miribel-Catala, C. P. Aviles, J. Colomer-Farrarons, M. Gonzalez-Pinero, and J. Samitier, "Design of an implantable nano-enabled biomédical device for in-vivo glucose monitoring," in *Design of Circuits and Integrated Systems*, 2014, pp. 1–6.

[9]   C.-Y. Chun-Yueb Huang, H.-Y. Huan-Yu Lin, Y.-C. Yu-Chien Wang, W.-Y. Wei-Yin Liao, and T.-C. Tse-Chuan Chou, "A portable and wireless data transmission potentiostat," in *The 2004 IEEE Asia-Pacific Conference on Circuits and Systems, 2004. Proceedings.*, 2004, vol. 2, pp. 633–636.

[10]   M. D. M. Dryden and A. R. Wheeler, "DStat: A versatile, open-source potentiostat for electroanalysis and integration," *PLoS One*, vol. 10, no. 10, p. 17, Oct. 2015.

[11]   M. Vergani, M. Carminati, G. Ferrari, M. Sampietro, L. Amato, A. Heiskanen, M. Dimaki, W. E. Svendsen, and J. Emneus, "Compact potentiostat for cellular electrochemical imaging with 54 parallel channels," in *2012 IEEE Biomedical Circuits and Systems Conference (BioCAS)*, 2012, pp. 136–139.

[12]   A. A. Rowe, A. J. Bonham, R. J. White, M. P. Zimmer, R. J. Yadgar, T. M. Hobza, J. W. Honea, I. Ben-Yaacov, and K. W. Plaxco, "CheapStat: An Open-Source, 'Do-

It-Yourself' Potentiostat for Analytical and Educational Applications," *PLoS One*, vol. 6, no. 9, p. e23783, Sep. 2011.

[13] H. M. Jafari, K. Abdelhalim, L. Soleymani, E. H. Sargent, S. O. Kelley, and R. Genov, "Nanostructured CMOS Wireless Ultra-Wideband Label-Free PCR-Free DNA Analysis SoC," *IEEE J. Solid-State Circuits*, vol. 49, no. 5, pp. 1223–1241, May 2014.

[14] C.-P. Huang, Y.-T. Shyu, T.-Y. Hsieh, C.-W. Cheng, W.-C. Liu, H.-T. Jian, Y.-W. Wang, B.-D. Liu, S.-J. Chang, L.-Y. Chiou, and C.-H. Chen, "The SoC design of a versatile biomedical signal processor for potentiostat," in *2015 International Symposium on Bioelectronics and Bioinformatics (ISBB)*, 2015, pp. 59–62.

[15] C. I. Dorta-Quinones, X. Y. Wang, R. K. Dokania, A. Gailey, M. Lindau, and A. B. Apsel, "A Wireless FSCV Monitoring IC With Analog Background Subtraction and UWB Telemetry," *IEEE Trans. Biomed. Circuits Syst.*, vol. 10, no. 2, pp. 289–299, Apr. 2016.

[16] B. Bozorgzadeh, D. P. Covey, C. D. Howard, P. A. Garris, and P. Mohseni, "A Neurochemical Pattern Generator SoC With Switched-Electrode Management for Single-Chip Electrical Stimulation and 9.3 µW, 78 pA rms , 400 V/s FSCV Sensing," *IEEE J. Solid-State Circuits*, vol. 49, no. 4, pp. 881–895, Apr. 2014.

[17] M. H. Kim, I. Nam, Y. Ryu, L. W. Wellman, L. D. Sanford, and H. Yoon, "Miniaturized neural sensing and optogenetic stimulation system for behavioral studies in the rat," 2015, p. 94340B.

[18] "EmStat | PalmSens." [Online]. Available: http://www.palmsens.com/en/instruments/emstat/. [Accessed: 07-Nov-2016].

[19] "WaveNow Potentiostat/Galvanostat System – Pine Research Instrumentation Store." [Online]. Available: https://www.pineresearch.com/shop/potentiostats/single-channel/wavenow/wavenow-main. [Accessed: 12-Jan-2017].

[20] G. F. Giordano, M. B. R. Vicentini, R. C. Murer, F. Augusto, M. F. Ferrão, G. A. Helfer, A. B. da Costa, A. L. Gobbi, L. W. Hantao, and R. S. Lima, "Point-of-use electroanalytical platform based on homemade potentiostat and smartphone for multivariate data processing," *Electrochim. Acta*, vol. 219, pp. 170–177, 2016.

[21] E. S. Friedman, M. A. Rosenbaum, A. W. Lee, D. A. Lipson, B. R. Land, and L. T. Angenent, "A cost-effective and field-ready potentiostat that poises subsurface electrodes to monitor bacterial respiration," 2012.

[22] A. J. Bard and L. R. Faulkner, "Electrochemical Instrumentation," in *Electrochemical Methods: Fundamentals and Applications*, Wiley, 2001, pp. 632–658.

[23] S. Z. Andreasen, D. Kwasny, L. Amato, A. L. Brøgger, F. G. Bosco, K. B. Andersen, W. E. Svendsen, and A. Boisen, "Integrating electrochemical detection with centrifugal microfluidics for real-time and fully automated sample testing," *RSC Adv.*, vol. 5, no. 22, pp. 17187–17193, 2015.

[24] X. Wang, G. Lin, G. Cui, X. Zhou, and G. L. Liu, "White Blood Cell Counting on

Smartphone Paper Electrochemical Sensor," *Biosens. Bioelectron.*, 2016.

[25]   H. S. El-Desoky and M. M. Ghoneim, "Assay of the anti-psychotic drug haloperidol in bulk form, pharmaceutical formulation and biological fluids using square-wave adsorptive stripping voltammetry at a mercury electrode," *J. Pharm. Biomed. Anal.*, vol. 38, no. 3, pp. 543–550, Jul. 2005.

[26]   M. C. Gardenal Santos, C. R. Teixeira Tarley, L. H. Dall'Antonia, and E. R. Sartori, "Evaluation of boron-doped diamond electrode for simultaneous voltammetric determination of hydrochlorothiazide and losartan in pharmaceutical formulations," *Sensors Actuators, B Chem.*, vol. 188, pp. 263–270, Nov. 2013.

[27]   S. Dehdashtian, M. B. Gholivand, M. Shamsipur, and Z. Karimi, "A nano sized functionalized mesoporous silica modified carbon paste electrode as a novel, simple, robust and selective anti-diabetic metformin sensor," *Sensors Actuators B Chem.*, vol. 221, pp. 807–815, Dec. 2015.

[28]   R. Bhattacharyya, B. Tudu, S. C. Das, N. Bhattacharyya, R. Bandyopadhyay, and P. Pramanik, "Classification of black tea liquor using cyclic voltammetry," *J. Food Eng.*, vol. 109, no. 1, pp. 120–126, Mar. 2012.

[29]   K. Tiwari, B. Tudu, R. Bandyopadhyay, and A. Chatterjee, "Identification of monofloral honey using voltammetric electronic tongue," *J. Food Eng.*, vol. 117, no. 2, pp. 205–210, Jul. 2013.

[30]   M. B. Gholivand, M. Shamsipur, G. Paimard, M. Feyzi, and F. Jafari, "Synthesis of Fe-Cu/TiO2 nanostructure and its use in construction of a sensitive and selective sensor for metformin determination," *Mater. Sci. Eng. C*, vol. 42, pp. 791–798, Sep. 2014.

[31]   M. B. Gholivand and L. Mohammadi-Behzad, "Differential pulse voltammetric determination of metformin using copper-loaded activated charcoal modified electrode," *Anal. Biochem.*, vol. 438, no. 1, pp. 53–60, Jul. 2013.

[32]   R. H. Farahi, T. L. Ferrell, A. Guiseppi-Elie, and P. Hansen, "Integrated electronics platforms for wireless implantable biosensors," in *2007 IEEE/NIH Life Science Systems and Applications Workshop*, 2007, pp. 27–30.

[33]   M. R. Siddiqui, Z. A. AlOthman, and N. Rahman, "Analytical techniques in pharmaceutical analysis: A review," *Arabian Journal of Chemistry*, vol. 44, 2013.

[34]   P. Zanello, "Voltammetric Techniques," in *Inorganic Electrochemistry: Theory, Practice and Applications*, Royal Society of Chemistry, 2003, pp. 49–138.

[35]   D. Ursutiu, C. Samoila, P. Kane, and F. Altoe, "Powerful Technologies Together for Engineering Education (PTT for EE)," in *Proceedings of 2015 12th International Conference on Remote Engineering and Virtual Instrumentation (REV)*, 2015, pp. 113–117.

[36]   V. Thangavel, Z.-X. Song, and R. F. Demara, "Intrinsic Evolution of Truncated Puiseux Series on a Mixed-Signal Field-Programmable SoC," *IEEE Access*, vol. 4, pp. 2863–2872, 2016.

[37]   M. F. Masters, T. Heral, and K. Tummala, "Low-cost coincidence counting

apparatus for quantum optics investigations," 2015, p. 97930V.

[38] G. Prasanna, J. Jayapandian, O. K. Sheela, and G. Amarendra, "A novel pulse processing scheme using embedded pulsed reset charge sensitive preamplifier," 2016, p. 60023.

[39] C.-Y. Huang, M.-J. Syu, Y.-S. Chang, C.-H. Chang, T.-C. Chou, and B.-D. Liu, "A portable potentiostat for the bilirubin-specific sensor prepared from molecular imprinting," *Biosens. Bioelectron.*, vol. 22, no. 8, pp. 1694–1699, Mar. 2007.

[40] A. Doboli, P. Kane, and D. Van Ess, "Dynamic reconfiguration in a PSoC device," in *2009 International Conference on Field-Programmable Technology*, 2009, pp. 361–363.

[41] P. Xuewei and A. K. Rathore, "Small-Signal Analysis of Naturally Commutated Current-Fed Dual Active Bridge Converter and Control Implementation Using Cypress PSoC," *IEEE Trans. Veh. Technol.*, vol. 64, no. 11, pp. 4996–5005, Nov. 2015.

[42] T. Mohiuddin, M. Nawrocki, and R. Bitter, "Introduction to LabVIEW," in *LabVIEW Advanced Programming Techniques*, 2nd ed., CRC Press, 2006, pp. 1–67.

[43] A. Bozatzidis, A. G. Anastopoulos, and T. Laopoulos, "An Automated Data Acquisition Setup for Electro-Chemical Measurements," in *2007 4th IEEE Workshop on Intelligent Data Acquisition and Advanced Computing Systems: Technology and Applications*, 2007, pp. 51–54.

[44] Z. Zou, A. Jang, E. T. MacKnight, P.-M. Wu, J. Do, J. S. Shim, P. L. Bishop, and C. H. Ahn, "An On-Site Heavy Metal Analyzer With Polymer Lab-on-a-Chips for Continuous Sampling and Monitoring," *IEEE Sens. J.*, vol. 9, no. 5, pp. 586–594, May 2009.

[45] N. Pour Aryan, V. Rieger, C. Brendler, and A. Rothermel, "An Economical and convenient experiment setup for electrode investigation," in *2012 Annual International Conference of the IEEE Engineering in Medicine and Biology Society*, 2012, pp. 815–818.

[46] T. Mohiuddin, M. Nawrocki, and R. Bitter, "State Machines," in *LabView Advanced Programming Techniques*, 2nd ed., CRC Press, 2006, pp. 135–179.

[47] T. J. Bress, "Producer–Consumer State Machines," in *Effective Labview Programming*, NTS Press, 2013, pp. 368–386.

[48] C. M. A. Brett and A. M. O. Brett, "Electrochemical Experiments," in *Electrochemistry : principles, methods, and applications*, Oxford University Press, 1993, pp. 129–150.

[49] J. Colomer-Farrarons and P. L. Miribel-Català, "Biomedical Integrated Instrumentation," in *A CMOS Self-Powered Front-End Architecture for Subcutaneous Event-Detector Devices*, Dordrecht: Springer Netherlands, 2011, pp. 93–132.

[50] M. Ciobanu, J. P. Wilburn, M. L. Krim, and D. E. Cliffel, "Fundamentals," in *Handbook of Electrochemistry*, Elsevier, 2007, pp. 1–30.

[51] R. M. Souto, "Electronic configurations in potentiostats for the correction of ohmic losses," *Electroanalysis*, vol. 6, no. 7, pp. 531–542, Jul. 1994.

[52] STMicroelectronics, "Application Note: Operational amplifier stability compensation methods for capacitive loading applied to TS507," no. 2653, pp. 1–22, 2007.

[53] S. Franco, "Static Op Amp Limitations," in *Design with operational amplifiers and analog integrated circuits*, 4th ed., 2015, pp. 221–276.

[54] S. Chen, "Practical Electrochemical Cells," in *Handbook of Electrochemistry*, Elsevier, 2007, pp. 33–56.

[55] X.-Z. Yuan, C. Song, H. Wang, and J. Zhang, "EIS Equivalent Circuits," in *Electrochemical Impedance Spectroscopy in PEM Fuel Cells*, London: Springer London, 2010, pp. 139–192.

[56] G. Instruments, "Universal Dummy Cell 3 Operator's Manual," *Cell*, 2005.

[57] "LMP7701 Precision, CMOS Input, RRIO, Wide Supply Range Amplifier | TI.com." [Online]. Available: http://www.ti.com/product/LMP7701. [Accessed: 19-Apr-2017].

[58] "LMP7721 3 Femtoampere Input Bias Current Precision Amplifier | TI.com." [Online]. Available: http://www.ti.com/product/LMP7721. [Accessed: 19-Apr-2017].

[59] Y.-H. Sheu and C.-Y. Huang, "A Portable Potentiostat for Electrochemical Sensors," in *3rd Kuala Lumpur International Conference on Biomedical Engineering 2006*, Berlin, Heidelberg: Springer Berlin Heidelberg, 2007, pp. 538–542.

[60] A. J. Peyton and V. Walsh, "Current-to-voltage and voltage-to-current converters," in *Analog electronics with Op Amps : a source book of practical circuits*, Cambridge University Press, 1993, pp. 37–58.

[61] S. Franco, "Circuits with Resistive Feedback," in *Design with Operational Amplifiers and Analog Integrated Circuits*, 4th ed., 2015, pp. 67–113.

[62] A. Bhat, "Stabilize Your Transimpedance Amplifier," 2012.

[63] V. Tabard-Cossa, "Chapter 3 – Instrumentation for Low-Noise High-Bandwidth Nanopore Recording," in *Engineered Nanopores for Bioanalytical Applications*, 2013, pp. 59–93.

[64] "LM741 Operational Amplifier | TI.com." [Online]. Available: http://www.ti.com/product/LM741. [Accessed: 27-Apr-2017].

[65] R. Schaumann, M. E. (Mac E. Van Valkenburg, and M. E. (Mac E. Van Valkenburg, *Design of analog filters*. Oxford University Press, 2010.

[66] M. J. M. Pelgrom, "Sampling," in *Analog-to-Digital Conversion*, New York, NY: Springer New York, 2013, pp. 163–195.

[67] M. J. M. Pelgrom, "Sigma–Delta Modulation," in *Analog-to-Digital Conversion*, New York, NY: Springer New York, 2013, pp. 419–468.

[68] S. Logan, "Understanding noise, ENOB, and effective resolution in ADCs," *EDN*, vol. 57, no. 10, pp. 39–41, 2012.

[69] B. Baker, "How delta-sigma ADCs work, Part 1," *Analog Appl. J.*, no. 3Q, pp. 13–16, 2011.

[70] B. Baker, "How delta-sigma ADCs work, Part 2," *Analog Appl. J.*, no. 4Q, pp. 5–7, 2011.

[71] S. W. Smith and S. W. Smith, "CHAPTER 15 – Moving Average Filters," in *Digital Signal Processing*, 2003, pp. 277–284.

[72] A. Doboli and E. H. Currie, "Hardware and Software Subsystems of Mixed-Signal Architectures," in *Introduction to Mixed-Signal, Embedded Design*, New York, NY: Springer New York, 2011, pp. 103–150.

[73] A. Doboli and E. H. Currie, "An Overview of Mixed-Signal, Embedded System Design," in *Introduction to Mixed-Signal, Embedded Design*, New York, NY: Springer New York, 2011, pp. 1–49.

[74] "PSoC® 5LP: CY8C58LP Family Datasheet: Programmable System-on-Chip (PSoC®)," no. 001–84932 Rev. *J. Cypress Semiconductor Corporation, p. 139, 2015.

[75] "CYBL10X6X Family Datasheet: Programmable Radio-on-Chip With Bluetooth Low Energy (PRoC BLE)," no. 001–90478 Rev. *K. Cypress Semiconductor Corporation, p. 42, 2015.

[76] H. Gomaa, "Catalog of Software Architectural Patterns," in *Real-Time Software Design For Embedded Systems*, Cambridge: Cambridge University Press, 2016, pp. 530–550.

[77] H. Gomaa, "Software Architectural Patterns for Real-Time Embedded Systems," in *Real-Time Software Design For Embedded Systems*, Cambridge: Cambridge University Press, 2016, pp. 184–210.

[78] T. G. Robertazzi, "Wireless Networks," in *Introduction to Computer Networking*, Cham: Springer International Publishing, 2017, pp. 35–60.

[79] S. Higson, "Electro-analytical techniques," in *Analytical Chemistry*, OUP Oxford, 2003, pp. 285–322.

[80] C. M. A. Brett and A. M. O. Brett, "Step and Pulse Techniques," in *Electrochemistry: principles, methods, and applications*, Oxford University Press, 1993, pp. 199–223.

[81] "CHI700E Series." [Online]. Available: http://www.chinstruments.com/chi700.shtml. [Accessed: 02-Jun-2017].

[82] "Project #020: UART to BLE Bridge | Cypress Semiconductor." [Online]. Available: http://www.cypress.com/blog/100-projects-100-days/project-020-uart-ble-bridge. [Accessed: 27-Mar-2017].

[83] I. C. Bertolotti and G. Manduchi, "Real-Time Concurrent Programming Principles," in *Real-time embedded systems: open-source operating systems perspective*, CRC Press, 2012, pp. 63–78.

[84] S. W. Smith, "Moving Average Filters," in *The scientist and engineer's guide to digital signal processing*, California Technical Pub, 1999, pp. 277–284.

[85] A. J. Bard and L. R. Faulkner, "Basic Potential Step Methods," in *Electrochemical Methods: Fundamentals and Applications*, Wiley, 2001, pp. 156–225.

[86] L. Li, X. Liu, W. A. Qureshi, and A. J. Mason, "CMOS Amperometric Instrumentation and Packaging for Biosensor Array Applications," *IEEE Trans. Biomed. Circuits Syst.*, vol. 5, no. 5, pp. 439–448, Oct. 2011.

[87] L. Li, W. A. Qureshi, X. Liu, and A. J. Mason, "Amperometric instrumentation system with on-chip electrode array for biosensor application," in *2010 IEEE Biomedical Circuits and Systems Conference (BioCAS)*, 2010, pp. 294–297.

[88] B. Lim, S. Takahashi, M. Futagawa, F. Dasai, M. Ishida, and K. Sawada, "On-chip square wave voltammetric pulse generator for redox measurement employing array structure," in *2014 IEEE Biomedical Circuits and Systems Conference (BioCAS)*, 2014, pp. 113–116.

[89] K.-Y. Chan and C.-Y. V. Li, "Microbial Fuel Cells and Other Bio-Electrochemical Conversion Devices," in *Electrochemically Enabled Sustainability: Devices, Materials and Mechanisms for Energy Conversion*, CRC Press, 2014, pp. 55–120.

[90] P. Levine, P. Gong, R. Levicky, and K. Shepard, "Active CMOS Biochips for Electrochemical DNA Assays," in *Microfluidics and Nanotechnology: Biosensing to the Single Molecule Limit*, CRC Press, 2014, pp. 19–86.

[91] S. Creager, "Solvents and Supporting Electrolytes," in *Handbook of Electrochemistry*, Elsevier, 2007, pp. 57–72.

[92] H. Kahlert, "Reference Electrodes," in *Electroanalytical Methods: Guide to Experiments and Applications*, Springer, 2013, pp. 291–308.

[93] G. M. Swain, "Solid Electrode Materials: Pretreatment and Activation," in *Handbook of Electrochemistry*, Elsevier, 2007, pp. 111–153.

[94] P. Zanello, "Basic Equipment for Electrochemical Measurements," in *Inorganic Electrochemistry: Theory, Practice and Applications*, Royal Society of Chemistry, 2003, pp. 139–158.

[95] F. G. Thomas and G. Henze, "Techniques," in *Introduction to Voltammetric Analysis: Theory and Practice*, Csiro Publishing, 2001, pp. 18–57.

[96] M. Zaib and M. M. Athar, "Electrochemical Evaluation of Phanerocheaete Chrysosporium Based Carbon Paste Electrode with Potassium Ferricyanide Redox System," *Int. J. Electrochem. Sci*, vol. 10, pp. 6690–6702, 2015.

[97] A. J. Bard and L. R. Faulkner, "Appendix C: Reference Tables," in *Electrochemical methods : fundamentals and applications*, Wiley, 2001, p. 833.

[98] A. Sayad, F. Ibrahim, S. Mukim Uddin, J. Cho, M. Madou, and K. L. Thong, "A microdevice for rapid, monoplex and colorimetric detection of foodborne pathogens using a centrifugal microfluidic platform," *Biosens. Bioelectron.*, vol. 100, pp. 96–104, 2018.

[99] S. Majumder, T. Mondal, and M. Deen, "Wearable Sensors for Remote Health Monitoring," *Sensors*, vol. 17, no. 1, p. 130, Jan. 2017.

[100] F. Miao, Y. Cheng, Y. He, Q. He, and Y. Li, "A Wearable Context-Aware ECG Monitoring System Integrated with Built-in Kinematic Sensors of the Smartphone," *Sensors*, vol. 15, no. 5, pp. 11465–11484, May 2015.

[101] M. Haghi, K. Thurow, and R. Stoll, "Wearable Devices in Medical Internet of Things: Scientific Research and Commercially Available Devices.," *Healthc. Inform. Res.*, vol. 23, no. 1, pp. 4–15, Jan. 2017.

[102] "Mouser Electronics - Distribuidor de Componentes Electrónicos." [Online]. Available: https://www.mouser.com/. [Accessed: 04-Nov-2017].

[103] "China PCB Prototype & Fabrication Manufacturer - PCB Prototype the Easy Way." [Online]. Available: https://www.pcbway.com/. [Accessed: 04-Nov-2017].

[104] A. P. Periasamy, Y.-J. Chang, and S.-M. Chen, "Amperometric glucose sensor based on glucose oxidase immobilized on gelatin-multiwalled carbon nanotube modified glassy carbon electrode," *Bioelectrochemistry*, vol. 80, no. 2, pp. 114–120, 2011.

[105] L. Zuo, S. K. Islam, I. Mahbub, and F. Quaiyum, "A Low-Power 1-V Potentiostat for Glucose Sensors," *IEEE Trans. Circuits Syst. II Express Briefs*, vol. 62, no. 2, pp. 204–208, Feb. 2015.

[106] "Amazon.com: 50 Test Strips Accu Chek Performa + Fingertip Blood Wiper Nano Glucose Sealed: Health & Personal Care." [Online]. Available: https://www.amazon.com/Accu-Chek-Performa-Fingertip-Glucose/dp/B00N3JMKA8. [Accessed: 24-May-2017].

[107] M. D. Steinberg, P. Kassal, I. Kereković, and I. M. Steinberg, "A wireless potentiostat for mobile chemical sensing and biosensing," *Talanta*, vol. 143, pp. 178–183, Oct. 2015.

[108] I. M. Apetrei and C. Apetrei, "Voltammetric determination of melatonin using a graphene-based sensor in pharmaceutical products.," *Int. J. Nanomedicine*, vol. 11, pp. 1859–66, 2016.

[109] C. Chen, C. Sun, and Y. Gao, "Amperometric sensor for hydrogen peroxide based on poly(aniline-co-p-aminophenol)," 2009.

[110] J. Duan, J. Duan, Z. Zhang, and T. Tong, "Irreversible cellular senescence induced by prolonged exposure to H2O2 involves DNA-damage-and-repair genes and telomere shortening," *Int. J. Biochem. Cell Biol.*, vol. 37, no. 7, pp. 1407–1420, Jul. 2005.

[111] C. Chen, X. Hong, T. Xu, A. Chen, L. Lu, and Y. Gao, "Hydrogen peroxide biosensor based on the immobilization of horseradish peroxidase onto a poly(aniline-co-N-methylthionine) film," *Synth. Met.*, vol. 212, pp. 123–130, 2016.

[112] N. Jaiswal, I. Tiwari, C. W. Foster, and C. E. Banks, "Highly sensitive amperometric sensing of nitrite utilizing bulk-modified MnO2 decorated Graphene oxide nanocomposite screen-printed electrodes," *Electrochim. Acta*, vol. 227, pp. 255–266, 2017.

[113] L. El Harrad and A. Amine, "Amperometric biosensor based on prussian blue and

nafion modified screen-printed electrode for screening of potential xanthine oxidase inhibitors from medicinal plants," *Enzyme Microb. Technol.*, vol. 85, pp. 57–63, 2016.

Curriculum Vitae

Adrián Iván Muñoz Martínez was born in Gustavo Diaz Ordaz, Tamaulipas, México, on December 17, 1990. He earned the Electronics Engineering degree from the *Instituto Tecnológico de Saltillo*, in February 2014. He was accepted into the graduate programs in Electronics Engineering in August 2014.

This document was typed in using Microsoft Word by Adrián Iván Muñoz Martínez.